Deciphering rare imprinting disorders within the Beckwith-Wiedemann spectrum

Siren Berland

Thesis for the degree of Philosophiae Doctor (PhD)
University of Bergen, Norway
2022

UNIVERSITY OF BERGEN

Deciphering rare imprinting disorders within the Beckwith-Wiedemann spectrum

Siren Berland

Thesis for the degree of Philosophiae Doctor (PhD)
at the University of Bergen

Date of defense: 28.10.2022

Year: 2022

Title: Deciphering rare imprinting disorders within the Beckwith-Wiedemann spectrum

Name: Siren Berland

Print: Skipnes Kommunikasjon / University of Bergen

Scientific environment

This PhD work was carried out during the period of 2016-2022 at the Department of Medical Genetics, Haukeland University Hospital, and the Department of Clinical Medicine (K2), University of Bergen, under the main supervisor, professor Gunnar Douzgos Houge and co-supervisor professor Stefan Johansson.

Haukeland University Hospital

UNIVERSITY OF BERGEN

Acknowledgements

Working with clinical genetics for the last 16 years has been a rewarding process. When I first started in genetics, two of my friends had children with a clinical diagnosis of Beckwith Wiedemann syndrome. I tried hard to learn about this disorder during my first weeks at the Department of Medical Genetics, Haukeland University Hospital. Happily, I learned that the genetics involved was way more complicated than I ever imagined. This was a massive inspiration for my interest in clinical genetics in general, but particularly in imprinting disorder. First, I want to thank the families contributing to this work. I have developed the most profound admiration for the families involved in this project. Without their enthusiasm and time-spending contribution, this work would not be possible. Fortunately, my main supervisor is an outstanding scientist, a brilliant clinician, and a great teacher with more patience than his student. Also, he shares my interest in imprinting disorders. A deep admiration and profound gratitude go to prof. Gunnar Houge.

A financial grant was provided by a three-year full-time PhD fellowship from Helse-Vest #912029. Unfortunately, a full-time PhD was not possible due to severe illness among colleagues, and half-time was also difficult. Therefore, after two years part-time (1st of July 2018), I dismissed this grant. The rest of the work was conducted part-time in between regular job at the Department of Medical Genetics.

This work had not have been possible without Bjørn Ivar Haukanes's invaluable contribution. His knowledge about molecular genetics, in particular RNA and epigenetics seems endless, and so is his patience. He has, along with Gunnar Houge, really inspired me to think outside the box. I will also express my gratitude to my co-supervisor Stefan Johansson for his inspiration for good science and writing and for always being helpful and supporting, and to my co-authors for their valuable contribution and for critically revising the manuscripts. Colleagues in the Lab; Sigrid Erdal, Guri Matre, Tomasz Stokowy, Rita Holdhus, Hilde Eldevik Rusaas; you were the backbone of the scientific lab work performed. Finally, I also thank the Department of Genetics for allowing me to finish my PhD. Here, I first want to thank the head of the Department, Prof. Vidar Steen, for being a role model in leadership,

wine tasting, formal genetics and science, and for his continuous support and feedback. I also want to thank my (lab)colleagues Ragnhild Berentsen, Simone Reiter, Ida Wiig Sørensen, Sofia Douzgou Houge, Andreas Benneche, and Ognjen Bojovic. Without your contribution, chocolate and support, I could never have left the diagnostic lab to finish this thesis. I also would like to thank to Hildegunn Høberg Vetti, who suberbly paved the way to balance PhD and work at the department. Thanks for our fruitful PhD discussions, but primarily for being a good friend and valuable colleague. My admiration for Gyri Gradek at the Department is getting deeper by the minute. I will thank her for her professional skills, clinical accuracy, never-ending working days, friendship, and for forcing me into Armauer Hansens Hus in the last months of my thesis. I also would like to thank my colleagues Ellen Økland Blinkenberg, for her insight beyond expectations in genetics, ethics, patients and life in general, Tone Nordtveit for telling me that there is no other solution than hard work, and Elen Siglen for her academical inspiration and for making writing it all up much more fun. I also want to thank the late Professor Helge Boman, who grounded our department and provided us with challenging tasks in formal genetics. Despite too long a distance due to Covid19, the endless cheering and support from Cecilie Rustad, Trine Prescott, and in particular Charlotte von der Lippe, have always been the light in the tunnel.

My family with Sigbjørn and our children, Vinjar, Tallak and Tyri, who were born after I started this project, have taught me what really matters in life. Without them, I could have worked 24/7 and might have finished early, resulting in lower quality and less fun in both life and scientific work.

Finally, I want to express my immense gratitude and endless admiration for my good friend and late colleague, Torunn Fiskerstrand, who sadly passed away 1st of Jan 2019. She is the biggest inspiration a young female scientist could ever imagine, and I deeply miss her as my close friend.

Norwegian summary of the thesis

Sammendrag av avhandlingen på norsk.

Beckwith-Wiedemann syndrom (BWS) er den hyppigste og mest komplekse tilstanden blant imprintingssykdommene. Avhandlingen presenterer tre ulike BWS spektrum familier, hvor vi utvider forståelsen av arvemønsteret ved BWS, og viser hvor viktig en presis diagnose er med tanke på individuell oppfølging av f.eks kreftrisiko og svangerskapskomplikasjoner, men også gjentakelsesrisiko i familien. Vi presenterer også en kompleks genvariant i *CDKN1C* som vi foreslår forårsaker ikke bare en, men hele tre ulike tilstander samtidig, bl.a grunnet en ikke tidligere beskrevet isoform av proteinet som kan tenkes å være viktig for hjernens utvikling. I tillegg beskriver vi for første gang en person med et dobbelt kromosomsett (UPD) fra far for to kromosomer (kromosom 7 og 15) som har gitt innsikt i nettverket av imprintede gener.

BWS karakteriseres av bl.a svangerskapskomplikasjoner, lavt blodsukker ved fødsel, høy fødselsvekt og stor morkake, stor tunge og store indre organer, midtlinjedefekter i buk og eventuelt tarmbrokk, økt risiko for barnekreft som Wilms tumour, og hos enkelte spesielle ansiktstrekk og mindre utviklingsavvik. Som hovedregel er den psykomotoriske utviklingen normal. Imprinting er en viktig genreguleringsmekanisme som ikke innebærer endringer i selve DNA-koden, men derimot en reversibel epigenetisk endring av DNA vha cytosin-metylering av hovedsaklig CpG posisjoner. For enkelte gener er ikke bare regulering av gendosen men også genkilden viktig, dvs om genet uttrykket på det kromosomet som er arvet fra mor eller fra far. Dette kalles kjønnsavhengig imprinting. Ved feil i dette kjønnsavgengige imprintingsystemet oppstår imprintingsykdommene. Ved BWS styres imprintingen av to imprintingssentre, IC1 og IC2, på den aktuelle kromosomregion på enden av kromosom 11 (11p15.5). I en normal situasjon er vektsfaktoren *IGF2* i IC1 kun aktivt på genkopien nedarvet fra far, mens veksthemmeren *CDKN1C* i IC2 kun uttrykkes fra genkopien nedarvet fra mor.

Metyleringsforstyrrelser i et (eller begge) av de to imprintingssentrene medfører BWS. Den hyppigste årsaken er sporadisk tap av metylering i IC2 på 11p15.5, som bl.a medfører at veksthemmeren *CDKN1C* slås helt eller delvis av. BWS kan også skyldes økt metylering av det maternelle IC1 som fører til at vekstfaktoren *IGF2* også uttrykkes fra mors genstreng, ikke bare fra fars. En slik økt metylering av IC1 kan være sporadisk, men kan også skyldes underliggende avvik i IC1 sin DNA sekvens, som kan nedarves og gi BWS dersom nedarving via morsledd.

Artikkel I beskriver en en slik familie, hvor familiemedlemmer i tre generasjoner har en sjelden IC1-genfeil som gir opphav til dominant arvelig BWS dersom maternell nedarving. Denne formen for BWS er forbundet med risiko for nyrekreft hos barn. Vi viser også at BWS symptomene øker fra andre til tredje generasjon (antesipasjon) og samtidig korrelerer med metyleringsgraden i IC1. Dette er ikke tidligere beskrevet ved imprintingssykdommer. Vi presenterer en hypotese for å forklare denne antesipasjonen. Som forventet medfører genfeilen forstyrrelse av skifte av metyleringsmønster på fars kromosom 11 i hans datters eggstokker, dvs at demetyleringen er inkomplett her. Det nye her er at denne metyleringsfeilen forsterkes til neste generasjon, dvs hos datterens barn, selv om genfeilen nå sitter på et maternelt nedarvet kromosom. Dette antyder at metyleringen på det maternelle kromosom 11 passivt nedarves til neste generasjon gjennom kvinneledd, mens kun det paternelle kromosom 11 aktivt demetyleres, altså at mors og fars BWS-regioner på kromosom 11 behandles ulikt i eggstokkene.

Artikkel II presenterer en familie med en kompleks variant i *CDKN1C*-genet, som medfører både tap og økning av genfunksjon, slik at gutten har en unik kombinasjon av både BWS-lignende overvekst og en veksthemming. Sistnevnte minner om speilbildetilstanden til BWS som kalles IMAGe. Ved å benytte RNA dypsekvensering viser vi at varianten i tillegg rammer en hittil ikke beskrevet transkriptutgave (isoform) av genet. Vi spekulerer i at genfeil i denne ubeskrevne isoformen kan forklare forsinket utvikling og liten hodeomkrets.

Artikkel III presenterer en gutt med en BWS-lignende trekk i tillegg til psykomotorisk utviklingsavvik. Han har normalt kromosomantall, men begge utgaver av både kromosom nr 7 og nr 15 er kun nedarvet fra far (paternelt), dvs at det

maternelle kromosom 7 og 15 ikke påvises. Dette kalles paternell uniparental disomi (UPD). Når UPD rammer kromosom som inneholder imprintede gener, kan imprintingsykdom oppstå. Begge disse kromosomene inneholder en rekke imprintede gener. Paternell UPD(15) er en av årsakene til Angelman syndrom, en velkjent imprintingssykdom som medfører psykomotorisk utviklingshemming, mens paternell UPD(7) ikke er assosiert med noen kjent imprintingssykdom. Vi finner imidlertid ingen annen forklaring enn paternell UPD(7) på hans BWS-lignende symptomer, som for øvrig overlapper med det man ser hos pasienter med generell paternell UPD mosaisisme. Ved RNA dypsekvensering finner vi oppregulering av flere vekstrelaterte gener. Mest interessant er en betydelig oppregulering av et imprintet gen på kromosom 7 kalt *PEG10*, som også kan tenkes å ha ev betydning for vekst. En slik dobbel UPD er ikke rapporert tidligere, og vi presenterer også en hypotese på hvordan dette har oppstått.

Summary

Background: Beckwith-Wiedemann syndrome spectrum (BWSp) is the most common and probably the most complex imprinting disorder in humans. BWSp is caused by different molecular and epigenetic mechanisms involving the chromosome 11p15.5 subdomain and is associated with overgrowth, endocrine disturbances, congenital malformation, and an increased childhood cancer risk. We see many BWSp families in our clinical practice, but the three families described in this dissertation have been selected because of their unique features, atypical inheritance patterns, or novel genetic causes.

Objective: We aimed to explore each family's clinical characteristics and the underlying molecular defects and further explain the genotype-phenotype correlation to improve clinical diagnostics and follow-up of these patients.

Materials and Methods: Three families were ascertained in our outpatient clinic, and we performed clinical and molecular investigations and gave genetic counseling. We used Sanger sequencing to identify the causal variants in the families described in articles I and II. In article III, SNP array-based copy number analysis in the affected boy revealed double isodisomy. In the family in article I, we determined the methylation status of Imprinting Centre 1 (IC1) in the BWS locus by MS-MLPA (Methylation Specific-Multiplex Ligation-dependent Probe Amplification) and bisulphite conversion followed by both subclone Sanger sequencing and NGS (Next-Generation Sequencing) of CTCF (CCCTC binding factor) binding sites in IC1. We compared the degree of methylation between the generations and between individual CTCF binding sites. In articles II and III, we performed NGS-based RNA deep sequencing to decipher the different *CDKN1C* transcripts and study the expression of individual genes or gene sets. Trio-based whole-exome sequencing (WES) were performed in articles II and III to exclude other molecular causes of the phenotype.

Results: In the three-generations BWS-family described in article I, we found evidence for anticipation through the generations, with increased methylation of IC1 correlating with increased severity of the developmental disturbance. This epimutation was secondary to a previously described heterozygous variant in the

OCT binding site NCBI36:11:g.1979595T4C in IC1. In the family presented in article II, an inherited and complex delins-variant in *CDKN1C* ((NM_000076.2) c.822_826delinsGAGCTG) was detected. This variant probably induced concurrent gain-of-function and loss-of-function effects, which correlated with the mirror phenotypes of both growth restriction and IMAGe features, and overgrowth and BWSp features, both present in the same individual. In addition, this variant affected a hitherto not reported *CDKN1C* transcript with a different C-terminal reading frame, that might explain his developmental delay. In article III, we studied a baby boy with a clinical presentation of BWS, but without a molecular correlate. Here we described for the first time a double uniparental disomy (UPD) affecting two imprinted chromosomes: 7 and 15. This caused paternal isoUPD(7) and isoUPD(15), the latter explaining Angelman syndrome. We also present a hypothesis for how the double UPD arose. However, we did not identify a known molecular explanation for the boy's BSWp, a phenotype reminiscent of general paternal UPD mosaicism. We explored if the UPDs could induce a global imprinting defect, but this was not detected. However, RNA-sequencing detected upregulation beyond expectation (>2 fold) of the maternally imprinted gene *PEG10* located to 7q21.3. Possibly, *PEG10* overexpression could cause an overgrowth phenotype, but this remains to be proven.
Conclusions: This work broadens the phenotypic and molecular spectrum of BWS and highlights the importance of a precise molecular diagnosis for clinical follow-up and recurrence risk. We show that anticipation can also occur in imprinting disorders and hypothesize that the paternal and maternal IC1 alleles are treated differently in the gonads. In addition, we present a hitherto not described *CDKN1C* transcript which might have importance for brain function. The study also gives insight into the so-called imprinted gene network. We investigated how this specific double paternal UPD(7) and UPD(15) could cause BWSp and ended up with *PEG10* overexpression as the most likely mechanism. Intriguingly, the two small, imprinted genes that we have studied, *CDKN1C* and *PEG10*, both have multiple reading frames, which is rare in human genes.

List of Publications

Paper I:

Berland S, Appelback M, Bruland O, Beygo J, Buiting K, Mackay DJ, Temple KI, Houge G (2013): "*Evidence for anticipation in Beckwith-Wiedemann syndrome*", Eur J Hum Genet. 2013;21(12):1344-8. PMID: 23572028 (1)

Paper II:

Berland S, Haukanes BI, Juliusson PB, Houge G. (2019): "*Deep exploration of a CDKN1C mutation causing a mixture of Beckwith-Wiedemann and IMAGe syndromes revealed a novel transcript associated with developmental delay".* J Med Genet. 2022;59(2):155-64. PMID 33443097 (2)

Paper III:

Berland S, Rustad CF, Bentsen MHL, Wollen EJ, Turowski G, Johansson S, Houge G, Haukanes BI. (2021): "*Double paternal uniparental isodisomy 7 and 15 presenting with Beckwith-Wiedemann spectrum features*". Cold Spring Harb Mol Case Stud. 2021;7(6) PMID: 34615670 (3)

Abbreviations

5mC: 5-methylcytosine, DNA methylation on cytosine

AS: Angelman syndrome

BWS: Becwith-Wiedemann syndrome

BWSp: Beckwith-Wiedemann spectrum

CBS: See CTS

CGI: CpG island, a cluster of CpGs

CH_3: Methyl group

CMA: Chromosomal Microarray Analysis

CNV: Copy number variant

CpG: Cytosin-Guanin dinucleotides

CTCF: CCCTC binding factor, a transcriptional repressor encoded by the CTCF gene that binds to target the sequence element and blocks enhancer interaction

CTS: CTCF Target Site, also called CTCF binding site (CBS)

DMR: Differentially methylated region (often includes several DMS)

DMS: differentially methylated site

DNA: Deoxyribonucleic acid

Enhancer: DNA elements binding to proteins that increase the likelihood of gene transcription, often multiple enhancers per gene, and localised upstream, intronic or downstream up to 1 Mb from the gene

GOF: Gain of function

GOM: Gain of methylation

GWUPD: Genome-wide uniparental diploidy, same as uniparental diploidy.

h/iUPD mixed iso/heterodisomy

Het: Heterozygous

Hom: homozygous

hUPD heterodisomy, a subtype of UPD with two homologous but different chromosomes from one parent

IC: Imprinting centre, same as ICR

ICR: Imprinting control region

IG: intergenic

ILO: Isolated lateralized overgrowth

In cis: in the same allele

In trans: on the opposite allele, or affecting another gene

Insulator: Sequences that block the interaction between promoters and enhancers

IUGR: Intrauterine growth restriction

iUPD isodisomy, a subtype of UPD, with the inheritance of two copies of one parental chromosome

iUPD(15)pat: paternal uniparental isodisomy of chr 15

KOS: Kagami-Ogata syndrome

LOF: Loss of function

LOM: Loss of methylation

LOS: Large Offspring Syndrome, which is BWSp in ruminants

LQTS: long-QT syndrome

Mat: maternal

MEGs: maternally imprinted genes

MLPA: Multiplex Ligation-dependent Probe Amplification

MS-MLPA: Methylation-specific-MLPA

ncRNA: non-coding RNA

NGS: Next-generation sequencing

NMD: Nonsense-mediated mRNA decay

OCT variant: Short for variant in the OCT4/SOX2 binding site on IC1

OCT4: OCTamer binding transcription factor 4 = OCT3 = OCT3/4

Pat: Paternal

PCNA: Proliferating cell nuclear antigen (a domain in *CDKN1C*-gene)

PEGs: Paternally imprinted genes

Promoter: DNA sequence upstreams of genes, binding to DNA polymerase and transcription factors to initiate RNA transcription

PTC: Premature termination codon

PUD: Paternal uniparental diploidy. Same as GWpatUPD

PWS: Prader Willi syndrome

RNA: Ribonucleic acid

SCMC: Subcortical Maternal Complex (of the oocyte)

SGA: Small for gestational age

SNV: Single nucleotide variant

SOX/OCT motif = OCT binding site, binding site on DNA for SOX/OCT4 heterodimer, see also OCT variant

SRS: Silver-Russel Syndrome

TAD: Topologically Associating Domain

TS14: Temple syndrome

TSS: transcription start site

UPD: Uniparental disomi

UPD(15): uniparental disomy of chromosome 15

UPDmat: maternal UPD

WES: Whole-exome sequencing (by NGS)

WGS: Whole-genome sequencing (by NGS)

Contents

Introduction

1.1 Introduction to imprinting disorders

All cells in our body contain the same genome, but not all genes express RNA at the same level or simultaneously. Non-coding epigenetic marks on the DNA or the histones decide when and where the RNA is expressed and, in summary, can direct what the cell should be doing and when it should act (4). Epigenetics regulates gene expression by changes outside the actual DNA sequence. The most known epigenetic mechanisms are de/methylation on DNA (CpG dinucleotides, i.e., cytosines followed by a guanine) and modifications on histones (methylation/acetylations). Most epigenetic marks are dynamic and often challenging to interpret but usually induce local chromatin conformation changes or gene silencing through methylation on promotors or other differentially methylated regions (DMRs). In addition, DMRs can act as imprinting control regions or centres (ICs) that regulate imprinting patterns of nearby genes in cis (5) (6).

Genomic imprinting is a parent-of-origin-specific stable gene inactivation, leading to monoallelic gene expression or functional hemizygosity in diploid cells (7). Disruption of this imprinting mark and hence distortion of the monoallelic expression pattern will create an imprinting disorder. The imprinting mark is epigenetic and mainly involves DNA methylation, but histone modification and non-coding RNA also contribute. An imprinting disorder will display epigenetic changes ("epimutation") with or without an underlying genetic defect. Imprinting defects can affect the establishment, the erasure, or the maintenance of the imprinting mark. The imprinting marks are erased in the early germ cells, followed by a new mark according to the parental gender. This methylation mark of imprinted genes is maintained throughout that individual's lifetime and present permanently in almost all cells, making it easy to use diagnostically. Due to imprinting mechanisms, humans and other mammals depend on sexual reproduction (5).

Imprinting disorders constitute a rare but essential group of genetic disorders and affect pre- and postnatal growth, metabolism and feeding behaviour, endocrine disturbances like neonatal hypo-and hyperglycemia and precocious puberty, development and a cancer predisposition (8). Many imprinting disorders have overlapping phenotypes and a broad phenotypic spectrum, exemplified by Beckwith-Wiedemann syndrome. Due to genetic heterogeneity, mosaicism below the threshold for detection, and broad clinical spectrum with mild or atypical presentations, imprinting disorders are underdiagnosed and impossible to rule out by genetic testing. Imprinting disorders are caused by the dysregulation of imprinted genes which are monoallelically expressed in a parent-of-origin-specific manner, and either the maternal or the paternal allele are expressed, not both. Imprinted genes can be either protein-coding or non-coding RNAs (ncRNAs). ~ 270 candidate imprinted genes in humans are reported to date (www.geneimprint.com, last checked March 2022). This number most likely represents an overestimation, as recent studies can only confirm stringent imprint by allele-specific RNA-seq in tissues in the GTEx project and placenta samples for a subset of these. A more conservative estimate is that probably <50 human genes are indeed imprinted genes (9) (10). These genes avoid the second wave of imprinting marks erasure in the early zygote and retain the parental imprint (6). The epigenetic marks can be DNA methylation on cytosines followed by guanines (CpG dinucleotides), usually located in promotors and lead to silencing of RNA transcription.

1.1.1 Imprinting centres

Imprinted genes are typically organised in clusters of larger conserved domains that can be several megabases long (5). These clusters contain both paternally and maternally imprinted genes as well as non-imprinted genes and non-coding RNA, which is essential for gene regulation. These domains always contain a primary or germline differently methylated region (gDMR) including CpGs, called imprinting control regions or centres (ICs). ICs are always monoallelically methylated and can control the expression of imprinted cis genes within the locus by regulatory elements.

It is estimated that there are about 35 gDMRs in the human genome (6), in contrast to somatically or secondary sDMRs, which are more numerous. The DMRs are also characterised by histone marks that in the methylated DMR allele are indicative of closed chromatin, and in the unmethylated DMR allele of an open chromatin configuration. All but two ICs are in promoters and are maternally methylated. The methylated maternal allele will prohibit the expression of the regulating lncRNA responsible for inhibition of nearby genes. Thus, other genes within the locus on the maternal strand will be expressed. The situation is the opposite for the paternal allele with an unmethylated IC, which will permit the expression of lncRNA that in turn interferes with the expression of other nearby genes in cis (on the same strand) and silence them. A well-known example is the maternally methylated IC2 (*KCNQ1OT1*:TSS-DMR) in the Beckwith-Wiedemann syndrome locus, located in the promoter of *KCNQ1OT1* (TSS: transcription start site), see **Figure 1**, where the normal situation of IC2 is illustrated. ncRNA produced by the *KCNQ1OT1* gene from the unmethylated paternal allele will silence the growth repressor *CDKN1C* in cis and therefore allow growth. The methylated promoter on the maternal allele will suppress *KCNQ1OT1* ncRNA and regulate growth by allowing *CDKNC1* expression.

Figure 1: BWS IC2

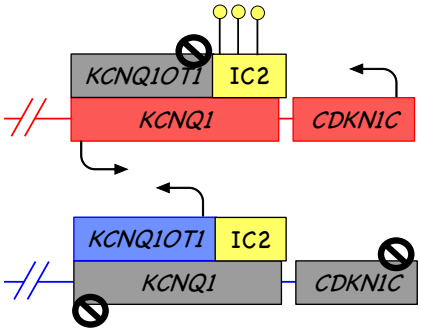

Overview of the human BWS IC2 on 11p15.5p15.4 in the centromeric domain, not drawn to scale. Red line: Maternal allele. Blue line: Paternal allele. Squares: Genes indicated by their names. Filled lollipops: DNA methylation. Crossed circle/grey genes: non-expressed genes. Arrows: Expressed genes and direction of transcription. IC2 is methylated on the maternal allele. The regulation in this domain involves lncRNA. KCNQ1OT1 (the antisense to KCNQ1), and in earlier literature called LIT1 (Long QT intronic transcript 1).

There are several disease mechanisms causing imprinting disorders. A well-known example is a maternal epimutation like Loss-of-Methylation (LOM) of BWS IC2, rendering a paternal methylation pattern on both strands, with *CDKN1C* dysregulation and, therefore, BWS. A maternal *CDKN1C* Loss-of-Function (LOF) variant on DNA level, although a normal methylation pattern, lead to an overlapping phenotype and BWS. The rare intergenic ICs are often paternally methylated and less CpG rich (11) (6). Intergenic (IG) ICs are located between genes and the regulation in this domain can be explained by an insulator model (**Figure 2).** Non-methylated maternal IC1 (*H19/IGF2*:IG-DMR) in the BWS locus allows CTCF binding to seven CTCF binding targets sites in IC1 called CTS 1-7, functioning as an insulator and blocking the interaction between a mutual enhancer and *IGF2*, and *H19* – but not *IGF2* – is expressed. The methylated paternal IC1 prevents CTCF binding to CTS and allows the enchancer to interact with *IGF2*, which is expressed. An epimutation involving Gain-of-Methylation (GOM) of the paternal IC1, with methylated pattern on both strands, lead to *IGF2* upregulation and BWS. The other known paternally methylated IG-type of IC is the *MEG3/DLK:*IG-DMR on chromosome 14q32.

Figure 2: BWS IC1

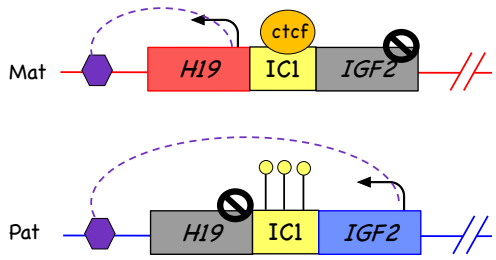

Overview of the human BWS Imprinting centre 1 on 11p15.5p15.4, not drawn to scale. CTCF is a transcription factor that regulates the 3D structure of chromatin. The purple hexagon represents a mutual enhancer of H19 and IGF2. The telomeric domain, controlled by IC1, is methylated on the paternal chromosome and includes the insulin-like growth factor 2 gene IGF2, which can promote growth, and the untranslated lncRNA H19.

The expression is regulated on the DNA level by methylation on CpG residues, non-coding RNAs (like H19 and antisense transcripts), 3D chromatin changes or histone modifications. Often, the imprinted genes are affected postzygotically and can be in a mosaic state with asymmetric growth.

Imprinted genes are usually tightly regulated, and imprinting is an important mode of regulation and can induce tissue- and time-specific imprinting. In addition, transcript-specific imprinting is also reported, for example, *PLAGL1* (6q24), where only transcripts expressed from promoter 1 (of a total of 4) are imprinted (7). *GNAS* locus on chromosome 20 is paternally imprinted (and maternally expressed) in the endocrine end-organs renal tubules, pituitary gland and gonads. Haploinsufficiency of the gene (i.e., a heterozygous LOF variant on either *GNAS* allele with 50% reduction of the constitutional gene expression) leads to a skeletal phenotype called Albright's hereditary osteodystrophy (AHO), with an autosomal dominant inheritance pattern (i.e. not imprinted). If this variant is maternally transmitted, there will be an additional phenotype with end-organ hormone resistance due to silencing (imprinting) of the paternal allele. This condition is traditionally called pseudo-hypoparathyroidism type 1a (PHP1a). An end-organ endocrine-only phenotype (PHP1b) can be caused when the *GNAS* is affected by an epimutation, as seen in sporadic LOM of the maternal allele or by paternal uniparental disomy (UPD) of chromosome 20. This affects *GNAS* expression in endocrine end-organs but not in skeletal tissue. Another example of an imprinting disorder is Angelman syndrome (15q11.2) involving the UBE3A gene, which is paternally imprinted (and maternally expressed) exclusively in the brain, while RNA expression of *UBE3A* in the blood is biallelic. Angelman syndrome is caused by loss of *UBE3A* brain expression, due to a maternal 15q11.2 microdeletion (including *UBE3A*), a pathogenic *UBE3A* variant on the maternal allele, or by paternal UPD(15).

The IC can direct downstream effects by establishing sDMRs, chromatin modification and TADs through CTCF-cohesins, lncRNA, and alternative splicing resulting in allele or tissue-specific isoforms (6).

1.2 Definition of epigenetics and how it differs from imprinting

Epigenetics ("over" genetics) study the mechanisms that cause a change in gene expression and can regulate the interaction between genes and the gene products and turn genes "on" and "off". However, these epigenetic modifications do not change the sequence of DNA. Furthermore, epimutations are permanent epigenetic alterations that affect the regulation of imprinted domains, as opposed to transient, late-onset or tissue-specific epigenetic changes that occur in somatically (or secondary) methylated DMRs during a lifetime.

1.2.1 DNA methylation

Epigenetic modification by DNA methylation in mammals refers to adding a methyl group (CH3, abbreviated Me) to the 5' position of the pyrimidine ring of a cytosine (C), one of the four bases of the DNA code. This forms a 5-methylcytosine (5mC) and occurs in non-stem cells in mammals at CpG dinucleotides, ("p" is shorthand for the phosphate-group that links two bases on the same strand). A cluster of CpGs is called a CGI (CpG island). The human genome contains about 28 000 CGIs and >20 million CpGs. This chemical Me-tag directly on the DNA does not change the DNA sequence but regulates gene expression. Correct repression of transcription is crucial for embryological development, normal somatic growth, and random X-inactivation in females. It is also important in controlling allelic gene expression in genomic imprinting. For example, epivariation in the genome resulting in different phenotypes has been known for more than 20 years when coat colour variation in mice was found to be caused by inherited changes in DNA methylation in the *Agouti* locus (12).

1.2.2 Histone modification

DNA wind itself around spools made of an octamer of histone proteins (H3, H4, H2A and H2B). Several modifications of the long tails or core of histones can alter the packaging of DNA, which is a weak acid. These chemical tags on histones can be, e.g. acetylation, methylation, phosphorylation and ubiquitination, leading to gene

expression repression or activation. For example, an open or permissive chromatin configuration will allow transcription associated with H3K4me3 (histone protein 3, trimethylation of lysine in position 4), while closed or repressive chromatin with H3K9me2, H3K9me3, H3K27Me3, and H4K20me3 will not. Such chromatin changes can be induced by gDMRs and sDMRs.

1.2.3 Gene regulation by RNA

The genome contains around 20 000 genes for RNA only, and most of these genes are thought to influence genome structure or regulate the expression of protein-coding genes. Such non-coding RNAs (ncRNA) are especially abundant in imprinted regions. Transcription of ncRNA can be a negative regulator of other genes. For example, the transcription of antisense RNA *UBE3A-ATS* will induce silencing of the paternal *UBE3A* allele in the brain, causing brain-restricted monoallelic expression. ncRNA can also be involved in gene regulation in trans, as demonstrated in the imprinted gene network, where lncRNA *IPW* (in the PWS locus on Chr 15) targets *EHMT2* (a histone methyltransferase) to the *MEG3* IC on Chr 14 and thereby regulate *MEG3* (13) .

gDMRs, including the ICs, will control the establishment of sDMRs within their respective loci. The gDMRs and sDMRs can induce allele-specific epigenetic marks by DNA methylation of promoters (see above), transcription factors, and lncRNA silencing of nearby genes in cis. MicroRNA (miRNA) and small nucleolar RNA (snoRNA) transcribed from IC loci might be involved in the post-transcriptional regulation of imprinted genes (6). In addition, alternative splicing can be directed by imprinting, exemplified by the *GNAS* locus and the different transcripts. Repeat expansions and 5'UTR variants can cause promoter hypermethylation events and gene inactivation.

Recent studies have shown that such epivariation is often secondary to rare genomic variants (SNPs or CNVs), for example affecting CTFC motifs (14), and is an important cause of both inherited disease and *de novo* cases of congenital disorders

(15). Epigenetic variations are less often inherited than expected from the Mendelian inheritance, which could indicate somatic mosaicism or a more extensive reset during gametogenesis.

1.2.4 Topologically associating domains (TADs)

Topologically associating domains (TADs) in the 3D genome are chromatin organised in loops formed by cohesion rings. Insulators together with CTCFs will act as boundaries of these loops and bind to specific surface sites on cohesion complexes. Such loops enable closer contact between genes and promoters/enhancer elements and regulate gene expression within the TAD. This is nicely illustrated for the BWS IC1 locus by others (6). The formation of a loop physically separates *IGF2* from its enhancer on the unmethylated maternal IC1 locus, whilst on the paternally methylated IC1, an alternative loop will allow connection between *IGF2* and the common *H19/IGF2* enhancer.

1.3 When does imprinting occur?

Imprinting marks (methylation at CpGs) last for one generation and will be reset for each offspring, disregardless of gender. Reprogramming occurs twice during reproduction: First, a less extensive wipe retaining imprinting regions (gDMRs) right after fertilisation but before implantation, and then a complete reset according to the gender in primordial germ cells in early gametogenesis, nicely reviewed by others (4, 6). Imprint erasure involves passive demethylation by less access to DNA methyltransferases (DNMT1 proteins) in the extensive reset of primordial germ cells. The erasure of methylation marks in imprinted regions takes longer than in the rest of the genome. This reset of the imprinted regions in the gonads is followed by reestablishment according to the gender by remethylation by *de novo* DNA methyltransferases and cofactors. This ensures gender-specific imprinted regions in the offspring. This active *de novo* methylation in germ cells is finished by birth in the primordial male germ cells but continues into adulthood in females. The methylation

of the DMRs is partly determined by the chromatin configuration, as the CGIs are marked by histone modifications that recruit *de novo* DNA methyltransferases (6).

Right after fertilisation, but before fusion of the male and female pronuclei, the epigenetic zygotic reprogramming takes place: A less extensive demethylation wipe, mostly studied in mice, with passive and slow demethylation of the maternal genome (involving replication dependant dilution and blocking of remethylation), and faster and active demethylation involving demethylating TET-enzymes of the paternal genome (6). Imprinted genes avoid the zygotic wave and keep the parental imprint as a memory in the form of DMRs under control by DNA elements like ICRs and insulators. Maternal effect oocyte factors involved in the subcortical maternal complex (SCMC) are essential for keeping gDMRs methylated and involved in the integrity of the early embryo. Defects of the SCMC factors can lead to loss of maternal imprint and hydatiform mole, infertility, and multilocus imprinting disorder (MLID). The zygotic gene activation continues in the maternal and paternal genome until the blastocyst stage, where the activation is completed, and the embryo starts transcribing its own RNA. Then, secondary tissue-specific imprinting starts (involving methylation, histone modification and more), regulating embryologic and placental development. The methylation marks on imprinted genes are kept constant and stable through mitosis and in different tissues with the help of maintenance DNA methyltransferases.

1.4 Overview of imprinting disorders in humans

Known imprinting disorders are localised to seven different chromosomal loci. They often have common features, and most of them affect growth and development. Many imprinted genes cluster around the same imprinting centre, and have a sister syndrome, often a mirror syndrome, according to the parental imprint. Below is a summary of their main characteristics. For more complete overviews, please see other publications (16) (17) (7) (8).

- **Chromosome 6** includes Transient neonatal diabetes mellitus type 1 (TNDM1) (OMIM #601410), caused by LOM of *PLAGL1*:alt-TSS-DMR, usually due to UPD(6)pat, paternal 6q24 duplications, sporadic epimutation/LOM or MLID. MLID can be caused by biallelic variants in *ZFP57*, encoding a transcriptional repressor important for maternal-effect methylation maintenance during early development. This causes increased expression of *PLAGL1* and *HYMAI*. Clinically this involves transient neonatal diabetes and increased risk of IUGR, macroglossia, omphalocele, other malformations, and diabetes type 2 in adulthood. Maternal UPD(6) with growth restriction has been reported, but the phenotype might be due to a low-level trisomy 6 mosaicism and not the UPD per se (18).

- **Chromosome 7** includes Silver Russel syndrome II (OMIM #618905) due to UPD(7)mat, but the causal gene(s) is not determined. See section 1.9 for details on SRS.

- **Chromosome 8** includes Birk-Barel syndrome (OMIM #612291) due to maternally inherited variants in *KCNK9* affecting p.Gly236 or p.Ala237.

- **Chromosome 11** includes Beckwith-Wiedemann syndrome due to either reduced *CDKN1C* expression (IC2 LOM, pathogenic *CDKN1C* variant, or MLID), *IGF2* overexpression due to IC1 GOM, or a combination (seen in mosaic segmental UPD(11)pat and paternal 11p15 duplications). See section 1.8 for more details. The sister syndrome Silver Russel syndrome 1 (OMIM #180860) is caused by reduced *IGF2* expression (IC1 LOM, MLID, LOF variants), or increased *CDKN1C* expression due to Gain-of-function (GOF) variants (also causing IMAGe syndrome), or a combination seen in UPD(7)mat or maternal 11p15 duplications.

- **Chromosome 14** includes Temple syndrome (TS14, OMIM #616222) due to LOM at *MEG3/DLK:*IG-DMR and the sDMR *MEG3*:TSS-DMR, caused by

UPD(14)mat, paternal 14q32.2 deletion, MLID or (sporadic) epimutations (19). TS14 presents with IUGR, short stature, relative macrocephaly, mild hypotonia, delayed development and early puberty. The TS phenotype can mimic both PWS (see below) and SRS. Deletions affecting only the paternal *DLK1* gene lead to isolated precocious puberty. The sister syndrome Kagami-Ogata syndrome (KOS, OMIM #608149) is due to GOM at the same DMRs, caused by UPD(14)pat, maternal 14q32.2 deletion, or (sporadic) epimutations (20). KOS include a skeletal phenotype, intrauterine overgrowth, placentomegaly and polyhydramnios, and can mimic BWS. They often have abdominal wall defects, and some present with overgrowth at birth, but growth restriction is more prominent later. Mild hypotonia and delayed development are common. There is also an increased risk of childhood tumours like hepatoblastoma, as in BWS (20)

- **Chromosome 15** includes Prader Willi syndrome (PWS, OMIM #176270) due to GOM of *SNURF*:TSS-DMR caused by paternal 15q11.2 deletions (*SNURF-SNRPN, SNORD116, MAGEL2* and more), UPD(15)mat and (sporadic) epimutations. Regarding the latter, small CNVs in the IC are reported. The phenotype includes severe neonatal hypotonia, initial feeding difficulties but later hyperphagia, short stature, hypogonadism, and mild intellectual disability, including psychiatric disorders. The sister syndrome Angelmann syndrome (AS, OMIM #105830) is caused by reduced *UBE3A* expression, caused by maternal 15q11.2 deletions, *UBE3A* pathogenic variants on the maternal allele, UPD(15)pat and (sporadic) epimutations (LOM of *SNURF*:TSS-DMR). Individuals with AS have milder hypotonia than in PWS, but have a more severely affected cognitive function. In addition, there are two other imprinted disorders in this region not caused by epimutations or UPD(15): Schaaf-Yang syndrome (OMIM #615547) due to paternal *MAGEL2* LOF variants and Central Precocious Puberty 2 (OMIM #615347) due to paternal LOF variants in *MKRN3*. Maternal duplications (and triplications) of

15q11.2 also cause neurodevelopmental phenotype (OMIM #608636), while reciprocal paternal duplications are considered phenotypic neutral.

- **Chromosome 20** includes pseudohypoparathyroidism type 1b (PHP1b, OMIM #603233) due to LOM of *GNAS A/B:*TSS-DMR, caused by sporadic epimutations, UPD(20)pat, and microdeletions within the locus, all causing loss of *Gsα* expression in endocrine tissues. Familial forms are common. The clinical spectrum includes short stature, PTH resistance and hypocalcemia, obesity, ectopic ossifications, and phenotypic overlap with PHP1a. See also section 1.1.1. The sister syndrome Mulchandani–Bhoj–Conlin syndrome (OMIM #617352) is phenotypically different and caused by UPD(20)mat, causing growth restriction and neonatal feeding difficulties (21). In addition, maternally inherited LOF variants in *GNAS* cause pseudohypoparathyroidism type 1a (PHP1a, OMIM #103580), while paternally inherited variant causes a milder phenotype called pseudopseudohypoparathyroidism (PPHP), or Albright's hereditary ostedystrophy (OMIM #612463). In addition, paternally inherited *GNAS* variants are also associated with progressive osseous heteroplasia (OMIM #166350).

1.5 Molecular mechanisms causing imprinting disorders

Imprinted genes have monoallelic gene expression; that is 50% of what is expected from a biallelically expressed gene. Having one instead of two expressed copies makes these genes particularly sensitive and altering this expression level (gain or loss) can cause disease. Abnormal expression of imprinted genes can happen from several mechanisms:

- **Pathogenic variant in an imprinted protein-coding gene:**
  A pathogenic (LOF or GOF) variant affecting the active allele of an imprinted gene leads to changes in gene expression. If the variant occurs on the inactive, non-expressed allele, this is phenotypically silent, and the gene expression remains intact (i.e., from the other allele only). The variant can be passed on to

the next generation, and depending on the transmitting gender, it can give rise to an affected child. This thesis includes an example of this in article II (2).

- **Structural rearrangements and CNVs:**
  A copy number variation (CNV), including an imprinted locus affecting the parentally expressed allele, can alter gene expression. A deletion/loss of the active unmethylated allele mimics a LOF variant with no gene expression. A duplication will lead to an increased expression level (two out of a total of three alleles will be expressed). Deletion of a non-expressed allele can be phenotypically silent and passed on to the next generation. This will cause disease if the sex of the parent changes in future generations. Such CNVs can be caused by structural chromosome rearrangements like translocations, small supernumerary marker chromosomes, and inversions.
- **Pathogenic variant in the imprinting centre (IC):**
  A pathogenic variant (SNV) or small CNV restricted to the IC, will lead to secondary epimutations (methylation defects) in the imprinted region. This can be heritable. This thesis includes an example of this in article I (1).
- **Epimutation:**
  A sporadic epimutation, without an underlying or primary DNA variant, alters the methylation in the IC.
- **Multilocus imprinting defects (MLID):**
  MLID, often comprising LOM or a mixture of GOM and LOM, occur at multiple, seemingly independent imprinted loci. MLID is most commonly due to biallelic variants in *ZFP57* (in children with TNDM and MLID) due to impaired postzygotic methylation maintenance of imprinted loci. Another important cause is maternal-effect biallelic or dominant-negative variants in a gene involved in SCMC with impaired DNA methylation establishment in the oocyte and LOM at imprinted loci postzygotically. Examples are *NLRP2/5/7, PADI6,* and *KHDC3L*. MLID due to a combination of UPD and sporadic hypomethylation of an unrelated imprinted locus are also reported (22) (23). For BWS individuals with IC2 LOM, up to 30%-50% might have MLID (24)

(25). MLID is more frequent among girls than boys with BWS. Uniparental diploidy (see below) has not been ruled out in most MLID-BWS individuals.

- **Uniparental disomy (UPD):**
  UPD occurs when both chromosomes originate from the same parent. This is usually a sporadic event (i.e. correction of an original trisomy or monosomy) and is not heritable. When UPD involves an imprinted chromosome, it leads to either zero or doubled expression level due to expression from none or both alleles. A postzygotic UPD caused by mitotic crossover can display a milder methylation defect due to somatic mosaicism. UPD is described in more detail below in section 1.5.1. This thesis includes an example of UPD in article III (3).
- **Uniparental diploidy:**
  Genome-wide UPD mosaicism, also called uniparental diploidy, presented in a female who is mosaic for a normal biparental and a paternal-only cell lineage (mosaic paternal uniparental diploidy/PUD or GWpatUPD) (26) (27) (28) (29) (30) (31) (32) (33) (34, 35) (36) (37) (38) (39) (40) (41) (42) (43). Male mosaics for uniparental diploidy are also reported (44) (36) (37) (45) (46). In affected females, the paternal lineage most often consists of a duplicated haploid (isodisomic) set originating from a single sperm. In affected males, two different sperms are involved in the origin of this mosaic condition. Even more rare, maternal uniparental diploidy (MUD or GWmatUPD) mosaicism with an SRS-like phenotype has been reported (47) (44) (48) (49) (50).

1.5.1 Uniparental disomy

Uniparental disomy (UPD) describes the situation where both copies of a pair of chromosomes in a euploid cell originate from the same parent (51). The meiotic and mitotic mechanisms in UPD are outlined in the figures below.

Figure 3: Normal meiosis I and II

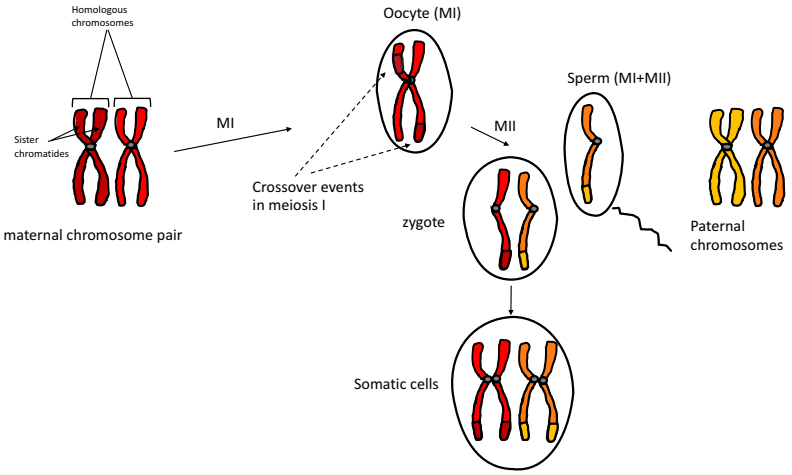

The parental chromosome homologues and the corresponding gametes in the maternal meiotic division and fertilization. To the left are the maternal (red) chromosomes, to the right the paternal (orange). Here, meiotic crossover and recombination has occurred in both chromosomal arms before the separation of the homologues in meiosis I (MI). Fertilization involves inclusion of the paternal chromatid into the oocyte, then the maternal chromatids separate in the second meiotic division (MII) before the pronuclei of the zygote fuses and mitotic divisions start. The somatic cells have two sister chromatids from both homologues. This brief illustration is simplified and omits steps and objects, including the polar bodies.

Figure 4: Trisomy rescue – MI

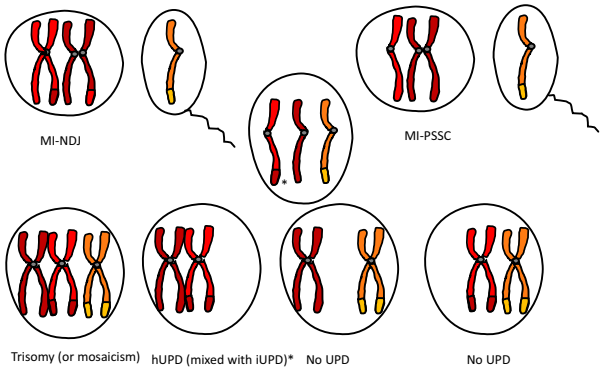

*Trisomy rescue after maternal MI error, where euploid restoration of the trisomic cell will have 1/3 risk of generation a UPD of heterodisomy type. Crossover in MI can give segments of isodisomy (excluding the centromere). To the left, a non-disjunction (NDJ) type of error occurred (missegregation of the homologues), and to the right, premature splitting and separation of the sister chromatids (PSSC). The * denotes that recombination and mixed iUPD is not relevant in PSSC.*

Figure 5: Trisomy rescue – MII

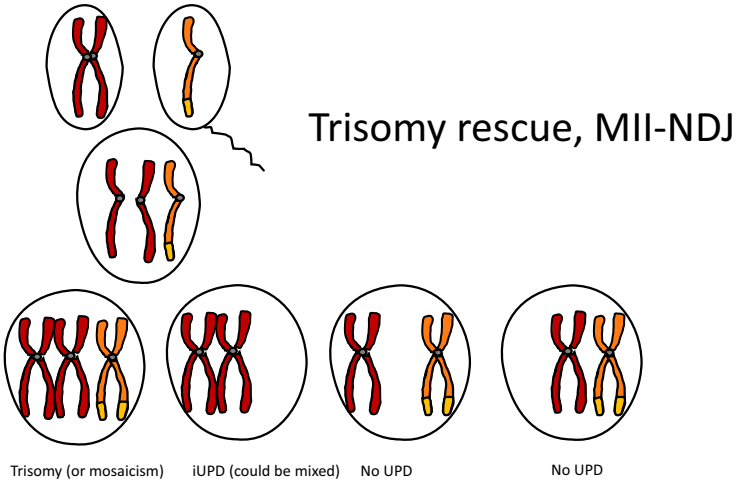

Trisomy rescue after maternal meiosis-II error, with isodisomic or mixed i/hUPD.

Figure 6: Trisomy rescue – MI-RS and MII error

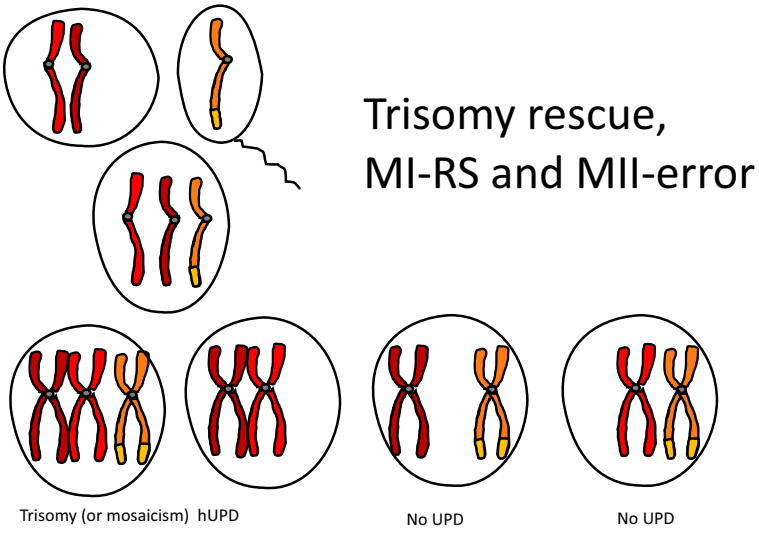

Reverse segregation (RS), involving segregation of the chromatids and not the chromosomes, to different oocytes in MI. Aneuploidy will occur if this is followed by an MII-RS missegregation (23% risk (52)) where the non-sister chromatids segregate, as illustrated.

Figure 7: a) Monosomy rescue b) Gamete complementation

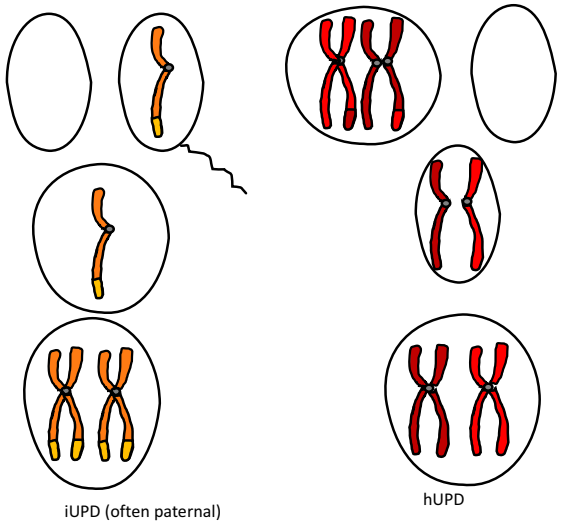

a) *Monosomy rescue (yellow chromosomes) after maternal error with a nullisomic ovum always result in isodisomy.*
b) *Complementation (red chormosomes) of a disomic and a nullisomic gamete is extremely rare, as it is preceded by both a maternal and paternal meiotic error.*

Figure 8: Postzygotic error

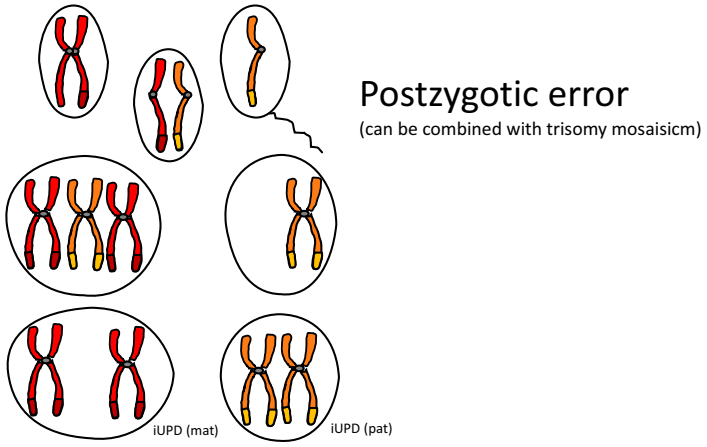

Postzygotic UPD formation after an initial euploid zygote, due to mitotic missegregation of the chromosomes, with trisomic and/or monosomic cell lines. A somatic endoduplication of the monosomy leads to iUPD, while the rescue of the trisomy results in iUPD in 50%.

UPD was first described in 1980 (53) but not clinically reported before 1988 (54). UPD can cause disease in multiple ways: Demasking a recessive disease where only one of the parents is a carrier; a secondary effect after the rescue of an original structural rearrangement or low-level trisomy; and finally due to imprinting defects. UPD has been reported in all chromosomes (see database of *Liehr T. 2021 Cases with uniparental disomy:* http://cs-tl.de/DB/CA/UPD/0-Start.html), but only UPD involving chromosomes 6, 7, 11, 14, 15 and 20 will give rise to an imprinting disorder, see Table 1.

Table 1: The consequence of UPD of imprinted chromosomes. The OMIM (Online Mendelian Inheritance of Man) morbid reference is noted if reported.

Chr	Paternal UPD	Maternal UPD
6	Transient neonatal diabetes mellitus 1 #601410	? (prenatal) growth restriction
7	?	Silver-Russel syndrome 2 #18905
11	Segmental/mosaic: Beckwith Wiedemann spectrum #130650	Silver-Russel syndrome 1 #180860
14	Kagami-Ogata syndrome #608149	Temple syndrome #616222
15	Angelman syndrome #105830	Prader-Willi syndrome #176270
20	Pseudohypoparathyroidism, type 1b #603233	Mulchandani–Bhoj–Conlin syndrome, #617352

A debate about whether UPD(16)mat also represent an imprinting disorder has been ongoing (55), but recent literature does not support this (56) (57) and proposes that the growth restriction in these individuals is probably caused by a low level of trisomy 16 mosaicism, often confined to placental tissue.

UPD could be paternal (UPDpat) or maternal (UPDmat) and can include low-level trisomy mosaicism, but also acquired somatically and in a specific tissue, for instance, as a driver in tumourigenesis. Constitutional UPD usually involves the whole chromosome, but segmental or partial mosaic UPDpat of 11p15.5 is common

in BWS. Although one could argue that such mosaicism should not be called UPD, but instead, a segmental loss of heterozygosity (57), the terminology of UPD will be used here. UPD can also involve the whole genome. A complete paternal diploid chromosome set (diandric zygote) gives rise to a non-viable complete molar pregnancy, also called an androgenetic hydatidiform mole. Such pregnancies do not involve any embryonic development but instead a trophoblastic disease of the placenta. A digynic zygote (fused haploid ova or retention of the second polar body, with no paternal contribution) will give rise to an ovarian teratoma without the development of placental tissue. On the other hand, a mosaic composition of both a genome-wide UPD and a biparental diploid chromosome set, called mosaic genome-wide UPD (mosGWUPD) or uniparental diploidy, are reported. Most individuals with GWUPD reported are of paternal origin, i.e., mos GWpatUPD, and often present with a BWS-like phenotype, but mosaic GWmatUPD has also been described, where the child's phenotype shows similarities to Silver-Russel Syndrome. For an overview of reported GWUPD, see the last bullet point in the former section.

UPD can also be subtyped into isodisomy (iUPD) and heterdisomy (hUPD), where isodisomy represents two identical chromosomes derived from the same grandparent, and heterodisomy two different homologous from the same pair. Full isodisomy is most often a result of monosomy rescue and paternal (**Figure 7a**), or a result of meiosis II (MII) error without recombination (almost always maternal) (**Figure 5**), or postzygotic origin from euploid gametes, where we expect equal rates of paternal and maternal iUPDs (**Figure 8**). Full heterodisomy results from MI error, involving non-disjunction (NDJ), premature splitting and separation of sister chromatids (PSSC), or reverse segregation (RS) in MI with missegregation in MII (**Figure 6)**. In RS, the aneuploidy arises in MII, but the centromeres are still heterodisomic due to the RS in MI. As most trisomies arise in MI, there will be two homologues, resulting in heterodisomy. If recombination and crossover occur, this will result in a mixed h/iUPD. For some chromosomes, in particular chromosome 15, complete heterodisomy (no recombination) is common (58). This has implications for the PWS detection rate on SNP-arrays, as isodisomic regions are needed for detection by

Chromosomal Microarray Analysis (CMA) screening (see section 1.5.3). For some UPDs, there is a predominance of maternal MI errors. The UPDs in PWS are most often a UPD(15)mat (~ 75%) due to such errors, while in Angelman syndromes, the UPD(15)pat often displays complete isodisomy due to postzygotic rescue after maternal meiotic errors, while paternal MI errors are rare. Most UPDs are secondary to aneuploidy or structural rearrangement, and sometimes a fraction of the original aberration is still present as low-level mosaicism, marker chromosomes or isochromosomes (51).

Postzygotic rearrangements like mitotic crossover result in segmental and mosaic UPDs. Segmental UPDs are usually isodisomies resulting from a rearrangement in a euploid zygote or a postzygotic rescue of partial aneuploidy (59), but segmental heterodisomy has been published (60). The incidence of constitutional whole-chromosome UPD was 1/2000 in a general population (61), while the incidence in clinical exomes was much higher; 0.31% (58). Half of these were mixed i/hUPDs, <40% complete isodisomies, of which 2/3% were of a paternal type and involved large chromosomes like Chr 1 and Chr 2. Isodisomies were less frequent in the general population (~ 25%) (61).

In the clinical exomes, about 15% were complete heterodisomies, only involving small, acrocentric chromosomes like Chr 15, but also 14, 16, 20 and 22 (62). There were only a few segmental UPDs, all terminal and isodisomies, with an incidence of about 1/2000 in this diagnostic cohort, and none of which included chromosome 11. This is probably explained by the clinical detection and pre-test pick-up rate of BWS and SRS. The incidence of segmental UPDs was found to be 1/173 (63), but the highest rate of UPD was found in discarded abnormal embryos after assisted reproduction techniques (3.7%) (64). The incidence of maternal UPDs was >70% both in the general populations and clinical exomes (61) (58).

1.5.2 Maternal meiosis and UPD formation

Paternally derived aneuploidies are extremely rare. A study of 5-day preimplantation (PGD)-blastomeres found paternal aneuploidy in <0.1% of affected embryos, which constituted <1% of all meiotic errors (65). The origins of UPDs are, therefore, mainly maternal meiosis and postzygotic.

Maternal trisomy due to segregation errors in the first meiotic division (MI) in the oocyte is a well-known cause of aneuploidy, and rescue of maternal MI errors is the most important contribution to UPD (57). MI-NDJ will also generate nullisomic oocytes, and PGD-blastomeres displayed equal proportions of trisomies and monosomies (0.113 vs 0.114), and the same was found for double trisomies and monosomies (both 0.019) (65). This indicated that monosomies are not less viable in very early embryos than trisomies. The likelihood of generating maternal trisomy and monosomy is comparable in all age groups and probably arises by the same mechanisms. This has implications for the formation of UPDs.

The study on blastomeres also confirmed that the risk of double monosomy or double trisomy is highly maternal age-dependent, and they found a risk of double monosomy at maternal age 40-42 years of 4-6% in both data and their mathematical model (66). They also show that the probability of an MII segregation error is ~2.2-fold increased after an initial MI error. The maternal age-effect in MII was also considerably stronger in an aneuploidy oocyte affected by an initial MI error than without (67). Chromosome 15, along with other acrocentric/short chromosomes 16, 21 and 22, have the highest rates of MI-aneuploidy and also present the strongest maternal age effect on PSSC and RS (67) (66) (65). MI-NDJ is probably less age-dependent than MI-PSSC and MI-RS, which are the major contributors to the age effect of aneuploidies and UPDs.

1.5.3 Molecular detection of UPD

As UPDs are copy number neutral, they can escape molecular detection. Methylation-sensitive analysis (either by screening or diagnostic testing) will detect UPD of imprinted chromosomes but not other UPDs. Standard chromosome analysis will also be inconclusive. If the CMA used for screening is an array-CGH (comparative genomic analysis), pure UPDs will be overlooked. An SNP-based CMA will detect iUPD but not complete hUPD. A mixed h/iUPD will often be detected, but with only one meiotic recombination and crossover, the SNP array will display only a single LCSH (Long contiguous stretches of homozygosity), also called runs of homozygosity (ROH) and loss of heterozygosity (LOH). This might escape recognition and be interpreted as identity by descent due to distantly related parents. In the case of consanguinity, where the SNP array of the child displays multiple LCSH on many chromosomes, a mixed UPD can be missed.

Given an individual diagnosed with PWS due to a CNV-neutral *SNURF*:TSS-DMR methylation aberration with a normal SNP-array without LSCH on chromosome 15, excluding a mixed or iUPD(15), traditionally, this was considered to represent a sporadic epimutation or a more rare a undisclosed IC defect. However, complete hUPD of small and often imprinted chromosomes like chromosomes 14, 15, 16, 20 and 22 are not that rare (62). hUPD(15)mat (PWS) is by far the most common hUPD, and is probably the most likely explanation in the example above. hUPD can be resolved by comparing SNPs and establishing the inheritance pattern in a trio analysis, either by WES, SNP-array by looking for opposite homozygosity (AA vs BB in the parents, and AA or BB in the child), or informative polymorphic microsatellites for the region of interest. Trio WES is clinically available as a screening tool for UPDs, as the SNVs in the UPD chromosome do not follow the expected mendelian inheritance pattern. However, this is not included as a bioinformatic option in all diagnostic labs, and relevant UPDs are likely to escape molecular detection unless clinically suspected. UPD screening usually demands parental samples (trios) or at least one parent (duos). However, with machine learning

tools, it was possible to identify UPDs in a large dataset with unlinked parental samples (61).

1.6 Inheritance pattern and recurrence risk in imprinting disorders

The recurrence risk for siblings or children of an affected individual with an imprinted disorder depends on the mechanism. As most imprinted disorders can arise from different and multiple causes, the recurrence risk will vary. For instance, BWS is most often caused by sporadic LOM of IC2, while TS14 is usually caused by UPD(14)mat, and PWS from *de novo* paternal 15q11.2 deletion or a UPD(15)mat, all with a very low or no recurrence risk. In contrast, up to 10% of Angelmann syndrome can be caused by maternally inherited *UBE3A* variants with a high recurrence risk, also introducing the risk of gonadal mosaicism. Familial cases presenting with a non-mendelian inheritance pattern can be difficult to recognize without taking an extended family history.
According to the classification above in section 1.5, guidance for recurrence risk is outlined below.

- **UPDs** are always *de novo* unless there is a predisposing factor for an imbalance that needs rescue, and recurrence of UPD has not been published. The risk of UPD due to a Robertsonian translocation is negligible (68).
- **Pathogenic variants in protein-coding imprinted genes** of interest, like *CDKN1C* in IMAGe and BWS or *UBE3A* in Angelman syndrome, are well-known examples of familial recurrence. The inheritance pattern is non-mendelian, with a 50% risk for (full/maternal) siblings if the mother is a carrier, while her carrier brother will not have affected children, only carriers. Another important factor in such SNVs is a risk of non-detected somatic germline or gonadal mosaicism in the parent.

- **A small CNV or SNV in the IC** are uncommon but important to detect. These infer a high recurrence risk of 50% in future pregnancies and for other family members, like pathogenic variants in imprinted genes, as seen above.
- **CNVs** can be inherited, i.e., CNVs not containing haploinsufficient protein coding genes, and be phenotypically silent on the non-expressed allele. This is particularly relevant for paternally inherited 15q11.2 duplications found in a healthy individual. A phenotypically silent duplication (or sometimes deletion) of a non-expressed gene can be passed on to the future generation and thus be inherited and will cause disease if the sex of the parent changes. Such CNV can often be detected by standard chromosome analysis, including FISH analysis of the parents (in case of balanced structural rearrangements) or CMA.
- **Sporadic epimutations** are often *de novo*, but the challenge is to exclude that the epimutation (LOM/GOM) is secondary to a primary underlying change in DNA.
- **MLID:** Apart for individuals with biallelic *ZFP57* variants in the proband with 25% recurrence risk in siblings, the recurrence risk in MLID is difficult to assess. In situations with severe biallelic maternal-effect variants causing recurrent biallelic complete hydatidiform moles with LOM at all maternal DMRs, the recurrence risk is 100% for the mother's offspring, regardless of the partner (69). In other situations, milder variants, incomplete penetrance, and mild and variable expression are reported in MLID (70). A dominant inheritance pattern is also reported (25).
- **Uniparental diploidy:** There is no increased recurrence risk in mosaic uniparental diploidy. Even though a slightly increased risk associated with maternal age can not be ruled out, recurrence has never been documented.

1.7 Beckwith-Wiedemann syndrome

Beckwith-Wiedemann syndrome (BWS) is an overgrowth syndrome first described in 1969 and involves a spectrum of clinical features (71, 72). BWS affects about 1/10 000 and is the most common imprinting disorder. The molecular aetiology is complex and involves an imprinted region on chromosome 11p15.5p15.4. The syndrome was redefined as Beckwith-Wiedemann spectrum (BWSp) by the international BWS consensus meeting in 2018 (73). Revised criteria were also introduced, and BWSp encompasses individuals fulfilling the BWSp criteria with a molecular finding (classical BWS, OMIM#130650), but also includes individuals with atypical presentations (fulfilling the score but without a molecular BWS diagnosis) and lastly, individuals not fulfilling the score (including isolated lateralised overgrowth (ILO), OMIM#235000) but where a molecular 11p15.5 anomaly is detected.

1.7.1 Clinical features

The clinical findings in BWSp include cardinal or common features like a large tongue (macroglossia), abdominal wall defects (exomphalos/omphalocele), and endocrine disturbances (hyperinsulinism), lateralised overgrowth, and Wilms tumour or nephroblastomatosis. I addition, histopathologic findings like cytomegaly of the adrenal cortex, pancreatic adenomatosis and placental mesenchymal dysplasia are also included in the cardinal features. Even though BWSp is considered an overgrowth syndrome, neonatal macrosomia/birth weight >2 SD is present in only about half of the affected individuals. Therefore, overgrowth is characterized as a suggestive and unspecific feature, along with ear pits/creases, large abdominal organs (liver, kidneys), milder abdominal defects including diastasis recti or umbilical hernia, transient neonatal hypoglycemia, and an increased risk of other childhood tumours. Global development is usually normal. There is a substantial variation in clinical presentation between different individuals, both among family members and especially in large cohorts. The latter can partly be explained by different molecular heterogeneity and mosaicism.

Other less frequent clinical findings in BWSp are not included in the scoring system due to lack of specificity, such as cleft palate, advanced bone age, polydactyly, typical face, genital abnormalities, inguinal hernias, congenital cardiac anomalies etc.

Table 2: BWSp Clinical score (73):

Cardinal features (2 points)	**Suggestive features (1 point per feature)**
Macroglossia	Birth weight >2 SD above the mean
Exomphalos	Facial naevus simplex
Lateralized overgrowth	Polyhydramnios and/or placentomegaly
Multifocal and/or bilateral Wilms tumour or nephroblastomatosis	Ear creased and/or pits
Hyperinsulinism (>one week and requiring escalated treatment)	Transient hypoglycaemia <1 week)
Pathology findings; Adrenal cortex cytomegaly, placental mesenchymal dysplasia or pancreatic adenomatosis	Typical BWSp tumours (neuroblastoma, rhabdomyosarcoma, unilateral Wilms, hepatoblastoma, adrenocortical carcinoma or pheochromocytoma)
	Nephromegaly and or hepatomegaly
	Umbilical hernia and/or diastasis recti

Score≥4: Classical BWS, molecular confirmation not needed for diagnosis, but for follow-up/counseling.
Score ≥2: Molecular testing indicated. If negative, further clinical evaluation, especially if there is a cardinal feature apart from isolated exomphalos present.
Score <2: Molecular testing not indicated.
A suggested flowchart for testing is published in the Consensus Statement (73).

1.7.2 Molecular background

BWS is caused by molecular anomalies in the BWS locus on chromosome 11p15.5p15.4. For an overview of the BWS locus, see section 1.1.1 and **Figures 2** (IC1) and **1** (IC2). This region involves several genes, many of which are imprinted. There are two domains, each controlled by an Imprinting Control Region or Imprinting Centre (IC), including a differentially methylated region (DMR). The

telomeric IC1 is officially called *H19/IGF2:IG-DMR* (HGVS nomenclature), but for simplicity, we use IC1.

IC1 is organised in two clusters containing one 450 bp A-repeat (with OCT4 octamer motifs), followed by three to four B-repeats. There are seven CTS (CpG repeats that are binding target sites for CTCF=CCCTC-binding factor), six of which are within B repeats, and the seventh CTS lies outside the imprinting centre, between A1 and the *H19* gene **(Figure 9).** *KCNQ1OT1:TSS-DMR* (IC2) is located centromeric to IC1 **.**

Figure 9: Details of BWS IC1

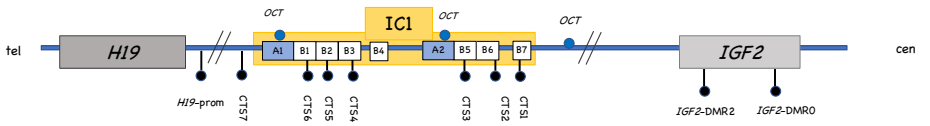

Schematic presentation of the paternal strand of the imprinted H19/IGF2 domain, including ~ 5 kb IC1, ~ 2 kb upstream of H19, IGF2 and relevant small differently methylated sites (DMS) on Chr. 11p15.5, not drawn to scale. The IC1 (yellow) contains two repeated blocks of A and B repeat elements and seven CTS. Six of the seven CTSs are located within the B-repeat elements. All 10 DMS (H19 prom, CTS1-7 and the two IGF2 DMRs) are methylated on the paternal allele and are illustrated with a filled lollipop. The IC1 includes six of these 10 DMS. The transcription factor OCT4 (encoded by POU5F1) form a heterodimer with SOX2 and binds to DNA in the OCT binding sites (blue circles) on the unmethylated maternal allele of IC1. If the target sites for binding proteins are mutated, the demethylation maintenance properties are lost, and the maternal IC will be methylated. An OCT binding site consists of a 59 bp element, including two SOX-OCT motifs and one OCT motif (74). Cohesins bind to OCT4, and by anchoring to OCT sites, loop formation can occur, forming topologically associated domains (TADs) (not shown).

The molecular anomalies in BWS can be classified into five large categories; IC2 LOM (**Figure 10**), IC1 GOM (**Figure 11**), UPD(11)pat (**Figure 12**), *CDKN1C* variants (**Figure 13**) and structural variants (**Figure 14**).

Figure 10: Loss-of-Methylation in Imprinting centre 2

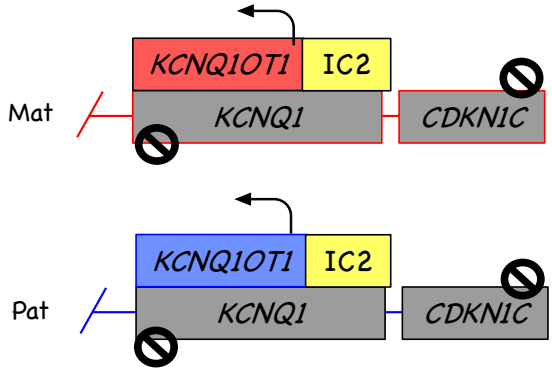

LOM of IC2. This is the most common anomaly in BWS, found in half of the individuals (50%) (73). Underlying CNVs/SNVs are uncommon, but MLID is seen in about 1/3 (73). This group is characterized by mosaicism, low tumour risk, high risk of exomphalos and abdominal wall defects. IC1 in the centromeric domain is unaffected, and not shown.

Figure 11: Gain-of-Methylation in Imprinting centre 1

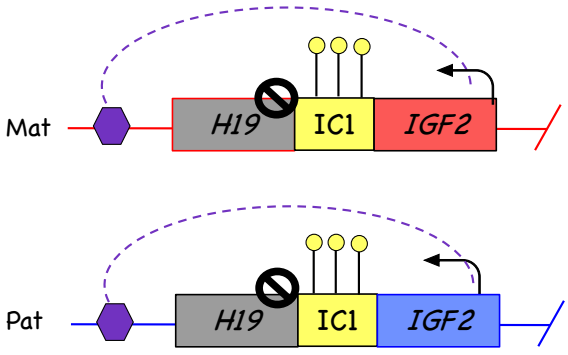

Isolated IC1 GOM is found in about 5-10%, and is associated with high tumour risk, low risk of exomphalos, and a considerable fraction carry an underlying CNV/SNV, implying an increased recurrence risk.

Figure 12: Paternal uniparental disomi 11p

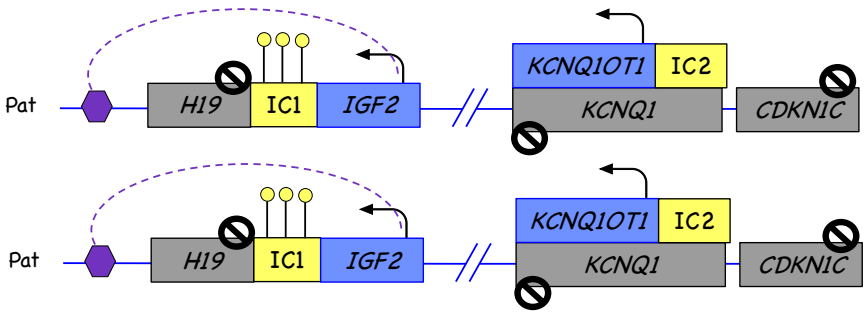

UPD(11)pat. Here a non-mosaic UPD is shown, but often somatic mosaicism is present, with a mixture of UPD(11)pat cells together with cells with normal methylation pattern. In UPD, the methylation patterns in both ICs are affected. UPD is found in 20% of the individuals with BWSp, who present with lateralized overgrowth, mosaicism, and high tumour risk. Exomphalos is rare, while hyperinsulinism is common. In about 10% of these individuals, there is an underlying mosaic GWpUPD/paternal unidiploidy (73).

Figure 13: Loss-of-function variant in *CDKN1C* gene

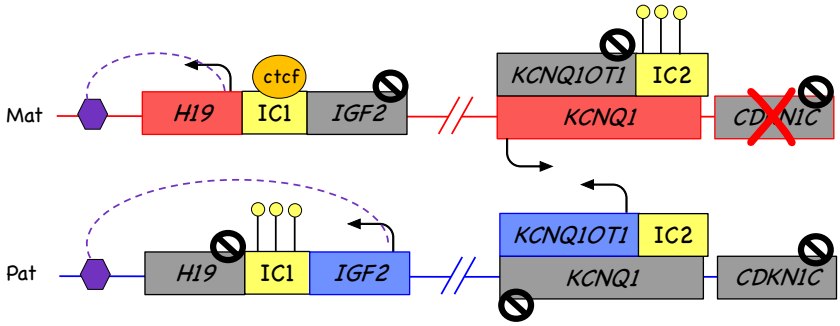

CDKN1C LOF variant on the maternal allele. This is found in about 8% of BWSp individuals but 40% of familial cases. Mosaicism is reported, and there is a high recurrence risk. These individuals present with low tumour risk, high risk of exomphalos and additional birth defects (genito-urinary, nevus flammeus, cleft palate etc) and pregnancy-related problems.

Figure 14: Structural variants of 11p15.5

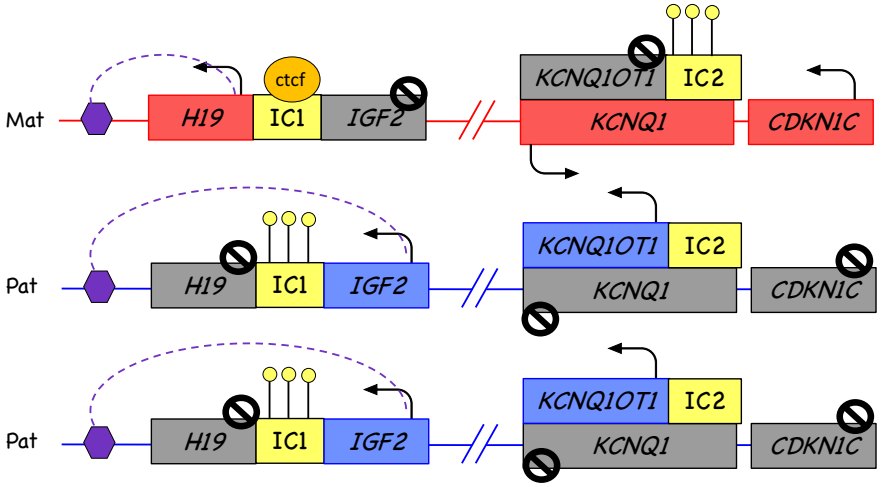

Structural variants of BWS locus, here represented by a duplication of the paternal Chr 11p15.5. This could be a small CNV (smaller than depicted here) but also involve larger chromosomal regions as in an unbalanced translocation. This is found in about 3% of the BWS individuals (73).

Molecularly diagnosed (by MS-MLPA, Methylation Specific-Multiplex Ligation-dependent Probe Amplification) BWS individuals, 41% show IC2 LOM, 27% have UPD(11)pat, and 11% have IC1 GOM (75). Regarding the latter, further high-density CNV and SNV studies of IC1 are warranted, as an underlying DNA aberration is found in 20% of isolated IC1 GOM (76) (77). However, the CNVs are often too small to be discovered by standard high-resolution CMA, either an IC1 microdeletion found in about 8% of IC1 GOM or small deletions and SNVs in the octamer-binding protein 4 (OCT4) or the transcription factor SOX2 bindings sites, found in about 12% of IC1 GOM (76) (78) (79) (80) (77). IC2 LOM comprises the largest subtype of BWS, and some authors imply an even higher incidence of IC2 LOM of up to 50-60% (73). IC2 is located in intron 10 of *KCNQ*1, which encodes a potassium channel involved in long-QT syndrome (LQTS). Underlying primary DNA variants in IC2 are extremely rare, and display complete LOM in contrast to sporadic IC2 methylation defects, which often show signs of mosaicism (81, 82). Such primary variants can be structural rearrangements and CNVs of *KCNQ1,* including IC2, but also *KCNQ1*-

CNVs and -SNVs outside IC2 in intron 10, which induce the termination of *KCN1Q1* transcription. Maternally inherited pathogenic variants lead to both BWS and LQTS in the child, while paternally inherited variants lead to LQTS only. This is explained by biallelic KCNQ1 expression in the heart (and adult tissue).

Pathogenic *CDKN1C* variants are found in 8% of the total group but up to 40% in familial cases (83). Missense variants in *CDKN1C* are associated with a less severe phenotype than complete LOF variants (84). Regarding (mosaic) segmental UPD(11)pat, up to 10% of these individuals had a paternal uniparental diploidy (PUD) background (26, 27) (75), and one study indicates an even higher risk of 7/36 (19%) (37). Chromosomal abnormalities (CNVs) like paternal duplication of the 11p15 region, or an unbalanced translocation, is present in less than 5% (75) and, dependent on the size of the duplication, will usually affect both DMRs. Up to 12% of individuals with IC2 LOM could be affected by a multilocus imprinting disturbance (MLID) (75). MLID could be due to biallelic maternal variants in SCMC genes like *NLRP2/5* affecting the subcortical complex of the oocyte. The mothers with biallelic variants are generally healthy but have an increased risk of affected pregnancy (hydatiform mole, infertility and miscarriages) and have children with BWSp and/or MLID, even though the BWS children themselves do not have biallelic variants. The clinical implication of recurrence of MLID is not fully elucidated. Females that carry SCMC variants induce LOM of maternal germline in the offspring, but not GOM or LOM of paternal germline. BWS in assisted reproductive technologies (ART) like *in vitro* fertilization might be increased 10-fold, particularly IC2 LOM (85). IC2 LOM is also enriched in monozygotic (female) twins, often clinically discordant for BWS, even though the lab test in blood and saliva shows methylation aberration in both (86).

In a few individuals with a BWS-like phenotype, other imprinting disorders have also been found: IC1-LOM (SRS pattern), MEG3-GOM (Kagami-Ogata syndrome), and UPD(6)pat (87). However, no molecular correlate is found in about 15% of patients.

This can be due to low-level mosaicism, molecular heterogeneity in BWSp, but also overlapping features with other syndromes.

1.7.3 Inheritance and recurrence risk

The recurrence risk in BWS depends on the molecular background. In mosaic genomic disorders like UPD and PUD, the recurrence risk for siblings and children is not higher than the risk in the general population. For individuals with BWS due to a *de novo* pathogenic *CDKN1C* variant, the risk for siblings is low but not negligible due to the risk of somatic or gonadal mosaicism. If the mother is a carrier of the variant, the recurrence risk is 50%. Only maternally inherited variants will cause BWS, while individuals with paternally inherited variants are asymptomatic carriers, as the gene is paternally imprinted. This implies that an affected male has a 50% risk of passing on the variant to his future children, but they will all be asymptomatic. His (maternal) siblings will have a 50% risk of inheriting the same variant as him.
In the case of a mosaic variant in the proband or carrier parent, the risk of children inheriting the variant can be as high as 50% depending on which tissue contains the variant and the mutation load. The mosaicism might not be detectable in DNA from blood, but in other tissues might be informative. There are also examples of asymptomatic parents with gonadal mosaicism, that is, that the variant is not present in the bloodline (or other tested tissue) but must be present in the gonads as the mother has two or more affected children with BWS. Testing of the ovaries is impossible.

For BWS individuals with epimutations, such as isolated LOM of IC2, this is usually a sporadic event, with a low recurrence risk both for siblings and children, but there are exceptions (82) (81). This is not true for individuals with seemingly isolated GOM of IC1 (hypermethylation). This is quite often (20%) caused by an IC defect, either a small CNV or an SNV (76) (80) (79). The risk of affected siblings can be as high as 50%, and the risk of passing on the variant allele to the offspring is also 50%, but only affected/carrier females will have affected children. Sequencing of ICs is not

available in the routine diagnostic for sporadic individuals, but high-resolution CNV calling is included in commercials MS-MLPA kits for BWS testing.

Individuals with mosaic UPD(11)pat will have combined partial GOM of IC1 and LOM of IC2. This picture can also be true for individuals with a partial trisomy 11p (either isolated or because of an unbalanced reciprocal translocation). The latter group will have a more severe syndromic presentation due to the underlying chromosomal aberration and not have their own children, but the recurrence risk for siblings can be high, depending on the size of the translocated elements. Most translocations are usually unique and with an individual risk, but there is one recurrent translocation involving 11p: t(4;11)(p16.2;p15.4), which has been reported in literature several times and also ascertained in a large family in our clinic. The risk of having a liveborn affected child with an unbalanced karyotype (der(4) t(4;11)(p16,2;p15.4) translocation is 15%, and hence a combined 4p- (Wolff-Hirschhorn syndrome) and BWS-phenotype if the balanced carrier parent is the father, and 4p- and SRS phenotype if the mother is a carrier (88). The molecular BWS anomaly in such cases is illustrated in **Figure 14**.

MLID can be caused by maternal factors, also called maternal-effect variants, with an unpredictable but high risk of affected children (up to 100%), as seen in mothers with a biallelic variant in *PADI6*, one of the genes involved in subcortical maternal complex (SCMC) with impaired DNA methylation establishment in the oocyte, and LOM at imprinted loci postzygotically. Mothers with biallelic variants in *NLRP7* can experience recurrent hydatiform moles, a phenotype mimicking non-mosaic genome-wide paternal uniparental diploidy. In MLID, the gender of the carrier parent is not relevant for the imprinting mechanism *per se* like in CNVs/SNVs/*CDKN1C* variants, but as many MLID is caused by mutations in genes involved in the SCMC affecting the oocyte, the mother is of particular interest also in these families.

1.7.4 *CDKN1C* overview

CDKN1C (cyclin-dependent kinase inhibitor IC) is a small paternally imprinted gene in IC2 in the BWS locus on chromosome 11p15. Only the methylated maternal *CDKN1C* allele is expressed, as unmethylated promoters on the paternal allele allow lncRNA expression of *KCNQ1OT1* that silence *CDKN1C* expression in cis (**Figure 1)**. The gene encodes p57kip2, localised in the nucleus, and functions as a negative regulator of growth and cell proliferation by inhibiting CDK complexes in the G1 phase by the N-terminal CDK inhibition domain (89). In addition, *CDKN1C* is implicated in the development of the embryo and tumourigenesis and is also expressed in neuronal tissues. The middle part of the protein-coding gene consists of a variable PAPA domain (proline-alanine repeat domain), and the C-terminal consists of a PCNA (proliferating cell nuclear antigen) binding motif involved in preventing DNA replication. For an overview, see (90). LOF variants (truncating and missense variants in the CDK domain) cause BWS, while reported IMAGe mutations are all missense variants located in the PCNA-binding motif. Even if these abrogate PCNA-binding, the pathogenicity in IMAGe is not by LOF as truncating mutations lacking PCNA lead to BWS, but by GOF, as IMAGe-mutants display increased protein stability leading to impaired cell cycle progression in vivo (91-93), although not found in earlier studies (94). The mechanism behind increased protein stability is not fully elucidated but might be due to impaired proteasome-mediated degradation caused by disruption of the putative C8 binding site (overlapping the PCNA-binding motif) of the 20S proteasome (92) or due to decreased ubiquitination of IMAGe mutants. *CDKN1C* variants associated with SRS probably bring about a milder functional effect than IMAGe-associating variants (91).

CDKN1C have multiple isoforms due to different UTR regions and multiple start sites, but also a transcript that uses a non-canonical reading frame for the last C-terminal region, including the PCNA motif. The use of such non-canonical reading frames is unusual for eukaryotic genes but is also seen in the “cousin” *CDKN2A*. Deep RNA analysis of *CDKN1C* has not been published, and a verification of all

described transcripts and predicted isoforms in humans are missing. *CDKN1C* is imprinted and predominantly maternally expressed, but with limited evidence and conflicting results for paternal RNA expression levels in humans (95) (96), from ~5% in fetal tissue and kidneys (97) to 20-50% in the blood (98).

1.7.5 Recommended follow-up and cancer risk

Cancer surveillance is recommended for (European) children with a risk of developing a malignant childhood tumour of at least 5% (73) (99). Depending on the molecular background, this is relevant for most BWSp individuals. Embryonal tumours occurred in almost 8% of BWS individuals with an established molecular diagnosis (99). There is not an increased risk of cancer in adult BWSp individuals. The risk is highest for the IC1 GOM group; with an overall risk of 23–28%; followed by UPD(11)pat with a risk of 14–16%, *CDKN1C* variants 7–9% and IC2 LOM 2–3% (100) (99). The risk is also substantial in individuals fulfilling the BWS criteria, but with no molecular diagnosis detectable, with 6.7% (100). A recent German population study found an overall risk for childhood (<15 ys) tumour of 4.4% in BWS, where the risk in the UPD(11)pat was the highest and reached 17.6% (101). Surprisingly, they did not find any cases of cancer within the 31 individuals with IC1 GOM, but this was not statistically significant. Even though differentiated screening protocols according to molecular subtypes have been proposed (100) (99), the BWS consensus group (2015) advised a similar screening protocol for the three subgroups with the highest risk, which involves abdominal ultrasound (screening for Wilms tumour) every three months until the age of 7 years (73). This protocol should also include individuals fulfilling the clinical BWS score but with no molecular cause, while individuals with BWS due to IC2 LOM will not be included in the screening.

For mosaic genome-wide paternal UPD (PUD), the cancer risk is higher and lasts into adulthood, and more comprehensive surveillance must be discussed (39) (43). Postema et al. postulated a tumour risk of 79% in this group, and many develop more than one tumour (39). As individuals with mosaic UPD(11)pat will present identical

to PUD on the standard MS-MLPA test, further studies must be performed to differentiate between these. Undisclosed PUD might have influenced the risk of cancer in the UPD(11)pat group.

Isolated lateralized overgrowth (ILO) (in earlier terms, hemihypertrophy or hemihyperplasia) is an asymmetric overgrowth of part of the body and a cardinal feature in BWSp. ILO and normal results on molecular BWS tests is not considered part of BWSp. However, cancer risk of 5% has been suggested, and these children have traditionally followed the same surveillance as children with BWSp. The cancer risk is based on the assumption that the risk is due to an undisclosed low-level mosaic UPD(11)pat, and even though the consensus group stated that specific studies of tumour risk were lacking, they advocate screening (73). A recent publication from the International Society of Pediatric Oncology advocates not including individuals with ILO in surveillance (102). Another study also showed no tumours in patients with ILO without fulfilling other criteria; and concluded that the risk of cancer in this group is low (103). This change is still under debate, but such intensive surveillance can probably be dismissed in this group with lateralized overgrowth without an additional point on the BWS score.

In BWSp, Wilms tumour (nephroblastoma) is the most common tumour, which has with high survival rate in the general population (90%). Wilms in BWS often has a better prognosis (less anaplastic and less metastatic) than in individuals without BWS, but bilateral and multifocal tumours are common. This will influence the choice of treatment. Other BWS-related tumours are hepatoblastoma, adrenal carcinoma, neuroblastic tumours, and rhabdomyoblastomas. Other considerations in the follow-up of BWSp patients are hypoglycemia due to hyperinsulinism, and this can last for several years in rare cases. Recently individuals with (complete) IC2 LOM and LQTS have been described (82) (81). The authors propose an echocardiogram in all BWS patients with IC2 LOM due to a small risk of *KCNQ1* haploinsufficiency as an underlying cause of familial BWS in some patients, but there is no consensus on this yet.

1.8 Overview of Silver Russel syndrome and IMAGe syndrome

Silver-Russel syndrome (SRS) is an imprinting disorder affecting about 1:30 000 to 1:100 000. Like BWSp, SRS shows a complex aetiology, including multiple imprinting loci and genes (104). Patients present with intrauterine and postnatal growth retardation but also severe feeding difficulties, hypoglycemia, asymmetry, mild global delay, early central puberty and insulin resistance, and often present with relative macrocephaly and prominent forehead. A scoring system is developed: NH-CSS, but the specificity is relatively low, and in the case of non-molecularly confirmed SRS diagnosis, the clinical diagnosis should only be used in patients scoring at least 4/6 in the NH-CSS, including both a relative macrocephaly and prominent forehead. Less specific but frequent findings (found in about half or more of the patients) are the triangular face, fith finger clinodactyly, shoulder dimples, micrognathia, excessive sweating, low muscle mass, low set and posteriorly rotated ears, high pitched voice, and prominent heels.
In about half of individuals with SRS, LOM of IC1 in 11p15.5 is found (**Figure 15)**.

Figure 15: IC1 LOM and SRS

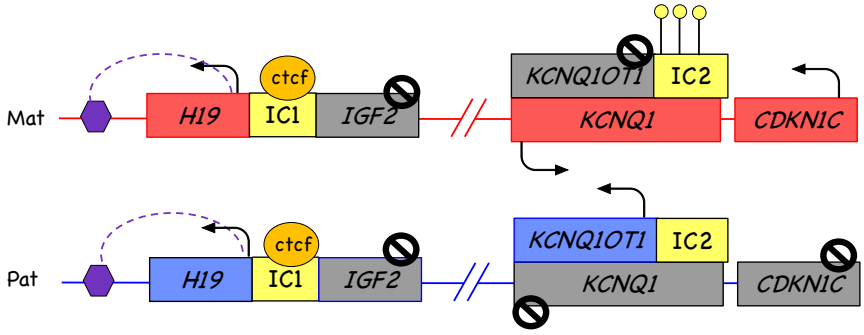

The most common cause of SRS is LOM of IC1 in the BWS locus on the paternal allele. The normal situation is shown in Figure 2.

An underlying microdeletion or SNV in IC1 is extremely rare (76). Less than 10% of SRS patients show UPD(7)mat, although the causal gene(s) for SRS in chromosome 7 is not elucidated. The molecular origin can be confirmed in about 60% of

individuals with SRS. CNVs are more prevalent in SRS than in BWS, and both large maternal 11p15.5 duplications and small duplications restricted to IC2 are reported. SNVs in imprinted genes are also found, with similar mechanisms to the maternally inherited *CDKN1C* GOF-variants and *IGF2* LOF-variants. Low-level mosaic UPD(11)mat is extremely rare in SRS and reported in four individuals only (105). This cause of SRS might be underestimated due to the technical difficulties in detecting mosaicism at such a low level. In addition, MLID and other overlapping imprinting disorders have been reported, including maternal UPD of chromosome 14 (Temple syndrome) and 20 (20), and mosaic maternal uniparental diploidy, and perhaps also maternal UPD(6). Maternal UPD(16) can also be found, but the molecular mechanism does not involve imprinting; rather, low-level mosaicism of trisomy 16. Surprisingly, discrepant molecular and clinical diagnoses have been reported in BWS and SRS individuals (106) (75).

IMAGe syndrome, caused by GOF variant in the PCNA-binding domain of *CDKN1C,* is partly overlapping the phenotype of SRS, and the acronym stands for Intrauterine growth restriction, Metaphyseal dysplasia, Adrenal hypoplasia congenita, and Genital abnormalities (107) (94). So far, less than 30 patients have been reported, and there are no consensus diagnostic criteria yet, as not all individuals have all features noted. Some have mildly delayed development, and there might be mildly dysmorphic facial features that are less described, like low-set ears and wide nasal bridge. One girl with IMAGe developed rhabdomyosarcoma, an embryological tumour earlier reported in BWS (108).

1.9 Molecular testing in imprinting disorders

The first obstacle is knowing when to suspect an imprinted disorder. Recognition of well-known and overlapping features such as disturbances of post-, pre- and perinatally growth, including the placenta, endocrinological dysfunction, childhood tumours, neurodevelopmental delay and hypotonia, and sometimes asymmetry or congenital anomalies. Molecular testing in imprinting disorders includes both methylation analysis and CNV analysis of the IC and corresponding loci. Commercial

assays such as MS-MLPA kit ME034 from MRC Holland investigate both methylation and CNVs and crudely covers most known imprinting disorders. In-house MS tests can also be very sensitive but must be combined with CNV analysis. For some disorders, further analysis, including screening for SNVs, is warranted, typically performed using Sanger sequencing or NGS of *CDKN1C*, *UBE3A*, *GNAS* etc. If a seemingly sporadic epimutation is found, including mosaicism, there can be reason to suspect an underlying genetic variant posing a risk of additional disease burden or an increased recurrence risk; an MLID, or a cytogenetic finding such as UPD. In these cases, further evaluation and investigations might be needed. To discriminate between a seemingly sporadic variant and UPD is relatively straight-forward in BWS, as UPD affects both imprinting centres, unlike sporadic LOM of IC2 or GOM of IC1, but in low-level mosaics, this distinction is challenging. In PWS, discrimination of sporadic LOM at *SNURF*:TSS-DMR and a UPD(15)mat can be crucial for establishing the recurrence risk, which is negligible in UPDs. Usually, maternal UPDs are heterodisomies due to trisomy rescue, but due to recombination, isodisomic regions are often present in the telomeric regions. Importantly though, UPD(15)mat often displays complete heterodisomy due to the lack of recombination (58). SNP arrays do not recognize these UPDs unless a haplotype analysis with a comparison with parental SNPs is performed. For other chromosomes, complete heterodisomies are extremely rare events. In case of a finding consistent with mosaic UPD(11)pat, investigation of possible mosaic PUD is warranted due to the risk of additional non-BWS features, risk of cancer and to establish the correct molecular diagnosis. This can be performed by SNP array looking for low-level mosaicism or by performing screening for MLID.

For individuals with sporadic BWS due to IC2 LOM without CNVs, further investigation is usually not recommended. As many as 1/3 of these individuals might have MLID, but clinical evaluation might be more informative than an MLID screening for sporadic cases. IC2 CNVs are rare, but small duplications involving IC2 are reported (109), as well as one deletion affecting nearby genes in the IC2 and induced IC2 LOM (110). For BWS individuals with IC1 GOM, 20% might have an

underlying CNV or SNV. MS-MLPA assay ME030 (commercial vendor name) will cover some of the small CNVs, but not SNVs. Sequencing of this region can be offered upon request at certain labs. Small deletions or SNVs in IC1 will cause BWS from a carrier mother but will be asymptomatic from a carrier father.
The risk must be carefully assessed in each case. In families with large duplications involving both domains and both ICs, there is a risk of BWS from a carrier father but SRS from a carrier mother. For smaller duplications or deletions, the outcome can be hard to predict, and BWS from a carrier mother was proposed for a small deletion inducing IC2 LOM. In contrast, a carrier father was predicted to have the risk of SRS in offspring as the deletion included *IGF2,* but also induced paternal *CDKN1C* expression due to lack of *KCNQ1OT1* despite normal methylation status in both domains (110).

1.10 Imprinted gene network

The imprinted gene network (IGN) provides an explanation for the suggested coregulation of imprinted genes. One possibility is that epigenetic misregulation of one locus can affect another imprinted locus in trans, or that the expression of the same or similar group of non-imprinted genes can be affected by different imprinted locus, explaining the clinical overlap between imprinted disorders. This has been shown for several imprinted genes in mice. One example in humans is that *IGF2* (on Chr 11) was found to be deregulated in TS14, explaining the clinical overlap with SRS. This is reviewed by others (111-113). So far, the IGN has not been confirmed in more extensive studies in humans.

1.11 Anticipation in human diseases – an overview

Anticipation describes an unusual non-mendelian inheritance pattern, where the disease strikes earlier and often also more severely in the succumbing generations than the previous. This concept was debated from its first report around 1850, rejected as a statistical artefact and explained by experimental errors like selection

bias or modifying a normal allele in trans (114). It took a long journey before final acceptance (115). Throughout the 1970s and later, other factors, including maternal factors, mitochondrial DNA, modifier genes and imprinting, were investigated but failed to fully explain the inheritance pattern in myotonic dystrophy and Huntington disease, and later the anomalous inheritance pattern called the Sherman paradox in families with fragile X syndrome. Höweler examined multiple families with myotonic dystrophy and rejected Penrose's statistical explanation (116), and finally, anticipation was accepted and incorporated into genetic textbooks after the discoveries of the molecular mechanism of these disorders in the early 1990ies. Anticipation is usually associated with a dynamic mutation such as a trinucleotide repeat expansion within a noncoding (or coding) segment that is unstable and can expand through meiosis and mitosis. Human diseased affected by anticipation are mainly of neurological origin and in addition to the aforementioned diseases, also include Kennedy disease (spinal and bulbar muscular atrophy) and several spinocerebellar ataxias. Dyskeratosis congenita represents another mechanism of anticipation, where impaired telomerase activity leads to declining telomere length in succumbing generations. Anticipation has not been reported in imprinting disorders before the work presented in this thesis.

2. Aims of the studies

Overall aim: To decipher the phenotypes and explore the molecular mechanisms in three families with novel presentations within the Beckwith-Wiedemann syndrome spectrum (BWSp).

2.1 Specific aims:

1) To investigate if the increased severity over generations in a BWS-family correlated with increased levels of IC1 methylation, compatible with anticipation (Article I).
2) To propose an explanation for this apparent anticipation (Article I).
3) To explain how a complex *CDKN1C* delins variant can have both gain-of-function and loss-of-function effects, causing a mixture of IMAGe and BWS-like features (Article II).
4) To find a potential link between this complex *CDKN1C* variant and developmental delay (Article II).
5) To explore how a double paternal uniparental isodisomy of chromosomes 7 and 15 can cause a BWSp like phenotype (Article III).

3. Methodology:

3.1 Data collection:

We ascertained the two families in articles I and II and the proband in article III through our diagnostic clinic. They were all clinically examined and were given genetic counseling. Routine lab analysis resulted in an initial molecular diagnosis in the three families, but there were more questions to be answered in all. The parents/guardians signed consent for further diagnostic studies and publication.

3.2 DNA analysis:

3.2.1 Sanger sequencing and NGS

Conventional Sanger sequencing of DNA in the region or gene in question was performed in both families in articles I and II, including Long-Range PCR to look for small CNVs in the IC1 in the family in article I. Furthermore, Next Generation Sequencing (NGS) of the whole exome filtered against the parents as reference (trio-analysis) was performed in articles II and III. Here, we looked for *de novo* variants in the proband, not present in either of the parents, and hemizygous X-linked and biallelic variants. In addition, we included inherited variants in a subset of genes, most of which were imprinted.

3.2.2 CNV analysis

Routine diagnostics in all three families involved a type of chromosomal microarray analysis called high-resolution SNP array (Cytoscan HD, Thermo Fischer), which includes both oligos revealing copy number variation (CNV) like deletions or gains, but also binary SNPs which in addition to CNVs can detect long continuous stretches of homozygosity (LCSH), also called runs of homozygosity (ROH). These stretches of homozygous SNPs can represent identity-by-descent where both haplotypes derive from a common ancestor, inferring that the parents must be related. Alternatively,

homozygosity is due to an ancient haplotype or uniparental disomy (UPD). Other types of chromosomal microarrays lacking SNPs will fail to detect UPDs. For MLPA-based CNV detection, see below.

3.2.3 Methylation analysis

MS-MLPA

To analyse the methylation pattern in the BWS locus in all three families, we performed a diagnostic test with a Methylation Specific-Multiplex Ligation-dependent Probe Amplification (MS-MLPA) analysis by MRC-Holland. MLPA analysis is a sensitive test that can detect small CNVs in a specific region defined by the probes. MLPA probes consist of two parts that must be perfectly hybridised to the sample DNA and then ligated, PCR-amplified and further analysed. An unperfect match to the sample will result in a lower relative peak and signal height of the specific probe (deletion). MS-MLPA involves the reaction described above for CNV detection and methylation analysis, including probes with a restriction site for the methylation-sensitive Hhal restriction endonuclease. The Hhal enzyme will digest unmethylated hybridised DNA, which will not be amplified, while methylated DNA will produce a signal. MS-MLPA was performed in the three families.

Bisulfite analysis

Bisulfite conversion of DNA will change unmethylated cytosine residues (“C”) in the DNA into Uracil (“U”). After amplification with bisulphite sequencing-specific PCR, U will be replaced by Thymine (“T). However, methylated cytosines will remain unchanged. Therefore, downstream assays can be performed to analyse the methylation load in CpG islands. In article I, a PCR product including 12 CpGs in a CpG island partly overlapping the MS-MLPA probes was subcloned, and Sanger sequenced. In this family, 6-8 subclones were analysed per individual. We also examined methylation patterns in two CTCF binding target sites in the IC1 CTS1 (B7) and CTS6 (B1), one on each side of the genomic IC1 variant, by NGS-based deep bisulfite sequencing with depth >1000 reads (117). After sequencing and alignment with the reference genome, we compared the DNA difference in CpGs in

the positive strands. The ratio of the reads C/(T+C) in the position will display the methylation ratio of that CpG.

3.2.4 Restriction enzymes and Sanger sequencing

In the family in article I, we wanted to investigate the parental origin of the IC1 variant. The variant is localised in an OCT binding site. If the variant was present on the methylated allele, it must be of paternal origin, and vice versa; an unmethylated allele must be of maternal origin. To differentiate, we first digested genomic DNA with the methylation-sensitive restriction enzyme McrBc, which digests away *methylated* DNA. After amplification and Sanger sequencing, we analysed the result and compared it with the result after undigested DNA sequencing. If the variant is apparently homozygous in digested DNA, the variant must be present on the unmethylated maternally inherited allele. Another restriction enzyme, BstUl, was also used when investigating an asymptomatic carrier. This enzyme will digest away *unmethylated* DNA. An apparently homozygous variant present after such predigestion indicates that the heterozygous variant originated from the methylated paternal allele.

3.2.5 Linkage analysis

In the family in article II, we wanted to investigate if the *de novo CDKN1C* variant in the grandfather arose on his maternal or paternal allele. DNA from his parents was available, so we chose to do a linkage analysis to analyse allele segregation by simple polymorphic tandem repeat markers (microsatellites, STR markers), localised inside and outside the *CDKN1C* gene. Finally, in article I, we compared the haplotype around the genomic position in IC1 in the Norwegian family to identify carriers of the variant. Also, we compared the haplotype to a French family harbouring the same variant to see if they shared a similar genetic background or a haplotype.

3.3 RNA-sequencing

We can analyse which genes are active and how much messenger RNA (mRNA) they transcribe with RNA-sequencing. This analysis also tells us what transcripts, or mRNA, are produced from a particular (mutated) allele. First, we prepared an RNA-sequencing library where total RNA was isolated and fragmented (<200-300 basepairs). Then, we converted the RNA fragments to stable double-stranded cDNA and added sequencer adapters. Lastly, we enriched the library by amplifying the DNA by PCR and sequenced by NGS. This raw data must be quality-checked before we fragment the reads and align these short reads to the reference genome. After normalising the data, we can count the number of reads per gene in each sample. For the boy in family III, we wanted to understand how the genetic aberration caused the phenotype. Active genes will produce (or transcribe) more mRNA than inactive genes, so by measuring the differences in transcription between fibroblast cells from the boy and other individuals, we can get an overview of which genes are dysregulated. Gene expression levels in big groups of genes were measured by counting the reads in the boy's mutated cells and compared to the gene expression levels in six controls. Here, we searched for fold changes in the expression of specific imprinted genes and particular gene sets. We aimed for a read depth of about 100 mill reads per sample for this general transcriptome analysis. For fold change computation and identifying differential gene expression, we used DESeq2. This involved adjustments and normalisation of data, and considered differences in library size, read count and content. Only genes fulfilling stringent data were further analysed.

In the family in article II, we were mainly interested in one gene: *CDKNC1C*, with presumably low and very variable levels of expression. Therefore, ultra-deep RNA sequencing was performed, i.e., about 250 million reads per sample. However, due to the complexity of the familial variant, no reads containing the variants were mapped to the reference genome, so we had to align the reads to a new reference that included the variant. In addition, we wanted to scrutinize and count all *CDKN1C* transcripts in this family to look for alternative transcripts and rare splicing events.

3.4 Ethical considerations

We obtained signed consents in all three families. As all analyses were performed in a diagnostic setting, approval from the Regional Ethics committee was not considered necessary (118).

4. Summary of results:

Below is a presentation of the main results from the three articles constituting this thesis.

4.1 Article I

Evidence for anticipation in Beckwith-Wiedemann syndrome

We investigated a family with six individuals in two generations affected with BWS. Unexpectedly, the symptoms were more severe in the 3rd than the 2nd generation, and the methylation levels also increased. We wanted to find the molecular cause of BWS in this family and to investigate if the gain of symptoms over generations correlated with increased levels of IC1 methylation, compatible with anticipation. Lastly, we aimed to propose an explanation for this apparent anticipation.

The younger individuals in the third generation presented with Wilms tumour, macroglossia demanding surgery, macrosomia, and one outcome of neonatal death. The three females in the second generation presented with tall stature, macrosomia at birth, and neonatal macroglossia. Some clinical details like possible pregnancy complications and placental size and histology were not reported in the article, and no validated scoring system was used. Therefore, we retrospectively set a BWSp score (73) (established in 2018) of 0 in the first asymptomatic generation, ≥ 2 in the 2nd generation and ≥ 5 in the 3rd generation. Methylation analysis by MS-MLPA confirmed a gain of methylation of IC1 in the BWS locus in all affected family members. However, the methylation level increased from average (0.48) in the asymptomatic 1st generation, to 0.70 and finally 0.85 in the 2nd and 3rd generation respectively, thus reflecting the clinical impression. We confirmed the increasing methylation of the same CpG island with bisulfite treatment and subclone sequencing. In contrast, deep NGS-based bisulfite analysis of two CTCF target binding sites (CTS) showed complete methylation in the 2nd generation in CTS1 (B7

repeat, on the *IGF2*-end of IC1). The NGS-based methylation pattern in CTS6 (B1 repeat, close to the CpG island) showed a methylation pattern similar to the results from MS-MLPA and bisulfite sequencing of the CpG island.
A heterozygous recurrent genomic variant in one of the OCT binding motifs of the IC1 was detected NCBI37:11:g.2023019T>C (= Chr11(GRCh37):g.2023019A>G), explaining the familial imprinting defect (76). We showed that the variant was present on the asymptomatic maternal grandmother's paternal allele with the use of a methylation-sensitive restriction enzyme in the analysis. Furthermore, we confirmed the carrier status in other family members by haplotype analysis and found that the variant arose on a different haplotype than in the previously published French family.

In the sumitted anticipation in BWS (1), *Table 1* displayed median values instead of mean values. This implied only minor changes and did not inflict the interpretation. A revised version of *Table 1* is with correct mean values is included below as Table 3:

Table 3: Mean degree of ICR1 methylation in the first, second and third generations with 95% confidence intervals (parentheses).

	MLPA analysis	Bisulphite sequencing
1. generation (n=2)	0.48 (0.45 – 0.51)	0.47 (0.39 – 0.55)
2. generation (n=3)	0.70 (0.65 – 0.75)	0.77 (0.74 – 0.80)
3. generation (n=3)	0.85 (0.82 – 0.88)	0.86 (0.81 – 0.91)

4.2 Article II

Deep exploration of a CDKN1C mutation causing a mixture of Beckwith-Wiedemann and IMAGe syndromes revealed a novel transcript associated with developmental delay.

Here we investigated a family with a young boy with a BWSp score of 8 ("classical" BWS), who also presented with additional features like growth restriction, postnatal

microcephaly, small kidneys, and dysmorphic features and delayed development, which are not included in BWSp. On the contrary, many of these additional features are present in mirror syndromes of BWS like IMAGe and SRS. Molecular diagnostic investigation for BWS detected a heterozygous, pathogenic delins variant in *CDKN1C* (NM_000076.2) c.822_826delinsGAGCTG, replacing five nucleotides with six others in the junction between exons 1 and 2 of the main isoform. Other diagnostic analyses (CMA, WES, MS-MLPA) were normal.

We aimed to determine how a delins in CDKN1C can have both gain-of-function and loss-of-function effects, causing a mixture of IMAGe and BWS features. We also wanted to explain his developmental delay.

Sanger sequencing confirmed that the delins-variant was heterozygous in the proband, his unaffected mother and maternal grandfather. However, the variant was not present in the grandfather's parents. Further analysis of different tissues clearly stated that the maternal grandfather was mosaic for the variant, and microsatellite analysis confirmed that the variant had occurred on his maternal allele and explained his mild BWS features. Due to the location of the indel at the intron-exon junction, we hypothesised that the variant induced frameshifting to a non-translated truncated transcript, with LOF explaining the BWS phenotype, but also that alternative splicing using different acceptor sites occurred. By investigating the sequence manually, we predicted different alternatives of the commonly used isoforms CDKN1C-A and -B, including truncated transcripts with a C-terminal being out-of-frame (alternative acceptor site I) and a non-truncated transcript including reported IMAGe-variants (alternative acceptor site II). Lastly, we speculated that the variant could affect an alternative transcript (*CDKN1C-201*) with a non-canonical reading frame in the last exon. This mutated alternative transcript would be in-frame, creating a mutated hybrid protein with a normal N-terminal like in alternative isoform D, while the C-terminal part would be of A/B type. In total, we proposed the possibility that the delins variant could give rise to four highly different mutant transcripts. Semi-quantitative real-time-PCR (qPCR) showed low expression of the *CDKN1C*

transcripts, especially in fibroblast-RNA. qPCR confirmed the presence of the alternative transcript *CDKN1C-201* in blood-RNA from all individuals but not in fibroblast-RNA, where only the common transcripts *CDKN1C-202/204* were found. We detected the mutated standard transcript in the affected males but not in the asymptomatic mother. We did not have qPCR-assays that enable us to investigate the existence of the mutated *CDKN1C-201* transcript, nor the transcripts derived from alternative acceptor sites.

We further analysed the transcripts by ultradeep RNAseq of the patient, the mother and the maternal grandfather. We included blood and fibroblast-derived RNA from the boy and blood-derived RNA only from the mother and grandfather. We had to map the reads to a custom-made reference genome which included the delins-variant, as no complex delins-reads were mapped to the initial analysis with the NCBI reference genome.

This analysis answered many of our questions:

- RNAseq confirmed the presence of three out of the four predicted mutant transcripts:
    - Mutated isoform A, consensus splice site (Asp274GlufsTer12)
    - Mutated isoform A, alternative acceptor site I (Asp274GlufsTer47)
    - Mutated Isoform D = hybrid D-A/B, 128aa
    - Not detected: Mutated isoform A, alternative acceptor site II (Asp274_276delinsAlaVal)
- The proportion of transcripts from the mutant allele was about 50% in the boy (higher in fibroblast than in blood), 25% in the mosaic grandfather and only 6% in the mother.
- Splice defects were confirmed, and alternative acceptor site I activation occurred in the boy's fibroblasts.
- The alternative transcript *CDKN1C-201* was documented in patients and controls and represented 16-42% of the total reads. However, the majority of

the delins reads involved this transcript, probably explained by the fact that most predicted mutant transcripts were expected to succumb to NMD.

4.3 Article III

Double paternal uniparental isodisomy 7 and 15 presenting with Beckwith-Wiedemann spectrum features

We investigated a newborn boy who presented with BWSp phenotype (placentomegaly, hyperinsulinism, enlarged viscera, hemangiomas, and earlobe creases) in addition to conjugated hyperbilirubinemia. He fulfilled the clinical BWSp score with five points, whereas four are required for the clinical diagnosis. However, we did not find a molecular BWS-correlate. On the contrary, SNP-array revealed iUPD(7) and iUPD(15) (**Figure 16)**. A double UPD has never been reported in patients before. This leads us to explore how a double paternal uniparental isodisomy of chromosomes 7 and 15 can cause a BWS-like phenotype. Further analysis with MS-MLPA confirmed a clinical suspicion that both iUPDs were of paternal origin.

Figure 16: Result from UPD analysis by SNP array

Chr. 11 (normal) Chr. 7 (iUPD) Chr. 15 (iUPD)

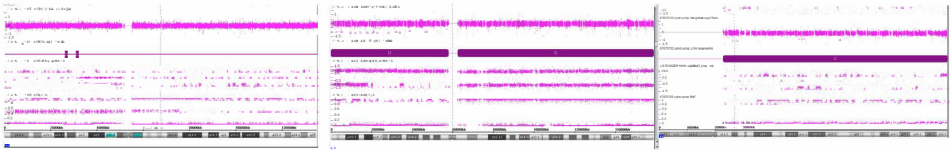

Screenshot of the result from SNP array, where we did not find any likely pathogenic CNVs. To the left, chromosome 11 shows normal results with no indication of UPD mosaicism in the BWS locus. The first row displays the copy number oligos aligned at Log2 ratio 0, interpreted as copy number neutral. In the middle and third row (allelic difference and BAF), the SNPs show normal distribution, with AA, AB and BB distributed as expected. In the middle frame, the result from chromosome 7 is presented. The first row shows normal CNV calling. Then there is an automatic LSCH interpretation from the software (the filled bar) due to the lack of a heterozygous AB line in rows 2 and 3, indicating LSCH of the whole chromosome due to iUPD. In the third frame, a similar result from the smaller acrocentric chromosome 15 displays iUPD.

This analysis also included DMRs on chromosomes 6 and 14, which showed a normal methylation pattern. UPD(15)pat implied a diagnosis of Angelman syndrome, which at the time was clinically unexpected. We confirmed the results in DNA from a separate blood sample and a skin biopsy. WES did not provide any additional findings that could explain his BWSp or hyperbilirubinaemia. Therefore, we hypothesized that the dysregulation of imprinted genes in chromosomes 7 and 15 could interfere with the expression of other imprinted genes on chromosome 11 or perhaps 14, in accordance with the theory of the imprinted gene network. We performed RNAseq on fibroblast-derived RNA normalized against six samples from another run to look for an unexpected expression pattern of imprinted genes. The paternally expressed *PEG10* (7q21) was overexpressed, with a six-fold versus an expected two-fold expression in UPD(7)pat. Among the up-regulated differently expressed genes (DEGs) in fibroblasts, about 1/10 referred to genes included in gene sets annotated in "growth" from geneontology.org.

In the submitted article on double UPDs (3), we wrongfully describe *PEG10* to be paternally imprinted. *PEG10* is a paternally expressed gene, and hence maternally imprinted. This mistake is made both in the abstract (page 1/14) and in the start of discussion (page 7/14, end of the first paragraph). A similar mistake is present in the end of the result section, (page 6/14) *"In summary, (…) highest FC where all paternally imprinted*", where "imprinted" should be replaced by "expressed". Alternatively, "paternally imprinted" should be replaced by "maternally imprinted".

5. Discussion

5.1 Methodological considerations

5.1.1 Article I – *Anticipation in BWS*

Clinical phenotyping:

The clinical details in the family presented in article I are incomplete, especially for the 2nd generation (the affected mothers). Some pregnancy-related details are omitted, and more details on the macroglossia and protruding abdomen in childhood would be interesting. In addition, the use of a scoring system should have been included. The consensus BWSp scoring system was not developed at the time of publication *(73),* but other scoring systems were available. A BWS score would have made it easier to compare the clinical scores across the generations and look for significant changes. More details would also make it easier to see if there were more numerous symptoms, not only a more severe presentation of the symptoms.

Methylation analysis:

As we wanted to investigate and validate increasing methylation levels, we chose three different methylation analyses:

- MS-MLPA, diagnostically easy-available MS-MLPA, is widely used in diagnostics and can be compared with the results from other centres.
- We chose subclone bisulfite sequencing as the first verification of the results from MS-MLPA. This analysis was readily available in-house without much extra cost. Our initial aim was to confirm the result from MS-MLPA, and we chose clones overlapping MS-MLPA.
- Finally, we chose NGS-bisulfite sequencing that gives multiple reads of the methylation depth from several differently methylated sites, not just surrounding the CGI described above. This analysis would gain additional information, not just verification.

Pyrosequencing with bisulphite sequencing could have been an alternative analysis, which can be used to detect small changes in methylation, including low-level mosaicism. Unfortunately, this technique demanded special equipment and adjustments at the laboratory and was unavailable for us.

To search for an underlying IC1 variant, we performed MLPA and CMA, while long-range PCR and Sanger sequencing of genomic DNA from one of the affected family members in the second generation were performed by a collaborating laboratory. We also tested the asymptomatic grandmother by Sanger sequencing when the familial variant was detected. However, we chose to do a haplotype analysis to confirm the segregation of the variant in the phenotype in other family members. We also used this information to easily compare with the French family's haplotype and investigate if the variant arose on different genetic backgrounds. Functional analysis of the variant had already been performed, which concluded that the variant affected OCT4/SOX2 binding, and further validation of this variant was not indicated (76).

Bisulfite sequencing:

Regarding the bisulfite sequencing of clones, there are some remarks. Firstly, the PCR product chosen for analysis partly overlaps the region already covered by the MS-MLPA probes, designed for confirmation only. Furthermore, the PCR product did not include the IC1 or the region surrounding the OCT binding site variant disclosed in the family. Secondly, the number of clones (6-8) obtained is low, and as only half of these alleles are expected to be maternal, a random skewing cannot be excluded. We considered five out of 12 data points noninformative as they were highly methylated in all samples, including controls (Article I, Suppl. Table 1). Two out of three controls (three individuals excluding the grandparents) had high methylation values also in the informative data points, not reflecting their normal phenotype, and had a normal MS-MLPA and NGS-based bisulfite result. Such a result can be regarded as a general challenge with the subcloning technique, and we cannot use the results alone to make conclusions.

Thirdly, we did not discriminate allele-specific (maternal or paternal) clones. This might have been possible by including an informative SNP. Hence, this analysis does

not prove that the maternal alleles are indeed hypermethylated (and not demethylated), as we cannot rule out a random overload of methylated paternal clones.

NGS-based bisulfite analysis

NGS-based bisulfite analysis addressed most of the remarks mentioned above. This analysis covered IC1 and the genomic region surrounding the OCT variant, and the ultra-deep sequencing addressed the second remark, although the identical CpGs were not analysed. We could potentially have missed a different methylation pattern in these two regions, but this is less likely as the methylation level in MLPA, bisulfite subclone sequencing, and NGS are consistent. Methylation analysis of additional CTSs (CTS1-7) might have answered if other CTSs showed a gradual increase in generations like CTS6 (B1), but the cost of such analyses was an obstacle. Finally, our analysis demonstrated an anticipation effect in the H19 promoter region and CTS6 (B1) but not in CTS1 (B7).

Control groups

We did not conduct a comparison with other (sporadic) IC1-GOM BWS patients and age-matched controls, as we did not have access to a relevant control group or inclusion of other patients in our case report.

5.1.2 Article II – *Three faces of CDKN1C*

The boy presented clinically with a very high suspicion of BWS, and we found the molecular cause through diagnostic work-up with MS-MLPA and Sanger sequencing of *CDKN1C*. CMA and trio WES analysis did not explain his non-BWSp features, so we decided to investigate the complex *CDKN1C* variant further. We suspected a combined LOF and GOF effect, the latter caused by different predicted splicing events. The *in silico* interpretation of the variant was crucial for generating hypotheses for further studies in this family. This extended interpretation included the BLAST search of the short, frameshifted C-terminal tail predicted from the use of alternative acceptor site I, which led us to the *CDKN1C-201* transcript.

Calculating the parental expression levels to analyse imprinting effect and leakage was challenging due to two main reasons: Variable nonsense-mediated mRNA decay (NMD), with a probable false low proportion of reads including premature termination codons (PTCs), and low mapping of the variable PAPA encoding region by RNA seq, with a positive selection of reads with the *CDKN1C-201* transcript not harbouring this region.

A new analysis with suppression of NMD before RNA-Seq might be more informative in our family, but due to technical reasons, we prefer comparing results only from the same RNA-seq flow cell.

We first conducted cDNA Sanger sequencing and qPCR to verify the different transcripts, but this was inadequate due to multiple hypothetical transcripts and low expression. Therefore, RNAseq to analyse *CDKN1C* transcripts was necessary. In planning this, we compared to already performed RNAseq in other patients and found a low expression of *CDKN1C*. This demanded a more costly ultra-deep RNAseq. As tissue-specific frameshifting was suspected, multiple tissued should preferably be investigated. However, RNA can be difficult to extract, and we did not have access to relevant control tissues. Therefore, we only included blood and fibroblast-derived RNA. Biopsies from other relevant tissues like the placenta, brain and adrenal cortex were not ethically justifiable nor possible to obtain. We also extracted RNA from urine by the “Urine Exfoliated Cell and Bacteria RNA Purification Kit, cat#2250” and “Urine Collection and preservation tubes” (Norgen Biotek Corp, Thorold, ON, Canada). Unfortunately, there was no urine-RNA yield from the patient or controls (not included in the article).

We also performed protein studies, and several Western blots on CDKN1C were made. We used lysates from fibroblasts from the patient and family members, healthy controls and HeLa-cells, HEC293 cells, and anonymous chorion villi, with two different Ab p57Kip2 antibodies with both N-terminal (EP2515Y, ab75974) and C-terminal (Cell signalling #2557) binding, all with inconclusive results with no or very

weak bands, and bands with variable sizes outside protocol standards. Cytosol/nuclear fractionation was also unsuccessful. This is probably due to a very low amount of CDKN1C expressed, and the results are not shown. Similar unsuccessful attempts at protein studies have been reported before (95). We did not include the protein studies in the published article.

The functional analysis performed by others has not always been straightforward, as technical analysis and interpretation are challenging. Due to low expression, functional analysis of the variant cannot be performed in fibroblast cells. Analysing HEC293-derived cell lines is possible, but there is no established test for GOF/LOF in this gene. *In vitro* analysis should also be interpreted with caution, exemplified by the analysis of R281X in HeLa-cells. This variant unexpectedly *stimulated* protein function in vitro, i.e. a GOF-effect. However, the patient had a classical BWS-phenotype without additional features apart from some missing teeth, and hence *in vivo* NMD and LOF was suspected (84). A similar analysis for our variant was therefore not initiated.

The alignment and mapping of reads, including the complex variant and variant calling, proved challenging in both NGS-based DNA and RNA sequencing. The variant was called as multiple single events in trio-based WES and was not even mapped to the reference genome in RNAseq. The latter is relevant for studies using RNAseq as a first-tier test when searching for potential splicing consequences in relevant tissues for an undisclosed variant.

5.1.3 Article III – *Double UPD*

The boy in article III presented with neonatal overgrowth and endocrine disturbances, and an imprinting disorder like BWS was immediately suspected. However, testing for BWS (MS-MLPA) was normal. UPDs can escape molecular detection, and the initial CMA performed in another hospital was based on an array CGH (comparative genomic analysis) that will only detect CNVs and not CNV-neutral UPDs. Alternative methods, such as SNP-based CMA, will detect iUPD and mixed UPD, visualised by single LCSH, but not total hUPD. Our clinical suspicion of an

imprinting disorder made us perform another CMA that indeed allowed us to detect the UPDs. It could be argued that a SNP-array as the first CMA screen in patients with developmental delay or congenital anomalies is more time-consuming and costly than array-CGH. However, we considered the higher resolution for CNVs and the ability to detect LSCH (UPD) clearly outweigh these concerns in clinical practice, particularly in the suspicion of an imprinting disorder.

The finding of a double UPD of two imprinted chromosomes warranted further investigations. For methylation analysis in the boy, we performed MS-MLPA involving both chromosomes 7 and 15 on blood-DNA as a diagnostic workup. After that, we confirmed the findings in separate samples from different tissues. His phenotype was reminiscent of a mosaic paternal uniparental diploidy (PUD), which would have had dramatic clinical consequences due to the increased risk of cancer. Therefore, we opted to completely rule this out, even though mosaic PUD was not found in SNP-array and is not readily compatible with non-mosaic iUPDs. A more global methylation analysis and a CMA and methylation analysis in skin biopsy were therefore performed with a normal result. The MS-MLPA analyses ruled out other known imprinting disorders affecting chromosomes 6, 11 and 14, in addition to 7 and 15. We did not test for methylation aberration on chromosome 20 as this was not clinically suspected.

An alternative analysis might have been the MS-MLPA kit ME034 (multilocus imprinting), which would include chromosomes 19 and 20, but this kit was not available in-house. We also considered a more comprehensive genome-wide methylation analysis. However, as all MS-MLPA was completely normal apart from chromosome 7 and 15, and the patient did not show asymmetry or other signs of mosaicism, this costly analysis was not indicated. In retrospect, results from commercially available platforms designed to analyse multiple imprinting defects across known genes and loci involved in imprinting disorders (like EpiSign) might be easily compared to other patients with isolated iUPD(7) and iUPD(15)pat in the future. However, this was beyond the scope of this study and was unlikely to have

clinical benefit for the boy. Instead, we were more interested in the clinical consequences of the imprinting defects and wanted to look at the transcription of genes by RNAseq.

For optimalisation of this analysis, several skin biopsies, separated in time and localisation, should have been drawn and analysed in the same run. Both ethical issues and costs were obstacles to this. It is likely impossible to obtain placenta biopsy for RNA extraction in clinical practice, even in similar patients. The need for additional healthy and age-matched controls is not that important. RNA from patients with isolated paternal iUPD(15) and (7) could have been included for comparison. However, such biopsies are extremely difficult to obtain, as even single iUPDs are rare. As a result, the normalisation of RNAseq data excluded many transcripts from further analysis, including *MEST,* one of the candidate genes implicated in growth restriction in UPD(7)mat.

5.2 Discussions of findings

5.2.1 Article I – *Anticipation in BWS*

Methylation analysis:

Based on studies of a three-generation family in article I, we have molecular data that support our clinical observation that anticipation can occur in Beckwith-Wiedemann syndrome. We detected the anticipation effect on methylation in DMS more proximal to H19: CTS6, CTS7 and the CpG island. In contrast, methylation at the CTS1 closest to the variant does not exhibit an anticipation effect but is fully hypermethylated already in the second generation with mild BWS symptoms. To the best of our knowledge, this is the first report of anticipation in an epigenetic syndrome. We recommend using the term “anticipation” only in families when there is both a clinical and molecular correlation. A “clinical anticipation” without a molecular correlate has been reported (117). Our finding is reinforced by a separate study on a three-generation-BWS family harbouring the same variant, reported as “methylation anticipation” by Sun et al. in 2019 (77). Here, additional DMSs were analysed

(CTS1-7, *IGF2*-DMR0, *IGF2*-DMR2). In CTS1-5, only a slightly increased degree of methylation of 2% from the second to the third generation occurred, and like our result, complete methylation of CTS1 already occurred in the second generation. The other DMSs (CTS6-7, IGF2-DMR0/2 and H19 promoter) analysed in their study showed a mild GOM in the second generation and high GOM in the third, which is also in accordance with our finding in CTS6, where the anticipation in methylation is found. They could not find an increased phenotypic severity across generations, as the second generations already had classical BWS. Clinical anticipation was therefore not confirmed. Furthermore, Sun et al. described a convex shape of the curves representing the methylation levels in the second generation in the OCT variant family, not found in controls nor individuals with sporadic IC-GOM. A larger GOM in DMSs closer to the variant than more distant DMSs explained the shape change in the overall methylation curve. A similar pattern was also documented in BWS individuals with other OCT variants but not in BWS individuals with sporadic IC1 GOM (119). Sun et al. included healthy children as controls in their study and confirmed a consistent normal methylation level of around 50% in all DMSs, although somewhat higher (about 60%) in CTS7. They also studied age-related somatic demethylation in IGF2-DMR0 and found a slight decline in methylation of about 5% from young children (median age 4) to adulthood (20-40 years) (77). However, the demethylation was stable from early childhood. If this age-related demethylation is comparable for all DMSs in this domain, an adjustment would probably not affect the result in our study, as two out of three of the individuals in the 3rd generation in article I were older than all the control children in that study. In families with BWS due to OCT variants in IC1, complete methylation of all DMSs will probably be reached within a few generations, and one generation might even be sufficient. However, this could depend on the variant, genetic background and external factors. For a female with seemingly sporadic BWS with complete GOM in IC1 due to an OCT variant, further (molecular) anticipation in the next generation (her children) is not possible. However, this implies that her mother must be carefully clinically examined, as she might have milder phenotypic features that escaped clinical attention, particularly in adulthood.

Hypothesis on impaired germline imprint switching

In contrast to random postzygotic remethylation explaining the apparent anticipation, our data suggest that the maternal and paternal *H19/IGF2* alleles are treated differently during oogenesis and that only the paternal alleles are subject to demethylation. Although this new idea needs animal studies for verification, it aligns with experimental studies on mouse embryonic carcinoma cell lines showing suppressed demethylation of *de novo* methylation upon OCT disruption (120). Furthermore, our hypothesis is the only in line with our data so far. We outline the hypothesis in **Figure 17**, an improved version of figure 4 in the published article (1). The different handling of the alleles regarding parental origin in the oocytes must be linked to the variant. A female with BWS due to sporadic IC1 hypermethylation will produce healthy offspring and, hence, the oocyte can demethylate both paternal and maternal hypermethylated alleles. Our hypothesis is hard to prove without additional families with identical or another tentative mild variant. However, the hypothesis could potentially have been dismissed by conflicting results in other family members, data from generation IV, or data on the paternal transmission of a partly hypermethylated OCT binding site variant allele.

The gonadal imprinting switch in the oocytes involves mainly the paternal allele demethylation but also the demethylation maintenance during post-fertilisation development, e.g., an ability to resist the *de novo* remethylation after implantation. Our hypothesis mainly involves a defect in the demethylation process in the gonads. Alternative explanations focusing on impaired maintenance of a hypomethylated maternal allele are not excluded. The OCT binding site variant impairs the ability to resist remethylation. Demethylation is used in establishing hypomethylation and maintenance due to the protection of somatic remethylation. OCT proteins are required for DNA demethylation, and the OCT motifs might function as methylation sensors and, in the hypermethylated state, will suppress demethylation activity in cis. Lack of OCT/SOX binding might have a double effect: Diminished demethylation in the gonads and impaired protection from remethylation (120).

Figure 17: Model of impaired germline imprint switching by BWS IC1 OCT variant

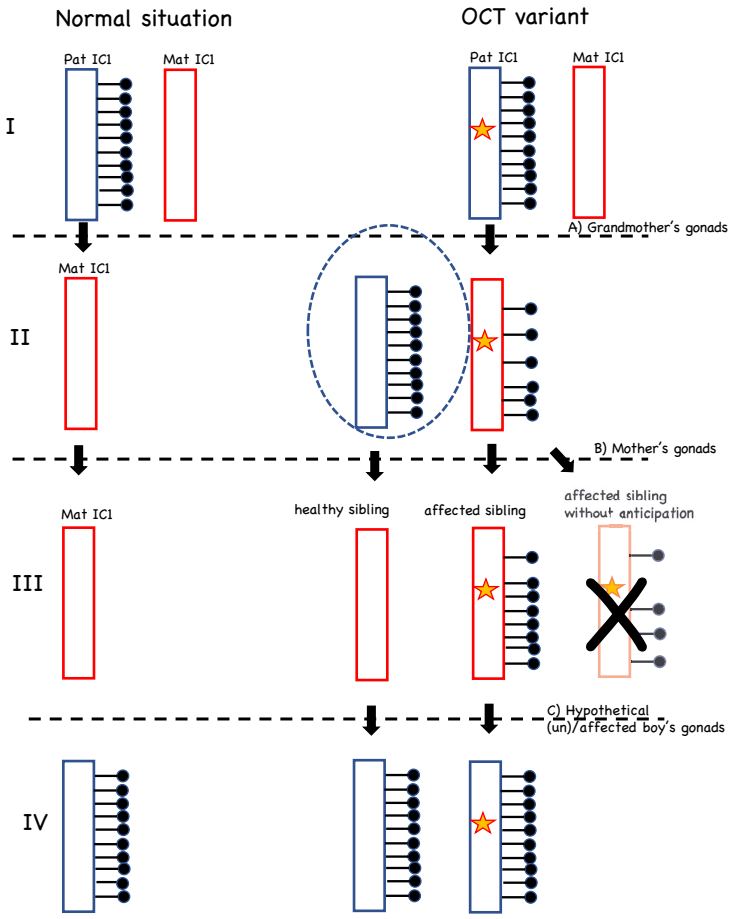

The methylation status of IC1 allele upon grandmaternal, maternal and hypothetical son's transmission, resulting in generation II, III and a hypothetical IV. The normal situation is shown to the left, OCT (binding site) variant (star) family to the right. After maternal and paternal transmission, the alleles are outlined in red and blue, respectively. In generation II, a normally methylated paternally inherited allele is shown in the open blue circle, omitted for simplicity in others. In the gonads, the imprinting marks are erased, and new marks are established. After implantation, remethylation according to the parental origin of the IC1 allele in cis occurs. The OCT variant results in incomplete demethylation and perhaps reduced somatic remethylation resistance upon maternal transmission in A). Further demethylation of the maternal allele was not seen in B), neither active demethylation as seen in A), nor unchanged (or mild, sporadic de or remethylation) as seen in the shaded alternative covered by an X in B) was found. This suggests that only paternal alleles can be demethylated in the maternal gonads. Transmission through an (un)affected male C) resulting in complete remethylation of the paternal allele (healthy offspring).

However, a recent study showed that SOX2 is a so-called super pioneer transcription factor, able to overcome repressive epigenetic marks like methylation (121). SOX2 binding accompanied by OCT4 binding inhibits DNMT1-dependent methylation maintenance during replication leading to passive demethylation. In our family, diminished SOX/OCT binding increased remethylation, placing the main pathomechanism as a postimplantation methylation defect, not related to the gonadal switch (74, 121). This is reinforced by a recent function study on different OCT binding site variants in the A2 repeat in the human IC1 transfected into a P19 cell system, including the variant in article I. They confirmed that the variants indeed disrupted postzygotic maintenance of hypomethylation by suppressing induction of demethylation (74). The variant in our family was associated with more DNA demethylation residual activity than others, confirming our *in-silico* assumptions that this substitution might be milder. Probably, the demethylation suppression is limited to the nearby CTSs, explaining the completely demethylated CTS7 in the 2nd generation in our family and the "curves" found by others. However, whether or how these variants affect demethylation in the gonads is still unknown.

This implies that the anticipation effect (in DMSs further away from the variant) is difficult to explain by suppressed demethylation maintenance and must involve stochastic methylation events and other transacting factors. However, we find it unlikely that our observations on anticipation combined with the recent publication are entirely due to random differences in protection from secondary remethylation (77), so our hypothesis is not rejected.

The genomic variant found in this family is recurrent (76) (77) and localised in the OCT4/SOX2 binding site in the A2 repeat. Other studies have also reported recurrent pathogenic IC1 variants, most of which are localised in A2, although one SNV was in the putative consensus site for SOX2 in B3. IC1 SNVs were also found to be more common than CNVs (12% vs 8%) (119). Extensive IC1 analysis is recommended in IC1 GOM individuals (73), but analysis restricted to the A2 repeat might be sufficient in most families.

5.2.2 Article II – *Three faces of CDKN1C*

RNAseq confirmed all the predicted transcripts but one; the mutated transcript due to the use of alternative acceptor site II. This transcript might not be expressed if this alternative acceptor site is not used. Alternatively, a tissue-specific expression could be present even though not detected in our limited blood- and fibroblast-derived RNA analysis. A low expression beyond our detection is not excluded, but the clinical significance of deficient expression is unknown.
The C-terminal delins variant in the *CDKN1C* family is predicted to cause both a LOF and a GOF. In addition, a novel isoform D is mutated with an unknown function and consequence. We further discuss the potential consequences of each of the mutant transcripts detected. Finally, we decipher the phenotype in the boy into three different "faces", linked to three different transcripts.

In our article, we argue that

- The mutated isoform from the main transcripts using the canonical splice sites, Asp274GlufsTer12, causes LOF and BWS.
- The use of alternative acceptor site I of the main transcripts, Asp274GlufsTer47, can lead to IMAGe features. However, the non-confirmed mutated product from the alternative acceptor site II, Asp274_276delinsAlaVal, would make a better candidate.
- The mutated hybrid isoform from the novel isoform D with C-terminus from the common A/B isoforms might cause a neurodevelopmental phenotype.

In our article, we postulated an NLS (N-terminal localisation signal) KRKR immediately terminal to the delins variant, and we were speculating whether an expressed mutant transcript missing this signal would induce pathogenicity. Another, even more, N-terminal NLS has later been confirmed as a nuclear localisation signal and that a missense change inferring a substituting of the last amino acid residue in CDKN1C – R316W– which is also the last arginine in the NLS: RKRLR. The variant was identified in an individual with BWS, and the mutated protein delocalised from the nucleus to cytosol in transfected HEK293 cells (90). This might have implications

for our patient, as the expressed mutated (hybrid) isoform D now includes a new nuclear signal that was not present in wt-isoform D. The localisation of wt-isoform D is so far unknown, but there is a possibility that the hybrid mutant will mislocalise into the nucleus.

Transcripts including stop codons and nonsense-mediated decay

As the truncated transcript from the consensus splice site encoding p.Asp274GlufsTer12 (common isoform A/B) was present in both blood and fibroblasts, NMD had not cleared all transcripts with premature stop codons (PCT) at the point of analysis. This was unexpected since the PCT was located ~ 100 nucleotides upstream of the last exon-exon boundary, more than 50 nucleotides that usually is required to trigger NMD (122). The predicted C-terminally truncated protein product contains substitutions of the same amino acids reported in IMAGe individuals, even though the substitutions do not produce reported IMAGe-variants. If the transcript is not degraded, this product might also have IMAGe-like effects. The RNA product from alternative acceptor site II would include known IMAGe substitutions a not be terminated. However, we did not detect this transcript in our analysis.

Non-degraded C-terminally truncated transcripts could potentially exhibit a toxic effect causing developmental delay, but we consider another candidate for the neurodevelopmental phenotype; the mutant *CDKN1C-201–* with an expression of ~ 40% of all *CDKN1C*-transcripts in the family. Expression level in the healthy control was lower, only 15.6%. The lower reading depth could partly explain the less accurate result in control. However, NMD partly clearing mutated non-*CDKN1C-201*-transcripts with PCTs will increase this family's relative amount of mutated *CDKN1C-201*. In contrast to wt*CDKN1C-201*, mutated *CDKN1C-201* uses the canonical reading frame, resulting in a potentially mislocalised fusion product that may cause the unusual features in the boy.

The reason why RNA analysis verified a high level of RNA suspected to succumb to NMD must be addressed elsewhere. However, NMD is known to be variable and

could also be an *in vitro* artefact. Furthermore, NMD-suppression in general for this gene is highly unlikely, as no other reported individuals with truncating *CDKN1C* variants in the same region have a developmental delay or IMAGe-phenotype (84).

Parental expression and paternal leakage

Due to variable NMD, the calculation of the relative transcripts can be misleading when measuring the degree of imprinting. Mutated *CDKN1C-201* is not predicted to degrade at the RNA level. Looking at this transcript only, the mother expressed 1/14=7.1% delins *CDKN1C-201* of total *CDKN1C-201,* grandfather 16/32=50.0% and the boy 30/44=68.2% (blood) and 50/81=61.2% (fibroblasts), demonstrating a slightly higher degree of imprinting than the other mutated *CDKN1C* transcripts, shown in figure 5 in the article. RNA-Seq does not map in the repetitive PAPA region. This means that any attempt to quantify transcripts, including the PAPA region, must be interpreted cautiously. The RNAseq read depth in the GC-rich PAPA region is almost zero (see Suppl 4 in article III). Other transcripts lacking PAPA (e.g. *CDKN1C-201*) could be wrongfully reported as more abundant. This reduces opportunities for detailed and unbiased parental expression analysis.

Our data add to earlier reports of maternal expression in humans (with ~1/20 expression of the presumed paternal allele) in all tissues examined but the fetal brain (94), where biparental and higher expression was found. Later studies have reported maternal only expression in fibroblasts (95), biallelic expression verified with RT-PCR in blood and kidney in 3/5 BWS individuals (96), and lastly, a leaky (20-50%) paternal allele in lymphoblasts verified with RNA-seq, although statistically insignificant due to the low number of reads (98). Mouse studies have shown that *external factors can challenge Cdkn1c-imprinting* in utero, i.e., maternal protein deprivation causes lifelong de-repression of the paternal allele (123), which indicates that imprinting status and expression are not static. Deep RNA-Seq analysis of several informative *CDKN1C* families with a substitution not predicted to undergo NMD could elucidate the degree of imprinting in blood and fibroblasts. However, since the *CDKN1C*-output from RNAseq was so variable and often low, such an

analysis would probably only give uncertain estimates, and only the ratios in that tissue could be determined, which probably does not reflect, e.g., brain tissue. Our findings imply that analysis of expression of different isoforms, including isoform D (A6NK88) in the brain, is clinically more relevant.

Neurodevelopmental phenotype

We argue that the *CDKN1C-201* is highly expressed in the brain, that the protein is involved in cortical development, and that a mild neurological phenotype is overrepresented in BWS. Additional studies supporting CDKN1Cs involvement in brain development are also published: A constitutive knockout of Cdkn1c in mice drives brain overgrowth (macrocephaly and cortical hyperplasia), while brain-specific conditional deletion drives cortical thinning, nonobstructive hydrocephalus and cerebellar malformation (124, 125). A conditional heterozygous Cdkn1c-flox mat induced microcephaly and severely affected cKO mice (126). The translation into human brain development is missing, but this remains to see whether isoform D might explain some of this in the future.

CDKN1C and other members of the CIP/KIP proteins are intrinsically disorganised proteins (IDPs), meaning that there is no rigid 3D conformation, and parts of the proteins are disorganised and often fold after binding to partners (127). The C-terminal region (Cyclin-dependent kinase inhibitor domain) is highly disorganised, a feature of functional promiscuity and plasticity, probably partly by post-translational modification like phosphorylation. *CDKN1C* has three phosphosites; Ser28 (conserved), Ser282 and Thr310. This implies that the complexity of the gene and its isoforms are even more significant than anticipated, making it more challenging to generate hypotheses on the functions of this gene, both wildtype and mutated isoforms.

Loss-of-Function versus Gain-of-Function effects

A combination of IMAGe and BWS in the same individual has not been described before. However, phenotypic elements from both gene activation and loss-of-function in the same individual were reported as early as 1994, with a fascinating example

involving another imprinted gene, *GNAS*, encoding the G-protein Gsa-subunit. Two unrelated boys harbouring A366S-substitutions presented with testotoxicosis and precocious puberty due to constitutive activation in the cool testis, but the thermolabile Gsa led to Gs-degradation at body temperature and hence LOF and clinically pseudohypoparathyroidism 1a (128). Other examples of both GOF and LOF effects from the same variant are *RET*-mutations leading to oncogenic activation and clinically Multiple Endocrine Neoplasia type 2A but also Hirschsprung disease (129), *FNLA*-mutations with both activating (Oto-palato-digital spectrum disorders) and inactivating (periventricular nodular heterotopia) effects (130) (131) (132), a *GDF5*-mutation causing simultaneous multiple synostoses and brachydactyly (133) and lastly an *SMCHD1*-variant present in both Bosma arhinia microphthalmia syndrome and facioscapulohumeral muscular dystrophy type 2, and likewise one individual with both conditions (134).

5.2.3 Article III – *Double UPD*

We verified a clinically suspected imprinting disorder in the newborn boy, but the result of double UPD was surprising and novel. For patients fulfilling the BWS score but having an alternative explanation for the findings, the diagnosis of BWSp is inappropriate. An example of this can be Kagami-Ogatas syndrome (KOS), i.e. due to UPD(14)pat, that can present with cardinal BWSp features including omphalocele and macroglossia, and suggestive features like polyhydramnios/placentomegaly, childhood tumour with hepatoblastoma, and macrosomia, possibly achieving BWSp score of eight points (19). Neither UPD(7)pat or UPD(15)pat (Angelmann syndrome) are associated with BWSp, but we still think the double UPD is the explanation for his phenotype. Trio WES was performed to look for alternative genetic disorders, particularly recessive diseases demasked by the UPDs, but this analysis was also negative within the limitations of the test.

A series of similar patients or a molecular correlate is needed to prove an association between BWSp phenotype and the double paternal UPDs (or UPD(7) alone).
A literature search indicated that UPD(7)pat could be implicated in overgrowth and placentomegaly, but the data is not convincing. However, the more specific and rare

feature of conjugated hyperbilirubinaemia with or without hyperinsulinism seemed to be enriched in patients with paternal UPD, including UPD(7) and mosaic PUD, and screening for imprinting disorder can be implemented in patients with unexplained conjugated hyperbilirubinemia. However, our analysis did not find a suitable candidate gene for this phenotype among the differentially expressed genes.

The RNAseq did not support the Imprinting Gene Network (IGN) as there were no other imprinted genes outside chromosomes 7 and 15 among the differently expressed genes fulfilling the criteria. On the other hand, we did find upregulation of several genes, of which 1/10 were enriched in gene sets involved in growth. Moreover, *PEG10* on chromosome 7 was found to be upregulated beyond expectation (sixfold vs doubling of the expression level). *PEG10* is also among 11 confirmed genes imprinted in the placenta and, therefore, an excellent candidate to be implicated in neonatal and placental overgrowth (10). Only 11 genes were confirmed to be imprinted in the placenta, including three genes in the BWS loci on 11p15.5 (*IGF2, H19* and *PHLDA2),* three in chromosome 14q32.2 (*DLK1, RTL1, MEG3*), and two in chromosome 7q (*PEG10, MEST)*, and no genes originating from chromosome 15. Another recent study on a BWSp correlate in ruminants, Large Offspring Syndrome (LOS), which overlapping symptoms and molecular background, found upregulation of *PEG10* in affected LOS animals, supporting the role of *PEG10* in BWS (135).

PEG10 upregulation should preferably have been confirmed in another experiment with a different tissue sample from the boy. However, even if this were confirmed, the cause of the upregulation would still be unknown. Are the upregulations solely due to the UPD(7)pat, the combination with UPD(15)pat, or perhaps a combination of any two paternal UPDs, or another undisclosed molecular cause? *PEG10* expression should be compared in other UPD and PUD patients. In summary, we suspect the UPDs to cause the BWSp, perhaps due to *PEG10* overexpression, but the molecular links remain to be proven.

Interestingly, our articles highlight two genes with a remarkable and rare feature; both *PEG10* (paternally expressed) and *CDKN1C* (maternally expressed) have alternative reading frames giving rise to very different protein isoforms. *PEG10* has a longer isoform PEG10-RF1/2 translated from -1 ribosomal frameshifting from the same mRNA (136). We also showed that *CDKN1C* has a translated isoform D (A6NK88) from the hitherto not confirmed transcript *CDKN1C-201* involving frameshifting of the last coding exon. Alternative transcripts are common in eukaryotes, but non-canonical reading frames are rare in human genes, as discussed in article II, but are more common in prokaryotes. *PEG10* is a retrovirus-like gene that belongs to a retrotransposon family and includes a retroviral GAG domain. Retroviruses that use RNA as the genetic code contain all three reading frames, exploiting the potential with as little RNA as possible. In contrast, eukaryotic cells usually only have one reading frame. Genes with multiple reading frames may need more robust regulations like monoallelic expression, or retroviral-like structures attract methylation.

5.2.4 Recurrence risk and implications for genetic counseling

The recurrence risk of BWSp in these families must be assessed individually and depends on the molecular background. In the families in the articles, I and II, an autosomal dominant inheritance pattern was found, where heterozygous carrier females, disregardless of being clinically affected or not, would have a 50% risk of having a child with BWSp. We offered family members testing, and prenatal diagnostic and preimplantation genetic diagnostics were discussed. The affected children will be offered counseling follow-ups in the future. The clinical features in these families are highly variable. In the family with the OCT variant, a high risk of childhood cancer (Wilms tumour) is highly relevant, as they belong to the molecular subgroup of BWSp (IC1 GOM) with the highest overall tumour risk of 28%.
In contrast, the *CDKN1C* family in article II belong to the group with an overall risk of childhood cancer of 6.9%, and abdominal ultrasound screening for neuroblastoma is warranted (73). Moreover, a pregnant mother carrying an affected child with *CDKN1C* associated BWSp will have a high risk of pregnancy-related complications, like preeclampsia, and polyhydramnios. In addition, a high risk of

abdominal wall defects and the child's high mortality risk must be addressed. All newborns with BWSp must be assessed for hypoglycemia and hyperinsulinism, but in this *CDKN1C* family, there might also be a risk of life-threatening congenital adrenal hypoplasia.

For the family presented in article III, the double UPD was considered a sporadic event associated with increased maternal age, with a low recurrence risk for UPD and negligible risk to other family members. Nevertheless, we offer prenatal diagnostics in this family due to advanced maternal age. The cancer risk in the affected boy is unknown. However, BWSp-like screening was offered, as individuals with classical BWSp with a positive score but without a molecular correlate have an overall risk for childhood tumour of 6.2% (73).

5.3 Limitations of the present studies

All three articles describe single families with novel molecular findings. However, the most significant limitation of this study is the lack of confirmation in additional families, and not being able to repeat the experiments and validate the hypotheses. Furthermore, when dealing with rare disorders and individual families we cannot adjust for socioeconomic factors or analyse the individual's genetic and environmental background. Besides the family presented in article I (*Anticipation in BWS*), only two other families with either clinical or molecular anticipation have been published (113) (74). The most significant limitation is the lack of confirmation in multiple families. Therefore, the clinical relevance is probably limited only to a minority of BWS families with IC GOM. However, the variant seems to be recurrent, so possibly similar families can be detected and described in the future, hopefully allowing for more conclusive evidence. Furthermore, other studies have not reinforced the hypothesis generated in article I. On the contrary, the defects are documented to involve postzygotic maintenance rather than the gonadal switch (71). However, the anticipation effect is yet to be explained by another hypothesis.

The likelihood of detecting the *CDKN1C* variant described in article II in other individuals is extremely low. However, the findings can still be of value for other patients, either with isoform D variants or combined BWS and IMAGe.

In the boys in articles II and III, we searched for alternative molecular explanations for their atypical phenotype by trio WES analysis. However, this analysis has known limitations, and variants can go undetected. This could happen due to inadequate lab analysis, pipelines or interpretations, or other obstacles like a quality failure, pseudogenes and repeats, complexity of the variant, inheritance pattern, synonymous variants, (deep) intronic variants, and CNVs.

The genetic findings in the articles in this thesis are all extremely rare. However, the basic genetics we learned will be helpful to scientists and clinical geneticists specializing in rare disorders. In addition, the molecular findings in the three families will hopefully inspire others dealing with imprinting disorders to search for a potential underlying mechanism, which is required to give adequate genetic counseling.

6. Main Conclusions

We present evidence for clinical and molecular anticipation in a family with Beckwith-Wiedemann syndrome (BWS) and gain of methylation in imprinting centre 1 (IC1) due to an underlying pathogenic OCT binding site variant in IC1 in cis. The methylation level increased through the generations in differently methylated sites in IC1 that had the longest physical distance to the variant. Furthermore, we presented a hypothetical explanation for this, inferring different handling of the parental chromosomes during the gonadal reset of imprinting.

We also documented tissue-specific frameshifting and different molecular pathomechanisms for a single delins-variant in *CDKN1C,* explaining both BWS and the mirror syndrome IMAGe in the index boy. Moreover, the complex variant affected a hitherto not reported D-isoform of CDKN1C (CDKN1C-D, also called A6NK88) with high expression in the brain. We speculate that mutated isoform D is the cause of neurodevelopmental delay in the boy, not earlier described as associated with *CDKN1C*.

Lastly, we report on a baby boy with a double paternal uniparental isodisomy (iUPD), involving the two imprinted chromosomes 7 and 15. The UPD(15)pat is a rare cause of Angelman syndrome, which only later became clinical evident in the boy, while the UPD(7)pat is not known to be pathogenic or associated with a phenotype. However, since we did not find any other molecular explanation for his BWSp, including methylation disturbances on 11p15.5 or evidence for an imprinted gene network, it remains possible that our finding of overexpression of the imprinted gene *PEG10* (7q21.3) caused his overgrowth, and *PEG10* appears to be a good candidate gene for intrauterine growth regulation.

Isodisomic UPDs are related to increasing maternal age and can result from meiotic errors different from the traditionally non-disjunction type of errors. We outline the most probable maternal meiotic errors causing the double paternal UPDs.

6.1 Implications for clinical practice:

- Anticipation is documented in BWS with IC1 GOM. A mother in a BWS family might present as mildly or unaffected carrier, and the pedigree can be misleading. Familial BWS is not excluded in a sporadic patient with partial or incomplete GOM in IC1, in whom we usually suspect a postzygotic, mosaic epimutation. All individuals with IC1 GOM should be tested for an underlying pathogenic variant in IC1, starting with CNV analysis, followed by an A2 repeat analysis to ensure correct information for genetic counseling.
- *CDKN1C-201* (isoform D) should be included as a transcript possibly associated with a neurodevelopmental delay and analysed in clinical studies. Since this transcript is not included in publicly available databases used in variant interpretation, such as gnomAD, Alamut and Decipher, it will be difficult to detect a missense VUS in the standard transcripts (*CDKN1C-202/203/204*) that may induce frameshifting in *CDKN1C-201*.
- Combined GOF and LOF caused by the same variant in a gene must be kept in mind as a possibility in individuals with unusual phenotypic presentations.
- Multiple reading frames leading to different isoforms with different functions can be present in small, imprinted genes, and this must be manually searched.
- This study highlights the relevance of UPD in clinical settings when an imprinting disorder is suspected due to huge placental size, neonatal overgrowth, endocrine abnormalities and specific developmental disorders.
- Imprinting disorder beyond BWS should be included as a differential diagnosis in neonatal hyperinsulinism and conjugated hyperbilirubinemia.
- High-density SNP-array is superior to array-CGH in clinical settings and detects UPDs, not limited to imprinting disorders. However, SNP-array will not detect complete heterodisomies, which is common in UPD(15)mat (Prader-Willi syndrome), and MS-MLPA is needed when screening for causes of neonatal hypotonia.
- In BWSp individuals with macrosomia and placentomegaly, UPD(7)pat or other paternal UPDs should be in the differential diagnosis spectrum.

7. Future perspectives

We were the first to describe molecular anticipation in BWS in article I in 2013. It has since been frequently cited, indicating its relevance to the science of imprinting disorders and mechanisms. Probably, it was an important inspiration for the publication of a similar family with molecular anticipation in BWS (77). Therefore, a natural next step after these studies would be to investigate how the IC1 variants affect gonadal imprinting. This could be done using transgenic mice with a human-type IC1 defect to model the molecular consequence of the different variants found by us and others.

The anticipation mechanism in imprinting disorders might not be limited to BWS. Another disorder involving an intergenic DMR is Kagami-Ogata syndrome (KOS) on chromosome 14q32 (gDMR): *MEG3/DLK1:IG-DMR*. 10-20% of KOS are due to an epimutation (GOM), often due to an underlying microdeletion. Indeed, an underlying SNV in the IG-DMR imprinting centre should also be investigated, even in milder KOS with partial GOM.

To investigate possible brain interaction partners of *CDKN1C-201* (A6NK88), we have recently performed yeast two-hybrid (Y2H) screening (unpublished). The results are still very preliminary with a candidate gene *KMT2C (MLL3)*, but this and similar approaches could potentially reveal more about how rare mutations in alternative transcripts might cause disease through disturbed functional networks. The article on *CDKCN1* is cited in NCBI's review on IMAGe syndrome https://www.ncbi.nlm.nih.gov/books/NBK190103/, highlighting the clinical relevance of the finding, and hopefully, this will inspire other clinicians and scientists to investigate similar complex variants.

Further studies on growth patterns might clarify whether a UPD(7)pat overgrowth phenotype exists. Our study points to *PEG10* as a candidate growth regulator, and individuals with UPD(7)pat might be eligible for gene expression and phenotype

correlation studies. UPD(7) pat should be tested in individuals with BWS-like overgrowth without 11p15.5 aberrations. It is also important to analyse *PEG10* expression in individuals with molecularly verified BWS to look for associated upregulation, as indicated in LOS ruminants (135).

Our articles may stimulate further studies on small, imprinted genes with non-canonical reading frames like *PEG10* and *CDKN1C*. In addition, there might be other clinically relevant undisclosed transcripts with a novel function.

Another study published at the same time as article III showed that PEG10 is a target of UBE3A and that UBE3A is a posttranslational negative regulator of PEG10, while *PEG10* mRNA levels remain unaltered in Angelman syndrome neurons and *UBE3A*-rescued neurons (137). In other words, individuals with AS, regardless of mechanism, might have elevated brain PEG10 protein due to decreased posttranslational degradation. They also found that increased PEG10 levels might affect neuronal migration and thus contribute to the pathophysiology in AS. There was no indication that the affected boy in article III with increased *PEG10* mRNA level and AS had a more severe neurological phenotype than expected. On the contrary, our initial impression was a slightly milder AS phenotype in him, but he is too young for formal assessments. Further studies on *PEG10* might shed light on this in the future.

8. References

Uncategorized References

1. Berland S, Appelback M, Bruland O, Beygo J, Buiting K, Mackay DJ, et al. Evidence for anticipation in Beckwith-Wiedemann syndrome. Eur J Hum Genet. 2013;21(12):1344-8.
2. Berland S, Haukanes BI, Juliusson PB, Houge G. Deep exploration of a CDKN1C mutation causing a mixture of Beckwith-Wiedemann and IMAGe syndromes revealed a novel transcript associated with developmental delay. J Med Genet. 2022;59(2):155-64.
3. Berland S, Rustad CF, Bentsen MHL, Wollen EJ, Turowski G, Johansson S, et al. Double paternal uniparental isodisomy 7 and 15 presenting with Beckwith-Wiedemann spectrum features. Cold Spring Harb Mol Case Stud. 2021;7(6).
4. Mackay DJG, Temple IK. Human imprinting disorders: Principles, practice, problems and progress. Eur J Med Genet. 2017;60(11):618-26.
5. Barlow DP, Bartolomei MS. Genomic imprinting in mammals. Cold Spring Harb Perspect Biol. 2014;6(2).
6. Monk D, Mackay DJG, Eggermann T, Maher ER, Riccio A. Genomic imprinting disorders: lessons on how genome, epigenome and environment interact. Nat Rev Genet. 2019;20(4):235-48.
7. Eggermann T, Perez de Nanclares G, Maher ER, Temple IK, Tumer Z, Monk D, et al. Imprinting disorders: a group of congenital disorders with overlapping patterns of molecular changes affecting imprinted loci. Clin Epigenetics. 2015;7:123.
8. Soellner L, Begemann M, Mackay DJ, Gronskov K, Tumer Z, Maher ER, et al. Recent Advances in Imprinting Disorders. Clin Genet. 2017;91(1):3-13.
9. Baran Y, Subramaniam M, Biton A, Tukiainen T, Tsang EK, Rivas MA, et al. The landscape of genomic imprinting across diverse adult human tissues. Genome Res. 2015;25(7):927-36.
10. Pilvar D, Reiman M, Pilvar A, Laan M. Parent-of-origin-specific allelic expression in the human placenta is limited to established imprinted loci and it is stably maintained across pregnancy. Clin Epigenetics. 2019;11(1):94.
11. Elhamamsy AR. Role of DNA methylation in imprinting disorders: an updated review. J Assist Reprod Genet. 2017;34(5):549-62.
12. Morgan HD, Sutherland HG, Martin DI, Whitelaw E. Epigenetic inheritance at the agouti locus in the mouse. Nat Genet. 1999;23(3):314-8.
13. Stelzer Y, Sagi I, Yanuka O, Eiges R, Benvenisty N. The noncoding RNA IPW regulates the imprinted DLK1-DIO3 locus in an induced pluripotent stem cell model of Prader-Willi syndrome. Nat Genet. 2014;46(6):551-7.
14. Martin-Trujillo A, Patel N, Richter F, Jadhav B, Garg P, Morton SU, et al. Rare genetic variation at transcription factor binding sites modulates local DNA methylation profiles. PLoS Genet. 2020;16(11):e1009189.
15. Barbosa M, Joshi RS, Garg P, Martin-Trujillo A, Patel N, Jadhav B, et al. Identification of rare de novo epigenetic variations in congenital disorders. Nat Commun. 2018;9(1):2064.

16. Grafodatskaya D, Choufani S, Basran R, Weksberg R. An Update on Molecular Diagnostic Testing of Human Imprinting Disorders. J Pediatr Genet. 2017;6(1):3-17.
17. Carli D, Riberi E, Ferrero GB, Mussa A. Syndromic Disorders Caused by Disturbed Human Imprinting. J Clin Res Pediatr Endocrinol. 2020;12(1):1-16.
18. Eggermann T, Oehl-Jaschkowitz B, Dicks S, Thomas W, Kanber D, Albrecht B, et al. The maternal uniparental disomy of chromosome 6 (upd(6)mat) "phenotype": result of placental trisomy 6 mosaicism? Mol Genet Genomic Med. 2017;5(6):668-77.
19. Prasasya R, Grotheer KV, Siracusa LD, Bartolomei MS. Temple syndrome and Kagami-Ogata syndrome: clinical presentations, genotypes, models and mechanisms. Hum Mol Genet. 2020;29(R1):R107-R16.
20. Kagami M, Kurosawa K, Miyazaki O, Ishino F, Matsuoka K, Ogata T. Comprehensive clinical studies in 34 patients with molecularly defined UPD(14)pat and related conditions (Kagami-Ogata syndrome). Eur J Hum Genet. 2015;23(11):1488-98.
21. Mulchandani S, Bhoj EJ, Luo M, Powell-Hamilton N, Jenny K, Gripp KW, et al. Maternal uniparental disomy of chromosome 20: a novel imprinting disorder of growth failure. Genet Med. 2016;18(4):309-15.
22. Begemann M, Spengler S, Kordass U, Schroder C, Eggermann T. Segmental maternal uniparental disomy 7q associated with DLK1/GTL2 (14q32) hypomethylation. Am J Med Genet A. 2012;158A(2):423-8.
23. Hara-Isono K, Matsubara K, Fuke T, Yamazawa K, Satou K, Murakami N, et al. Genome-wide methylation analysis in Silver-Russell syndrome, Temple syndrome, and Prader-Willi syndrome. Clin Epigenetics. 2020;12(1):159.
24. Sanchez-Delgado M, Riccio A, Eggermann T, Maher ER, Lapunzina P, Mackay D, et al. Causes and Consequences of Multi-Locus Imprinting Disturbances in Humans. Trends Genet. 2016;32(7):444-55.
25. Fontana L, Bedeschi MF, Maitz S, Cereda A, Fare C, Motta S, et al. Characterization of multi-locus imprinting disturbances and underlying genetic defects in patients with chromosome 11p15.5 related imprinting disorders. Epigenetics. 2018;13(9):897-909.
26. Bertoin F, Letouze E, Grignani P, Patey M, Rossignol S, Libe R, et al. Genome-wide paternal uniparental disomy as a cause of Beckwith-Wiedemann syndrome associated with recurrent virilizing adrenocortical tumors. Horm Metab Res. 2015;47(7):497-503.
27. Kalish JM, Conlin LK, Bhatti TR, Dubbs HA, Harris MC, Izumi K, et al. Clinical features of three girls with mosaic genome-wide paternal uniparental isodisomy. Am J Med Genet A. 2013;161A(8):1929-39.
28. Borgulova I, Soldatova I, Putzova M, Malikova M, Neupauerova J, Markova SP, et al. Genome-wide uniparental diploidy of all paternal chromosomes in an 11-year-old girl with deafness and without malignancy. J Hum Genet. 2018;63(7):803-10.
29. Darcy D, Atwal PS, Angell C, Gadi I, Wallerstein R. Mosaic paternal genome-wide uniparental isodisomy with down syndrome. Am J Med Genet A. 2015;167A(10):2463-9.

30. Wilson M, Peters G, Bennetts B, McGillivray G, Wu ZH, Poon C, et al. The clinical phenotype of mosaicism for genome-wide paternal uniparental disomy: two new reports. Am J Med Genet A. 2008;146A(2):137-48.
31. Gogiel M, Begemann M, Spengler S, Soellner L, Goretzlehner U, Eggermann T, et al. Genome-wide paternal uniparental disomy mosaicism in a woman with Beckwith-Wiedemann syndrome and ovarian steroid cell tumour. Eur J Hum Genet. 2013;21(7):788-91.
32. Johnson JP, Waterson J, Schwanke C, Schoof J. Genome-wide androgenetic mosaicism. Clin Genet. 2014;85(3):282-5.
33. Inbar-Feigenberg M, Choufani S, Cytrynbaum C, Chen YA, Steele L, Shuman C, et al. Mosaicism for genome-wide paternal uniparental disomy with features of multiple imprinting disorders: diagnostic and management issues. Am J Med Genet A. 2013;161A(1):13-20.
34. Lee CT, Tung YC, Hwu WL, Shih JC, Lin WH, Wu MZ, et al. Mosaic paternal haploidy in a patient with pancreatoblastoma and Beckwith-Wiedemann spectrum. Am J Med Genet A. 2019;179(9):1878-83.
35. Kapur RP, Cole B, Zhang M, Lin J, Fligner CL. Placental mesenchymal dysplasia and fetal renal-hepatic-pancreatic dysplasia: androgenetic-biparental mosaicism and pathogenesis of an autosomal recessive disorder. Pediatr Dev Pathol. 2013;16(3):191-200.
36. Morales C, Soler A, Badenas C, Rodriguez-Revenga L, Nadal A, Martinez JM, et al. Reproductive consequences of genome-wide paternal uniparental disomy mosaicism: description of two cases with different mechanisms of origin and pregnancy outcomes. Fertil Steril. 2009;92(1):393 e5-9.
37. Ohtsuka Y, Higashimoto K, Oka T, Yatsuki H, Jozaki K, Maeda T, et al. Identification of consensus motifs associated with mitotic recombination and clinical characteristics in patients with paternal uniparental isodisomy of chromosome 11. Hum Mol Genet. 2016;25(7):1406-19.
38. Ohtsuka Y, Higashimoto K, Sasaki K, Jozaki K, Yoshinaga H, Okamoto N, et al. Autosomal recessive cystinuria caused by genome-wide paternal uniparental isodisomy in a patient with Beckwith-Wiedemann syndrome. Clin Genet. 2015;88(3):261-6.
39. Postema FAM, Bliek J, van Noesel CJM, van Zutven L, Oosterwijk JC, Hopman SMJ, et al. Multiple tumors due to mosaic genome-wide paternal uniparental disomy. Pediatr Blood Cancer. 2019;66(6):e27715.
40. Robinson WP, Lauzon JL, Innes AM, Lim K, Arsovska S, McFadden DE. Origin and outcome of pregnancies affected by androgenetic/biparental chimerism. Hum Reprod. 2007;22(4):1114-22.
41. Romanelli V, Nevado J, Fraga M, Trujillo AM, Mori MA, Fernandez L, et al. Constitutional mosaic genome-wide uniparental disomy due to diploidisation: an unusual cancer-predisposing mechanism. J Med Genet. 2011;48(3):212-6.
42. Christesen HT, Christensen LG, Lofgren AM, Brondum-Nielsen K, Svensson J, Brusgaard K, et al. Tissue variations of mosaic genome-wide paternal uniparental disomy and phenotype of multi-syndromal congenital hyperinsulinism. Eur J Med Genet. 2020;63(1):103632.

43. White M, McGillivray G, White SM, Zacharin MR. First report of congenital adrenal cysts and pheochromocytoma in a patient with mosaic genome-wide paternal uniparental disomy. Am J Med Genet A. 2016;170(12):3352-5.
44. Horike S, Ferreira JC, Meguro-Horike M, Choufani S, Smith AC, Shuman C, et al. Screening of DNA methylation at the H19 promoter or the distal region of its ICR1 ensures efficient detection of chromosome 11p15 epimutations in Russell-Silver syndrome. Am J Med Genet A. 2009;149A(11):2415-23.
45. Sheppard SE, Lalonde E, Adzick NS, Beck AE, Bhatti T, De Leon DD, et al. Androgenetic chimerism as an etiology for Beckwith-Wiedemann syndrome: diagnosis and management. Genet Med. 2019;21(11):2644-9.
46. Spier I, Engels H, Stutte S, Reutter H, Bartels E, Matos Meder S, et al. Male infant with paternal uniparental diploidy mosaicism and a 46,XX/46,XY karyotype. Am J Med Genet A. 2019;179(11):2252-6.
47. Bens S, Luedeke M, Richter T, Graf M, Kolarova J, Barbi G, et al. Mosaic genome-wide maternal isodiploidy: an extreme form of imprinting disorder presenting as prenatal diagnostic challenge. Clin Epigenetics. 2017;9:111.
48. Strain L, Warner JP, Johnston T, Bonthron DT. A human parthenogenetic chimaera. Nat Genet. 1995;11(2):164-9.
49. Yamazawa K, Nakabayashi K, Kagami M, Sato T, Saitoh S, Horikawa R, et al. Parthenogenetic chimaerism/mosaicism with a Silver-Russell syndrome-like phenotype. J Med Genet. 2010;47(11):782-5.
50. Repnikova E, Roberts J, Kats A, Habeebu S, Schwager C, Joyce J, et al. Biparental/androgenetic mosaicism in a male with features of overgrowth and placental mesenchymal dysplasia. Clin Genet. 2018;94(6):564-8.
51. Liehr T. Uniparental Disomy (UPD) in Clinical Genetics: Springer; 2014.
52. Ottolini CS, Newnham L, Capalbo A, Natesan SA, Joshi HA, Cimadomo D, et al. Genome-wide maps of recombination and chromosome segregation in human oocytes and embryos show selection for maternal recombination rates. Nat Genet. 2015;47(7):727-35.
53. Engel E. A new genetic concept: uniparental disomy and its potential effect, isodisomy. Am J Med Genet. 1980;6(2):137-43.
54. Spence JE, Perciaccante RG, Greig GM, Willard HF, Ledbetter DH, Hejtmancik JF, et al. Uniparental disomy as a mechanism for human genetic disease. Am J Hum Genet. 1988;42(2):217-26.
55. Yong PJ, Marion SA, Barrett IJ, Kalousek DK, Robinson WP. Evidence for imprinting on chromosome 16: the effect of uniparental disomy on the outcome of mosaic trisomy 16 pregnancies. Am J Med Genet. 2002;112(2):123-32.
56. Scheuvens R, Begemann M, Soellner L, Meschede D, Raabe-Meyer G, Elbracht M, et al. Maternal uniparental disomy of chromosome 16 [upd(16)mat]: clinical features are rather caused by (hidden) trisomy 16 mosaicism than by upd(16)mat itself. Clin Genet. 2017;92(1):45-51.
57. Benn P. Uniparental disomy: Origin, frequency, and clinical significance. Prenat Diagn. 2020.
58. Scuffins J, Keller-Ramey J, Dyer L, Douglas G, Torene R, Gainullin V, et al. Uniparental disomy in a population of 32,067 clinical exome trios. Genet Med. 2021.

59. Caldwell S, Sagaser K, Nelson Z, Frey J, Wardrop J, Boomer T, et al. Deletion rescue resulting in segmental homozygosity: A mechanism underlying discordant NIPT results. Am J Med Genet A. 2020;182(11):2666-70.
60. Nazarenko S, Sazhenova E, Baumer A, Schinzel A. Segmental maternal heterodisomy of the proximal part of chromosome 15 in an infant with Prader-Willi syndrome. Eur J Hum Genet. 2004;12(5):411-4.
61. Nakka P, Pattillo Smith S, O'Donnell-Luria AH, McManus KF, andMe Research T, Mountain JL, et al. Characterization of Prevalence and Health Consequences of Uniparental Disomy in Four Million Individuals from the General Population. Am J Hum Genet. 2019;105(5):921-32.
62. Scuffins J, Keller-Ramey J, Dyer L, Douglas G, Torene R, Gainullin V, et al. Uniparental disomy in a population of 32,067 clinical exome trios. Genet Med. 2021;23(6):1101-7.
63. Sasaki K, Mishima H, Miura K, Yoshiura K. Uniparental disomy analysis in trios using genome-wide SNP array and whole-genome sequencing data imply segmental uniparental isodisomy in general populations. Gene. 2013;512(2):267-74.
64. Xu J, Zhang M, Niu W, Yao G, Sun B, Bao X, et al. Genome-wide uniparental disomy screen in human discarded morphologically abnormal embryos. Sci Rep. 2015;5:12302.
65. McCoy RC, Demko ZP, Ryan A, Banjevic M, Hill M, Sigurjonsson S, et al. Evidence of Selection against Complex Mitotic-Origin Aneuploidy during Preimplantation Development. PLoS Genet. 2015;11(10):e1005601.
66. Tyc KM, McCoy RC, Schindler K, Xing J. Mathematical modeling of human oocyte aneuploidy. Proc Natl Acad Sci U S A. 2020;117(19):10455-64.
67. Gruhn JR, Zielinska AP, Shukla V, Blanshard R, Capalbo A, Cimadomo D, et al. Chromosome errors in human eggs shape natural fertility over reproductive life span. Science. 2019;365(6460):1466-9.
68. Moradkhani K, Cuisset L, Boisseau P, Pichon O, Lebrun M, Hamdi-Roze H, et al. Risk estimation of uniparental disomy of chromosome 14 or 15 in a fetus with a parent carrying a non-homologous Robertsonian translocation. Should we still perform prenatal diagnosis? Prenat Diagn. 2019;39(11):986-92.
69. Demond H, Anvar Z, Jahromi BN, Sparago A, Verma A, Davari M, et al. A KHDC3L mutation resulting in recurrent hydatidiform mole causes genome-wide DNA methylation loss in oocytes and persistent imprinting defects post-fertilisation. Genome Med. 2019;11(1):84.
70. Cubellis MV, Pignata L, Verma A, Sparago A, Del Prete R, Monticelli M, et al. Loss-of-function maternal-effect mutations of PADI6 are associated with familial and sporadic Beckwith-Wiedemann syndrome with multi-locus imprinting disturbance. Clin Epigenetics. 2020;12(1):139.
71. Beckwith JB. Macroglossia, omphalocele, adrenal cytomegaly, gigantism, and hyperplastic visceromegaly. Birth defects original article series. 1969;2:188-96.
72. Wiedemann HR. [The EMG-syndrome: exomphalos, macroglossia, gigantism and disturbed carbohydrate metabolism]. Z Kinderheilkd. 1969;106(3):171-85.
73. Brioude F, Kalish JM, Mussa A, Foster AC, Bliek J, Ferrero GB, et al. Expert consensus document: Clinical and molecular diagnosis, screening and management of

Beckwith-Wiedemann syndrome: an international consensus statement. Nat Rev Endocrinol. 2018;14(4):229-49.
74. Kubo S, Murata C, Okamura H, Sakasegawa T, Sakurai C, Hatsuzawa K, et al. Oct motif variants in Beckwith-Wiedemann syndrome patients disrupt maintenance of the hypomethylated state of the H19/IGF2 imprinting control region. FEBS Lett. 2020;594(10):1517-31.
75. Eggermann T, Bruck J, Knopp C, Fekete G, Kratz C, Tasic V, et al. Need for a precise molecular diagnosis in Beckwith-Wiedemann and Silver-Russell syndrome: what has to be considered and why it is important. J Mol Med (Berl). 2020;98(10):1447-55.
76. Demars J, Shmela ME, Rossignol S, Okabe J, Netchine I, Azzi S, et al. Analysis of the IGF2/H19 imprinting control region uncovers new genetic defects, including mutations of OCT-binding sequences, in patients with 11p15 fetal growth disorders. Hum Mol Genet. 2010;19(5):803-14.
77. Sun F, Higashimoto K, Awaji A, Ohishi K, Nishizaki N, Tanoue Y, et al. The extent of DNA methylation anticipation due to a genetic defect in ICR1 in Beckwith-Wiedemann syndrome. J Hum Genet. 2019;64(9):937-43.
78. Demars J, Rossignol S, Netchine I, Lee KS, Shmela M, Faivre L, et al. New insights into the pathogenesis of Beckwith-Wiedemann and Silver-Russell syndromes: contribution of small copy number variations to 11p15 imprinting defects. Hum Mutat. 2011;32(10):1171-82.
79. Poole RL, Leith DJ, Docherty LE, Shmela ME, Gicquel C, Splitt M, et al. Beckwith-Wiedemann syndrome caused by maternally inherited mutation of an OCT-binding motif in the IGF2/H19-imprinting control region, ICR1. Eur J Hum Genet. 2012;20(2):240-3.
80. Higashimoto K, Jozaki K, Kosho T, Matsubara K, Fuke T, Yamada D, et al. A novel de novo point mutation of the OCT-binding site in the IGF2/H19-imprinting control region in a Beckwith-Wiedemann syndrome patient. Clin Genet. 2014;86(6):539-44.
81. Valente FM, Sparago A, Freschi A, Hill-Harfe K, Maas SM, Frints SGM, et al. Transcription alterations of KCNQ1 associated with imprinted methylation defects in the Beckwith-Wiedemann locus. Genet Med. 2019;21(8):1808-20.
82. Essinger C, Karch S, Moog U, Fekete G, Lengyel A, Pinti E, et al. Frequency of KCNQ1 variants causing loss of methylation of Imprinting Centre 2 in Beckwith-Wiedemann syndrome. Clin Epigenetics. 2020;12(1):63.
83. Brioude F, Lacoste A, Netchine I, Vazquez MP, Auber F, Audry G, et al. Beckwith-Wiedemann syndrome: growth pattern and tumor risk according to molecular mechanism, and guidelines for tumor surveillance. Horm Res Paediatr. 2013;80(6):457-65.
84. Brioude F, Netchine I, Praz F, Le Jule M, Calmel C, Lacombe D, et al. Mutations of the Imprinted CDKN1C Gene as a Cause of the Overgrowth Beckwith-Wiedemann Syndrome: Clinical Spectrum and Functional Characterization. Hum Mutat. 2015;36(9):894-902.
85. Mussa A, Molinatto C, Cerrato F, Palumbo O, Carella M, Baldassarre G, et al. Assisted Reproductive Techniques and Risk of Beckwith-Wiedemann Syndrome. Pediatrics. 2017;140(1).

86. Weksberg R, Shuman C, Caluseriu O, Smith AC, Fei YL, Nishikawa J, et al. Discordant KCNQ1OT1 imprinting in sets of monozygotic twins discordant for Beckwith-Wiedemann syndrome. Hum Mol Genet. 2002;11(11):1317-25.
87. Wesseler K, Kraft F, Eggermann T. Molecular and Clinical Opposite Findings in 11p15.5 Associated Imprinting Disorders: Characterization of Basic Mechanisms to Improve Clinical Management. Int J Mol Sci. 2019;20(17).
88. Reid E, Morrison N, Barron L, Boyd E, Cooke A, Fielding D, et al. Familial Wolf-Hirschhorn syndrome resulting from a cryptic translocation: a clinical and molecular study. J Med Genet. 1996;33(3):197-202.
89. Eggermann T, Binder G, Brioude F, Maher ER, Lapunzina P, Cubellis MV, et al. CDKN1C mutations: two sides of the same coin. Trends Mol Med. 2014;20(11):614-22.
90. Stampone E, Bencivenga D, Barone C, Di Finizio M, Della Ragione F, Borriello A. A Beckwith-Wiedemann-Associated CDKN1C Mutation Allows the Identification of a Novel Nuclear Localization Signal in Human p57(Kip2). Int J Mol Sci. 2021;22(14).
91. Brioude F, Oliver-Petit I, Blaise A, Praz F, Rossignol S, Le Jule M, et al. CDKN1C mutation affecting the PCNA-binding domain as a cause of familial Russell Silver syndrome. J Med Genet. 2013;50(12):823-30.
92. Hamajima N, Johmura Y, Suzuki S, Nakanishi M, Saitoh S. Increased protein stability of CDKN1C causes a gain-of-function phenotype in patients with IMAGe syndrome. PLoS One. 2013;8(9):e75137.
93. Borges KS, Arboleda VA, Vilain E. Mutations in the PCNA-binding site of CDKN1C inhibit cell proliferation by impairing the entry into S phase. Cell Div. 2015;10:2.
94. Arboleda VA, Lee H, Parnaik R, Fleming A, Banerjee A, Ferraz-de-Souza B, et al. Mutations in the PCNA-binding domain of CDKN1C cause IMAGe syndrome. Nat Genet. 2012;44(7):788-92.
95. Lew JM, Fei YL, Aleck K, Blencowe BJ, Weksberg R, Sadowski PD. CDKN1C mutation in Wiedemann-Beckwith syndrome patients reduces RNA splicing efficiency and identifies a splicing enhancer. Am J Med Genet A. 2004;127A(3):268-76.
96. Algar E, Brickell S, Deeble G, Amor D, Smith P. Analysis of CDKN1C in Beckwith Wiedemann syndrome. Hum Mutat. 2000;15(6):497-508.
97. Matsuoka S, Thompson JS, Edwards MC, Bartletta JM, Grundy P, Kalikin LM, et al. Imprinting of the gene encoding a human cyclin-dependent kinase inhibitor, p57KIP2, on chromosome 11p15. Proc Natl Acad Sci U S A. 1996;93(7):3026-30.
98. Bodian DL, Solomon BD, Khromykh A, Thach DC, Iyer RK, Link K, et al. Diagnosis of an imprinted-gene syndrome by a novel bioinformatics analysis of whole-genome sequences from a family trio. Mol Genet Genomic Med. 2014;2(6):530-8.
99. Mussa A, Molinatto C, Baldassarre G, Riberi E, Russo S, Larizza L, et al. Cancer Risk in Beckwith-Wiedemann Syndrome: A Systematic Review and Meta-Analysis Outlining a Novel (Epi)Genotype Specific Histotype Targeted Screening Protocol. J Pediatr. 2016;176:142-9 e1.

100. Maas SM, Vansenne F, Kadouch DJ, Ibrahim A, Bliek J, Hopman S, et al. Phenotype, cancer risk, and surveillance in Beckwith-Wiedemann syndrome depending on molecular genetic subgroups. Am J Med Genet A. 2016;170(9):2248-60.
101. Coktu S, Spix C, Kaiser M, Beygo J, Kleinle S, Bachmann N, et al. Cancer incidence and spectrum among children with genetically confirmed Beckwith-Wiedemann spectrum in Germany: a retrospective cohort study. Br J Cancer. 2020;123(4):619-23.
102. Hol JA, Jewell R, Chowdhury T, Duncan C, Nakata K, Oue T, et al. Wilms tumour surveillance in at-risk children: Literature review and recommendations from the SIOP-Europe Host Genome Working Group and SIOP Renal Tumour Study Group. Eur J Cancer. 2021;153:51-63.
103. Radley JA, Connolly M, Sabir A, Kanani F, Carley H, Jones RL, et al. Isolated- and Beckwith-Wiedemann syndrome related- lateralised overgrowth (hemihypertrophy): Clinical and molecular correlations in 94 individuals. Clin Genet. 2021;100(3):292-7.
104. Wakeling EL, Brioude F, Lokulo-Sodipe O, O'Connell SM, Salem J, Bliek J, et al. Diagnosis and management of Silver-Russell syndrome: first international consensus statement. Nat Rev Endocrinol. 2017;13(2):105-24.
105. Pignata L, Sparago A, Palumbo O, Andreucci E, Lapi E, Tenconi R, et al. Mosaic Segmental and Whole-Chromosome Upd(11)mat in Silver-Russell Syndrome. Genes (Basel). 2021;12(4).
106. Mackay DJG, Bliek J, Lombardi MP, Russo S, Calzari L, Guzzetti S, et al. Discrepant molecular and clinical diagnoses in Beckwith-Wiedemann and Silver-Russell syndromes. Genet Res (Camb). 2019;101:e3.
107. Vilain E, Le Merrer M, Lecointre C, Desangles F, Kay MA, Maroteaux P, et al. IMAGe, a new clinical association of intrauterine growth retardation, metaphyseal dysplasia, adrenal hypoplasia congenita, and genital anomalies. J Clin Endocrinol Metab. 1999;84(12):4335-40.
108. Bolomiti M, Batnes-Pedersen E, Telman G, Januszkiewicz-Lewandowska D. A Case report: Co-occurrence of IMAGe syndrome and Rhabdomyosarcoma. Cancer Genet. 2021;256-257:100-5.
109. Heide S, Chantot-Bastaraud S, Keren B, Harbison MD, Azzi S, Rossignol S, et al. Chromosomal rearrangements in the 11p15 imprinted region: 17 new 11p15.5 duplications with associated phenotypes and putative functional consequences. J Med Genet. 2018;55(3):205-13.
110. Eggermann T, Begemann M, Pfeiffer L. Unusual deletion of the maternal 11p15 allele in Beckwith-Wiedemann syndrome with an impact on both imprinting domains. Clin Epigenetics. 2021;13(1):30.
111. Abi Habib W, Brioude F, Azzi S, Rossignol S, Linglart A, Sobrier ML, et al. Transcriptional profiling at the DLK1/MEG3 domain explains clinical overlap between imprinting disorders. Sci Adv. 2019;5(2):eaau9425.
112. Patten MM, Cowley M, Oakey RJ, Feil R. Regulatory links between imprinted genes: evolutionary predictions and consequences. Proc Biol Sci. 2016;283(1824).
113. Eggermann T, Davies JH, Tauber M, van den Akker E, Hokken-Koelega A, Johansson G, et al. Growth Restriction and Genomic Imprinting-Overlapping

Phenotypes Support the Concept of an Imprinting Network. Genes (Basel). 2021;12(4).
114. Penrose LS. The problem of anticipation in pedigrees of dystrophia myotonica. Ann Eugen. 1948;14(2):125-32.
115. Friedman JE. Anticipation in hereditary disease: the history of a biomedical concept. Hum Genet. 2011;130(6):705-14.
116. Howeler CJ, Busch HF, Geraedts JP, Niermeijer MF, Staal A. Anticipation in myotonic dystrophy: fact or fiction? Brain. 1989;112 (Pt 3):779-97.
117. Beygo J, Citro V, Sparago A, De Crescenzo A, Cerrato F, Heitmann M, et al. The molecular function and clinical phenotype of partial deletions of the IGF2/H19 imprinting control region depends on the spatial arrangement of the remaining CTCF-binding sites. Hum Mol Genet. 2013;22(3):544-57.
118. Houge G. [Where is the boundary between diagnostics and research?]. Tidsskr Nor Laegeforen. 2015;135(18):1632.
119. Abi Habib W, Azzi S, Brioude F, Steunou V, Thibaud N, Das Neves C, et al. Extensive investigation of the IGF2/H19 imprinting control region reveals novel OCT4/SOX2 binding site defects associated with specific methylation patterns in Beckwith-Wiedemann syndrome. Hum Mol Genet. 2014;23(21):5763-73.
120. Hori N, Yamane M, Kouno K, Sato K. Induction of DNA demethylation depending on two sets of Sox2 and adjacent Oct3/4 binding sites (Sox-Oct motifs) within the mouse H19/insulin-like growth factor 2 (Igf2) imprinted control region. J Biol Chem. 2012;287(52):44006-16.
121. Vanzan L, Soldati H, Ythier V, Anand S, Braun SMG, Francis N, et al. High throughput screening identifies SOX2 as a super pioneer factor that inhibits DNA methylation maintenance at its binding sites. Nat Commun. 2021;12(1):3337.
122. Fatscher T, Boehm V, Gehring NH. Mechanism, factors, and physiological role of nonsense-mediated mRNA decay. Cell Mol Life Sci. 2015;72(23):4523-44.
123. Van de Pette M, Abbas A, Feytout A, McNamara G, Bruno L, To WK, et al. Visualizing Changes in Cdkn1c Expression Links Early-Life Adversity to Imprint Mis-regulation in Adults. Cell Rep. 2017;18(5):1090-9.
124. Mairet-Coello G, Tury A, Van Buskirk E, Robinson K, Genestine M, DiCicco-Bloom E. p57(KIP2) regulates radial glia and intermediate precursor cell cycle dynamics and lower layer neurogenesis in developing cerebral cortex. Development. 2012;139(3):475-87.
125. Matsumoto A, Susaki E, Onoyama I, Nakayama K, Hoshino M, Nakayama KI. Deregulation of the p57-E2F1-p53 axis results in nonobstructive hydrocephalus and cerebellar malformation in mice. Mol Cell Biol. 2011;31(20):4176-92.
126. Laukoter S, Beattie R, Pauler FM, Amberg N, Nakayama KI, Hippenmeyer S. Imprinted Cdkn1c genomic locus cell-autonomously promotes cell survival in cerebral cortex development. Nat Commun. 2020;11(1):195.
127. Fahmi M, Ito M. Evolutionary Approach of Intrinsically Disordered CIP/KIP Proteins. Sci Rep. 2019;9(1):1575.
128. Iiri T, Herzmark P, Nakamoto JM, van Dop C, Bourne HR. Rapid GDP release from Gs alpha in patients with gain and loss of endocrine function. Nature. 1994;371(6493):164-8.

129. Decker RA, Peacock ML. Occurrence of MEN 2a in familial Hirschsprung's disease: a new indication for genetic testing of the RET proto-oncogene. J Pediatr Surg. 1998;33(2):207-14.
130. Zenker M, Rauch A, Winterpacht A, Tagariello A, Kraus C, Rupprecht T, et al. A dual phenotype of periventricular nodular heterotopia and frontometaphyseal dysplasia in one patient caused by a single FLNA mutation leading to two functionally different aberrant transcripts. Am J Hum Genet. 2004;74(4):731-7.
131. Hehr U, Hehr A, Uyanik G, Phelan E, Winkler J, Reardon W. A filamin A splice mutation resulting in a syndrome of facial dysmorphism, periventricular nodular heterotopia, and severe constipation reminiscent of cerebro-fronto-facial syndrome. J Med Genet. 2006;43(6):541-4.
132. Parrini E, Mei D, Pisanti MA, Catarzi S, Pucatti D, Bianchini C, et al. Familial periventricular nodular heterotopia, epilepsy and Melnick-Needles Syndrome caused by a single FLNA mutation with combined gain-of-function and loss-of-function effects. J Med Genet. 2015;52(6):405-12.
133. Degenkolbe E, Konig J, Zimmer J, Walther M, Reissner C, Nickel J, et al. A GDF5 point mutation strikes twice--causing BDA1 and SYNS2. PLoS Genet. 2013;9(10):e1003846.
134. Shaw ND, Brand H, Kupchinsky ZA, Bengani H, Plummer L, Jones TI, et al. SMCHD1 mutations associated with a rare muscular dystrophy can also cause isolated arhinia and Bosma arhinia microphthalmia syndrome. Nat Genet. 2017;49(2):238-48.
135. Li Y, Boadu F, Highsmith MR, Hagen DE, Cheng J, Rivera RM. Allele-specific aberration of imprinted domain chromosome architecture associates with large offspring syndrome. iScience. 2022;25(5):104269.
136. Clark MB, Janicke M, Gottesbuhren U, Kleffmann T, Legge M, Poole ES, et al. Mammalian gene PEG10 expresses two reading frames by high efficiency -1 frameshifting in embryonic-associated tissues. J Biol Chem. 2007;282(52):37359-69.
137. Pandya NJ, Wang C, Costa V, Lopatta P, Meier S, Zampeta FI, et al. Secreted retrovirus-like GAG-domain-containing protein PEG10 is regulated by UBE3A and is involved in Angelman syndrome pathophysiology. Cell Rep Med. 2021;2(8):100360.

European Journal of Human Genetics (2013) 21, 1344–1348

www.nature.com/ejhg

EJHG Open

ARTICLE

Evidence for anticipation in Beckwith–Wiedemann syndrome

Siren Berland[1], Mia Appelbäck[1,2], Ove Bruland[1], Jasmin Beygo[3], Karin Buiting[3], Deborah JG Mackay[4,5,6], I Karen Temple[4,5,6] and Gunnar Houge*[,1,2]

Classical Beckwith–Wiedemann syndrome (BWS) was diagnosed in two sisters and their male cousin. The children's mothers and a third sister were tall statured (178, 185 and 187 cm) and one had mild BWS features as a child. Their parents had average heights of 173 cm (mother) and 180 cm (father). This second generation tall stature and third generation BWS correlated with increased methylation of the maternal *H19/IGF2*-locus. The results were obtained by bisulphite treatment and subclone Sanger sequencing or next generation sequencing to quantitate the degree of CpG-methylation on three locations: the *H19* promoter region and two CTCF binding sites in the *H19* imprinting control region (ICR1), specifically in ICR1 repeats B1 and B7. Upon ICR1 copy number analysis and sequencing, the same maternal point variant NCBI36:11:g.1979595T>C that had been described previously as a cause of BWS in three brothers, was found. As expected, this point variant was on the paternal allele in the non-affected grandmother. This nucleotide variant has been shown to affect OCTamer-binding transcription factor-4 (OCT4) binding, which may be necessary for maintaining the unmethylated state of the maternal allele. Our data extend these findings by showing that the OCT4 binding site mutation caused incomplete switching from paternal to maternal ICR1 methylation imprint, and that upon further maternal transmission, methylation of the incompletely demethylated variant ICR1 allele was further increased. This suggests that maternal and paternal ICR1 alleles are treated differentially in the female germline, and only the paternal allele appears to be capable of demethylation.
European Journal of Human Genetics (2013) **21,** 1344–1348; doi:10.1038/ejhg.2013.71; published online 10 April 2013

Keywords: Beckwith–Wiedemann syndrome; anticipation; imprinting; *H19*; *IGF2*

INTRODUCTION

Beckwith–Wiedemann syndrome (BWS, OMIM no. 130650) is an overgrowth condition caused by epigenetic or genetic alterations in the imprinted *H19/IGF2-KCNQ1/CDKN1C* locus, spanning nearly 1 Mb in 11p15.5.[1] The two major causes of BWS are increased *IGF2* expression or decreased *CDKN1C* expression. The growth inhibitor *CDKN1C* is normally expressed from the maternal chromosome 11. On the paternal chromosome, inhibition of *CDKN1C* is associated with the expression of a long noncoding RNA called *KCNQ1OT1* or *LIT1* antisense to *KCNQ1*, the potassium channel gene involved in long-QT-syndrome type 1 and Jervell/Lange-Nielsen syndrome. In contrast, the growth factor *IGF2* gene is expressed from the paternal chromosome only. On the maternal chromosome, the noncoding RNA gene *H19* is expressed instead. The choices between *H19* or *IGF2* expression, and *LIT1* or *CDKN1C* expression, are regulated epigenetically. *IGF2* expression is associated with methylation of the insulator (CTCF) binding sites between *H19* and *IGF2*, also called imprinting centre region 1 (ICR1), and *CDKN1C* expression is associated with methylation of the *LIT1* promoter, also called imprinting centre region 2 (ICR2).

The regulation of 11p15.5 imprinting that causes monoallelic paternal *IGF2* expression and monoallelic maternal *CDKN1C* expression is complex, which also explains why there are many different molecular causes of BWS.[2] The most common cause is reduced expression of *CDKN1C*, which is usually due to sporadically occurring reduction in maternal ICR2 methylation (~50% of BWS cases), but sometimes associated with maternal *CDKN1C* mutations (5–10%). The second most common cause is *IGF2* overexpression, usually due to paternal uniparental disomy of 11p (~20% of BWS cases), but also to inappropriate ICR1 methylation on the maternal allele, which inhibits *H19* and stimulates *IGF2* expression (~5%).[1] In the latter situation, small deletions or mutations in the ICR1 that are likely to disrupt the insulator function of the region have been observed with a high sibling recurrence risk.[3–8] Recently, it was found that such small and overlapping deletions of ICR1 had variable effects on methylation of the maternal ICR1, indicating that maintenance of maternal hypomethylation was partly dependent on the spatial arrangement of the CTCF binding sites.[8]

Here, we describe a family with a previously reported ICR1 single nucleotide variant (NCBI36:11:g.1979595T>C) in an OCTamer-binding transcription factor-4 (OCT4) binding site and a gradual increase in ICR1 methylation over the next two generations, the first generation being tall statured, the second generation having full-BWS phenotype with Wilms tumours. This family indicates that ICR1 mutations may affect the ability to establish a maternal ICR1 methylation pattern of the paternal allele in female gonads, that is,

[1]Center for Medical Genetics and Molecular Medicine, Haukeland University Hospital, Bergen, Norway; [2]Department of Clinical medicine, University of Bergen, Bergen, Norway; [3]Institut für Humangenetik, Universitätsklinikum Essen, Essen, Germany; [4]Faculty of Medicine, University of Southampton, Southampton, UK; [5]Wessex Genetics Service, Southampton University Hospitals Trust, Southampton, UK; [6]Salisbury Hospital NHS Foundation Trust, Salisbury, UK
*Correspondence: Professor G Houge, Center for Medical Genetics and Molecular Medicine Haukeland University Hospital, Jonas Liesvei N-5021, Bergen, Norway.
Tel: +47 55 97 54 44; Fax: +47 55 97 54 78; E-mail: gunnar.houge@helse-bergen.no
Received 3 October 2012; revised 2 March 2013; accepted 12 March 2013; published online 10 April 2013

to demethylate the paternal ICR1 region. Our data also indicate that the maternal and paternal ICR1 alleles are treated differently in the maternal gonads, that is, that the maternal alleles are not demethylated (if methylated) in the maternal germ line, and may later be subject to a passive (stochastic) increase in methylation. To the best of our knowledge, this is the first description of anticipation in an epigenetic syndrome.

PATIENTS AND METHODS

Family

BWS was diagnosed in two sisters (III-1 and III-2) and their male cousin (III-3, see Figure 1). Elective caesarean section was performed in both sisters due to large babies. Both sisters had classical BWS features including Wilms tumour and visceromegaly. III-1 was born in week 38 with macroglossia and large kidneys, birth weight was 4860 g (860 g > 97.5th centile), length 53 cm (97.5th centile). As an infant, she was successfully treated for Wilms tumour with chemotherapy. At age 6 years, an operative tongue reduction was performed. III-2 was born at term with macroglossia and large kidneys, birth weight 5280 g (880 g > 97.5th centile). At age 9 months, she was nephrectomised due to Wilms tumour in her right kidney and mild nephroblastomatosis in her left kidney was also detected. The sisters are now 10 and 13 years, and both have good school performances and growth parameters in upper percentiles (III-1 97.5th centile and III-2 95th centile). Their male cousin (III-3, DZ twin) died from medical complications after a caesarean section in week 29. There was marked polyhydramnios. Birth weight was 2130 g (330 g > 97.5th centile), length 44 cm, head circumference 28 cm and he had visceromegaly (especially of the kidneys), macroglossia and general subcutaneous oedema. In comparison, his healthy unaffected DZ sister III-4 was 1170 g (5th centile), 38 cm and had the same head circumference at birth. None of the three affected children had neonatal hypoglycaemia, were markedly asymmetric or had transverse creases on their ear helices. The children's two mothers and the mothers' sister were tall statured (178, 185 and 187 cm, that is, lengths from the 96th centile and above) with large hands, and at least one had mild BWS features (large tongue, protruding stomach) as a child (II-1 in Figure 1). The sisters' parents had heights of 173 cm (mother, 85th centile) and 180 cm (father, 75th centile), and none of them had any BWS-like features as infants. II-1 was born at term with a large tongue and birth weight 5 kg (0.4 kg > 97.5th centile). II-3 and II-4 are DZ twins born in week 31 with birth weights 1800 g (50th centile) and 2350 g (99th centile), respectively, and II-4 also had a large tongue. All sisters have very mild and asymptomatic scoliosis, no hemihyperplasia and normally sized tongues as adults.

Methylation specific multiplex ligation-dependent probe amplification (MS-MLPA) analysis and bisulphite treatment followed by subclone sequencing

Blood DNA samples were obtained from all individuals except III-1 and III-2, where only saliva DNA samples could be obtained. MS-MLPA copy number and methylation analysis of the BWS/Silver-Russell syndrome region on chromosome 11 was done in the routine diagnostic laboratory using the SALSA MLPA ME030 kit version C2 (MRC-Holland, Amsterdam) and following the manufacturer's instructions. We also obtained saliva DNA samples from II-1 and II-4 to compare with the results of MS-MLPA analysis of blood DNA, and similar levels of methylation was found: 0.7 in saliva DNA from both individuals, compared with 0.71 and 0.75 in their blood DNA (Figure 1). The bisulphite conversion of DNA was performed with Applied Biosystems methylSEQr Bisulphite Conversion Kit (Life Technologies, Carlsbad, CA, USA), according to the manufacturer's protocol. PCR was performed using primers designed by Methyl Primer Express Software v1.0 (Applied Biosystems, Life Technologies) for bisulphite sequencing-specific PCR. Forward primer: 5′-ATTATTTTGGTTTTTGGTGAGG-3′ (unconverted: 5′-ACCACCT TGGCCTTTGGTGAGG-3′); reverse primer: 5′-ATACCATAAAAATTCCCC-CATA-3′ (unconverted: 5′-ATGCCATGGAAATTCCCCCATG-3′) (HG19: chr11: 2019867-2020153). M13 tails were added to all the primers as part of our routine to obtain uniform PCR conditions. PCR was performed in a 25 µl reaction containing 1x AmpliTaq Gold 360 Master Mix Forward (Invitrogen, Life Technologies, Carlsbad, CA, USA), 16% 360 CG enhancer (Invitrogen, Life Technologies), 10 µM forward primer and 10 µM reverse primer. The PCR conditions were as follows: denaturation at 95 °C for 5 min, 5 cycles of 95 °C for 30 s, 50 °C for 2 min and 72 °C for 3 min, followed by 35 cycles of 95 °C for 30 s, 58 °C for 1 min and 72 °C for 3 min, and finally a hold at 60 °C for 60 min. The PCR products were then cloned using TOPO TA Cloning Kit for Sequencing (Invitrogen, Life Technologies), following the manufacturer's instructions. Ten clones were purified using QIAprep Spin Miniprep kit (Qiagen, Hilden, Germany) and sequenced by Sanger sequencing using the BigDye Terminator v1.1 Cycle Sequencing Kit (Applied Biosystems, Life Technologies, Calrsbad, CA, USA) with T3 or T7 primers. Clean up was performed using the using Big DyeX Terminator purification (Applied Biosystems, Life Technologies). The sequences were resolved on a 3730 Genetic Analyser (Applied Biosystems, Life Technologies) and analysed with QUMA (Riken, Japan). To calculate the average methylation level in controls ($n = 5$, including the grandmother of the family) and affected ($n = 3$ per generation, see Figure 1), the average of all measurements per sample was first calculated, and thereafter the mean per group (Table 1). For MS-MLPA, four repeated measurements per sample were done, and for bisulphite sequencing, seven informative positions with differential methylation were measured once per patient (see Supplementary Table 1 and Supplementary Figure 1 with legend for details). Five data points were noninformative because they were highly methylated in all samples with no difference between patients and controls (Supplementary Table 1), and these data points were therefore excluded. The individual MS-MLPA and bisulphite data can also be seen in Figure 1, and mean data with 95% confidence intervals can be found in Table 1.

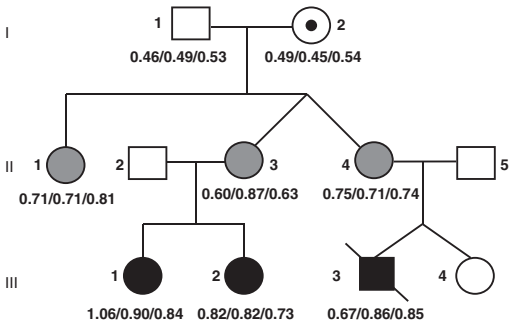

Figure 1 Family pedigree. The degree of methylation of the locus between *H19* and ICR1 was investigated by routine MLPA testing and bisulphite subclone sequencing, indicated by the (first ratio/) and (/middle ratio/), respectively. The methylation of the CTCF binding site 6 (CTS6) within the B1 repeat was investigated by bisulphite next generation sequencing, indicated by the (/final ratio) below the pedigree symbols.

Table 1 Mean degree of ICR1 methylation in the first, second and third generations with 95% confidence intervals (parentheses)

	MLPA-test	Bisulphite sequencing
1. generation ($n = 2$)	0.48 (0.45–0.51)	0.47 (0.39–0.55)
2. generation ($n = 3$)	0.71 (0.66–0.76)	0.75 (0.72–0.78)
3. generation ($n = 3$)	0.84 (0.81–0.87)	0.86 (0.81–0.91)

Abbreviations: ICR1, imprinting control region; MLPA, multiplex ligation-dependent probe amplification.

Bisulphite treatment followed by next generation sequencing

Bisulphite treatment was conducted using the EZ DNA Methylation-Gold Kit (Zymo Research Europe, Freiberg, Germany) according to the manufacturer's manual. For each individual bisulphite amplicon libraries were generated and sample-specific barcode sequences were added. The amplicons were purified, diluted and clonally amplified in an emulsion PCR before sequencing on the

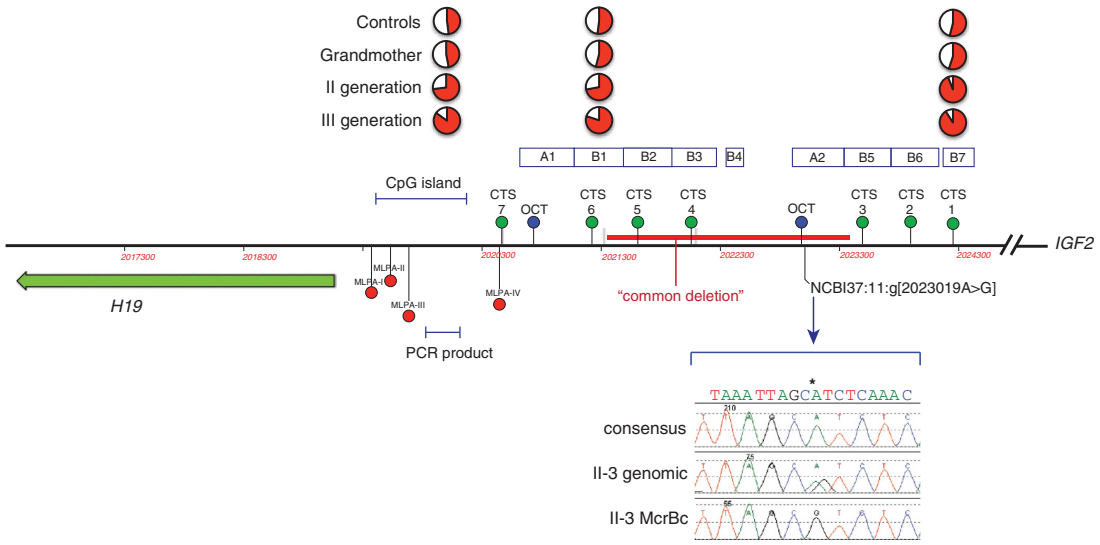

Figure 2 Illustration of the H19/IGF2 ICR1. Above the line approximate positions of CTCF binding sites are marked with green dots, and OCT4 sites are marked with blue dots. The position of a CpG island in the *H19* promoter is shown above the line. Below the line the differentially methylated CpG sites investigated by the routine MLPA kit are marked with red dots, and these sites are not included in the segment from the CpG island (marked as 'PCR product') that was investigated by bisulphite treatment followed by subclone sequencing and that contained seven differentially methylated CpG sites. The position of the common ~1.8 kb microdeletion[4] associated with BWS is marked with a red bar, and the OCT4 binding site mutation is also shown, as well as the sequencing result of II-3 before and after McrBc digestion of methylated DNA. Please note that the g.2023019A>G mutation corresponds to the T>C mutation on the antisense strand, which was described by[10]. The position of CTCF binding sites (CTS) in ICR1 are shown, and of these CTS6 and CTS1 were investigated by next generation bisulphite sequencing.

Roche/454 GS junior system was carried out. For subsequent data analysis the Geneious software (Biomatters, Auckland, New Zealand) and BiqAnalyzer HT were used.[9] A detailed description has been published elsewhere.[8] A minimum of 1058 reads for each sample was obtained. The average conversion rate was 99.0% for CTS1 and 99.1% for CTS6.

ICR1 sequencing

After confirmation of complete 11p15 grandmaternal haplotype segregation with large growth/BWS (Supplementary Figure 2), ICR1 and the H19 proximal promoter (HG19:chr11:2,020,402-2,024,682) were sequenced by standard methods from a product of 4281 bp generated using primers 5′-TGCACATACTTTG CACATGG/CGCTGTGGCTGATGTGTAG-3′, as described;[3] further details are available on request. To determine the parental origin of the sequence variant, 200 ng genomic DNA was cleaved using restriction enzyme McrBc (New England Biolabs, Ipswich, MA, USA) following the manufacturer's instructions; then DNA was desalted and concentrated using Amicon 30K microconcentrator columns (Millipore, Billerica, MA, USA) before amplification using primers 5′-CAACACA AGGATCCTAGACC/TCTTCGTATCGGGCCATATC-3′ and Sanger sequencing.

RESULTS

Our family shows dominant inheritance of BWS with a clinical picture that is compatible with anticipation (Figure 1). This impression was in line with the results of the routine MS-MLPA methylation testing of the BWS locus, which showed an increase in ICR1 methylation from normal level (0.49) in the grandmother to ~0.71 in the second generation with tall stature and ~0.84 in the third generation (Table 1, Supplementary Table 1), in the three children with classical BWS (Figure 1). These data were reproduced by bisulphite treatment and subclone sequencing to measure the degree of CpG-methylation of the *H19* differentially methylated promotor region (Figure 2).

To investigate whether the same tendency could be found in the CTCF binding sites (called CTS and numbered from 1 to 7) of the ICR1 repeats (Figure 2), the degree of methylation of two such sites was investigated by highly quantitative next generation bisulphite sequencing: CTS6 in B-type repeat B1, on the *H19*-side of ICR1, and CTS1 in B-type repeat B7, on the *IGF2*-side of ICR1 (Figure 2). Although CTS1 was fully methylated already in the grandmother's children (II-1, II-3 and II-4; Supplementary Table 1), CTS6 showed the same tendency towards increased methylation from generation II to III. In the mothers of generation II, the average degree of methylation was 73%, and in their children, the average degree of methylation was 81% (Figure 1). It thus seems that CTS1 was more prone to acquire methylation than CTS6.[8] To further illustrate the molecular correlation to the observed clinical anticipation, methylation heat maps of the degree of CTS1 and CTS6 methylation from the grandmother to daughters to grandchildren are shown in Figure 3. Of note, the degree of methylation in CTS6 correlates well with the clinical severity (Figure 3), that is, the number of BWS symptoms and findings (see above; II-3<II-4<II-1 and III-2<III-1<III-3). All normal individuals had heat map plots showing average (~50%) methylation (Supplementary Figure 3).

As dominant BWS can be associated with mutations in ICR1, between the *H19* noncoding RNA gene and the growth factor gene *IGF2*, this region was examined for mutations or deletions. Long-range PCR did not detect any microdeletions in ICR1 that could explain imprinting disturbances. However, ICR1 sequencing revealed the same maternal point variant NCBI36:11:g.1979595T>C (NCBI37:11:g.2023019T>C, see Figure 2) that had been described previously as a cause of BWS in three brothers.[10] To determine the parental origin of the variant, genomic DNA was digested with the

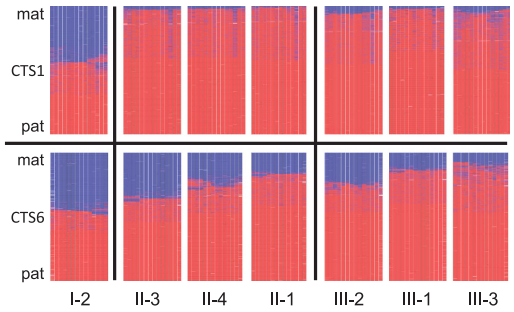

Figure 3 DNA methylation analysis: Heat maps of the methylation patterns obtained by next generation bisulphite sequencing of two CTCF binding sites: CTS1 and CTS6. The heat maps are ordered from left to right by the degree of methylation, and this also corresponds to the clinical severity. Only data from individuals harbouring the allele with the OCT4 binding site mutation is shown. The pedigree marks below the panels are the same as in Figure 1. Lines represent sequence reads, columns CpGs. Blue – unmethylated – maternal (mat); red – methylated – paternal (pat); white – missing sequence information.

methylation-sensitive restriction enzyme McrBC, which digests methylcytosine-containing DNA, and then amplified and sequenced. In the digested DNA from II-1 and II-3, the variant became apparently homozygous (II-3 result shown in Figure 2), indicating that it was present on the partially unmethylated, and therefore maternally inherited allele. In I-2, the non-affected grandmother, the opposite was found, indicating that the point variant was on the grandmother's paternal allele. Haplotype and sequencing information showed that the three sisters in generation II and the three affected children in generation III inherited this point variant, but not by the unaffected DZ sibling in generation III (Supplementary Figure 2).

DISCUSSION

From a clinical point of view, the second generation tall stature and third generation BWS in our family suggested anticipation (Figure 1). Alternatively, the increased clinical severity might be a random result of variable expression, not uncommon in BWS (see e.g. Scott *et al.*[11]). However, the increasing degree of methylation from the unaffected carrier grandmother of a paternal ICR1 variant over the two subsequent generations gave a molecular correlate to the observed anticipation (Figures 1 and 3, Table 1). The increased degree of ICR1 methylation was found both on routine MLPA-based methylation testing and bisulphite subclone sequencing of the CpG island region in the *H19* promoter, and bisulphite next generation sequencing of the CTCF binding site in the B1 repeat region of ICR1 (CTS6), but not the more *IGF2*-proximal CTCF binding site in the B7 repeat (CTS1) (Figures 2 and 3). Upon ICR1 sequencing to find a cause of the apparent anticipation, a previously found variant affecting OCT4 binding was found (Figure 2).[10] It was highly unlikely that this represented a founder mutation as the other family was French and the Norwegian family had no known French roots. Nevertheless, to exclude that this could be a founder mutation, Christine Gicquel was most helpful and sent us the SNP information of the ICR1 locus in their family, and when compared to our family, a common haplotype was excluded. We could therefore conclude that the same NCBI37:11:g.2323019T>C (NCBI36:11:1979595T>C) variant had occurred on two different genetic backgrounds.

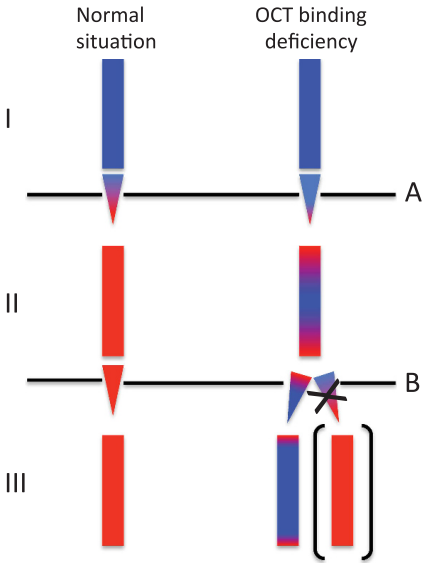

Figure 4 The imprinting status of the grand-grand-paternal allele after grandmaternal and maternal transmissions. The OCT4 binding site mutation apparently causes incomplete demethylation upon grandmaternal transmission (A), and further methylation upon maternal transmission (B). Of note, further demethylation, as in A, was not seen in B (marked by the X), suggesting that only paternal alleles can be demethylated in the maternal gonads. Blue = methylated (paternal pattern) and red = unmethylated (maternal pattern).

Recently, a family with another variant reducing OCT4 binding was described.[3] This variant 1979624A>C was 31 nt centomeric to the 1979595T>C variant found by Demars *et al.*[10] and us. Of note, in this family there were two affected brothers with prolonged post pubertal growth and final heights above the 99th centiles (204 cm and 208 cm, respectively), which is atypical for BWS patients. They also had renal problems, one had cysts and the other had a Wilms tumour, and neither was markedly asymmetric. This suggests that there may be clinical features that distinguish ICR1 mutation patients from other patients with BWS. None of the reported patients had the characteristic ear creases and growth did not decelerate in their teens, resulting in final statures above the 97.5th centile. If the latter also will hold true for the third generation in our family is yet unknown, as they are all children. Nevertheless, if a child with BWS and ICR1 hypermethylation has a tall statured mother, this should alert to the possibility of dominant inheritance, especially if the child also has Wilms tumour. Absence of ear creases should strengthen this suspicion.

It has previously been shown that the T>C variant in the ICR region affects OCT4/SOX2 binding,[10] and our data can be interpreted to imply that the variant interferes with gonadal switching from paternal to maternal imprinting. The same may be true for the A>C variant reported by Poole *et al.*[3] In the latter case, however, classical BWS occurred already in the first generation. One explanation for this discrepancy could be that the A>C variant is more detrimental to OCT4 binding than the T>C variant. Alternatively, the cause could be random variability in clinical expression. Our family suggests, however, that true anticipation as an explanation for increased clinical

severity may take place in BWS. This is supported by a recent report on the consequences of ICR1 microdeletions, where at least two of the six families had features compatible with anticipation, described as 'a kind of epigenetic memory effect' by the authors.[8] Possibly, the phenomenon of anticipation in BWS is not limited to OCT4 binding site mutations, but could be an explanation for non-penetrance in ICR1 deletion families as well. This has implications for genetic counselling of BWS families with ICR1 deletions or mutations. Transmission through the male germline implies a potential BWS risk not necessarily in the next, but in subsequent generations if the mutation is passed through the female germline. Second, transmission of the mutation through the maternal germline may first give rise to BWS in later (third and fourth) generations if the mutation is 'mild'.

From a more fundamental biological perspective, our findings give clues to how gonadal imprinting switching is regulated. The grandmother inherited a fully methylated paternal allele containing the T>C variant from her father, and a normal demethylated maternal allele from her mother. In the next generation, her three daughters inherited the grandpaternal ICR1 allele (with the T>C variant) and they had methylation levels of around 73%. This implies either that the grandpaternal allele was incompletely demethylated in their mother's gonads or that the variant allele was completely demethylated in the germline, but had reduced resistance to subsequent postzygotic remethylation. There are experimental data to support both of these suggestions.[12] A recent study showed that interference with OCT4 binding in P19 embryonic carcinoma cells rendered the H19 allele partially resistant to demethylation, but also that when partially methylated, further methylation seeding (remethylation) could easily take place.[13] Methylation seeding implies that inappropriate methyl groups recruit binding proteins that directly and indirectly promote both histone compaction and further DNA methylation. Moreover, on a more general genomic scale it has been shown that maintenance of imprinting marks in early zygotic development requires not only protection against postfertilisation demethylation, but also protection against somatic remethylation.[14] A similar requirement for OCT4/SOX2-binding elements to maintain the maternal demethylated state has been found in the Prader-Willi/Angelman syndrome imprinting centre.[15]

To explain anticipation, reduced protection against somatic remethylation is not enough. There must also be an element of demethylation resistance in the germline. However, even if the mutation caused only partial ICR1 demethylation to take place in the female germline (grandmother and daughters), one would still expect less ICR1 methylation in third generation (the children with BWS), not more. This remains true even if a susceptibility to somatic remethylation should vary somewhat from individual to individual. Of note, the grandpaternal (normal) allele inherited by III-4 (also confirmed by haplotyping, see Supplementary Figure 2) was completely demethylated in the same maternal gonad that could not demethylate the grandmaternal allele (II-4 in Figure 1). This indicates that mutations interfering with OCT4 binding may have different effects in paternal and maternal inheritance. Apparently, unlike the paternal allele, the maternal allele is incapable of being actively demethylated in the maternal germline—otherwise there would have been no anticipation. Our hypothesis on differential handling of paternal and maternal alleles in the maternal gonads is illustrated in Figure 4.

In conclusion, we have both clinical and molecular evidence for the occurrence of anticipation in rare cases of BWS, and our data also indicate that only paternally inherited *H19/IGF2* loci are demethylated in the maternal germline.

CONFLICT OF INTEREST

The authors declare no conflict of interest.

ACKNOWLEDGEMENTS

We are most grateful to the family for giving us the opportunity to gain further insight into mechanisms for BWS and Melanie Heitmann for expert technical assistance. This work was supported by HelseVest project no. 911744 and by the Bundesministerium für Bildung und Forschung (Network Imprinting diseases, grant No. 01GM1114A to K.B.).

1 Weksberg R, Shuman C, Beckwith JB: Beckwith-Wiedemann syndrome. *Eur J Hum Genet* 2010; **18**: 8–14.
2 Choufani S, Shuman C, Weksberg R: Beckwith-Wiedemann syndrome. *Am J Med Genet C Semin Med Genet* 2010; **154C**: 343–354.
3 Poole RL, Leith DJ, Docherty LE *et al*: Beckwith-Wiedemann syndrome caused by maternally inherited mutation of an OCT-binding motif in the IGF2/H19-imprinting control region, ICR1. *Eur J Hum Genet* 2012; **20**: 240–243.
4 De Crescenzo A, Coppola F, Falco P *et al*: A novel microdeletion in the IGF2/H19 imprinting centre region defines a recurrent mutation mechanism in familial Beckwith-Wiedemann syndrome. *Eur J Med Genet* 2011; **54**: e451–e454.
5 Riccio A, Sparago A, Verde G *et al*: Inherited and sporadic epimutations at the IGF2-H19 locus in Beckwith-Wiedemann syndrome and Wilms' tumor. *Endocr Dev* 2009; **14**: 1–9.
6 Demars J, Rossignol S, Netchine I *et al*: New insights into the pathogenesis of Beckwith-Wiedemann and Silver-Russell syndromes: contribution of small copy number variations to 11p15 imprinting defects. *Hum Mutat* 2011; **32**: 1171–1182.
7 Prawitt D, Enklaar T, Gartner-Rupprecht B *et al*: Microdeletion of target sites for insulator protein CTCF in a chromosome 11p15 imprinting center in Beckwith-Wiedemann syndrome and Wilms' tumor. *Proc Natl Acad Sci USA* 2005; **102**: 4085–4090.
8 Beygo J, Citro V, Sparago A *et al*: The molecular function and clinical phenotype of partial deletions of the IGF2/H19 imprinting control region depends on the spatial arrangement of the remaining CTCF-binding sites. *Hum Mol Genet* 2012; **22**: 544–557.
9 Lutsik P, Feuerbach L, Arand J, Lengauer T, Walter J, Bock C: BiQ analyzer HT: locus-specific analysis of DNA methylation by high-throughput bisulfite sequencing. *Nucleic Acids Res* 2011; **39**: W551–W556.
10 Demars J, Shmela ME, Rossignol S *et al*: Analysis of the IGF2/H19 imprinting control region uncovers new genetic defects, including mutations of OCT-binding sequences, in patients with 11p15 fetal growth disorders. *Hum Mol Genet* 2010; **19**: 803–814.
11 Scott RH, Douglas J, Baskcomb L *et al*: Constitutional 11p15 abnormalities, including heritable imprinting center mutations, cause nonsyndromic Wilms tumor. *Nat Genet* 2008; **40**: 1329–1334.
12 Hori N, Nakano H, Takeuchi T *et al*: A dyad oct-binding sequence functions as a maintenance sequence for the unmethylated state within the H19/Igf2-imprinted control region. *J Biol Chem* 2002; **277**: 27960–27967.
13 Hori N, Yamane M, Kouno K, Sato K: Induction of DNA demethylation depending on two sets of Sox2 and adjacent Oct3/4 binding sites (Sox-Oct motifs) within the mouse H19/insulin-like growth factor 2 (Igf2) imprinted control region. *J Biol Chem* 2012; **287**: 44006–44016.
14 Proudhon C, Duffie R, Ajjan S *et al*: Protection against de novo methylation is instrumental in maintaining parent-of-origin methylation inherited from the gametes. *Molecular cell* 2012; **47**: 909–920.
15 Kaufman Y, Heled M, Perk J, Razin A, Shemer R: Protein-binding elements establish in the oocyte the primary imprint of the Prader-Willi/Angelman syndromes domain. *Proc Natl Acad Sci USA* 2009; **106**: 10242–10247.

Supplementary Information accompanies this paper on European Journal of Human Genetics website (http://www.nature.com/ejhg)

incl
excl
I-2
II-4
III-3

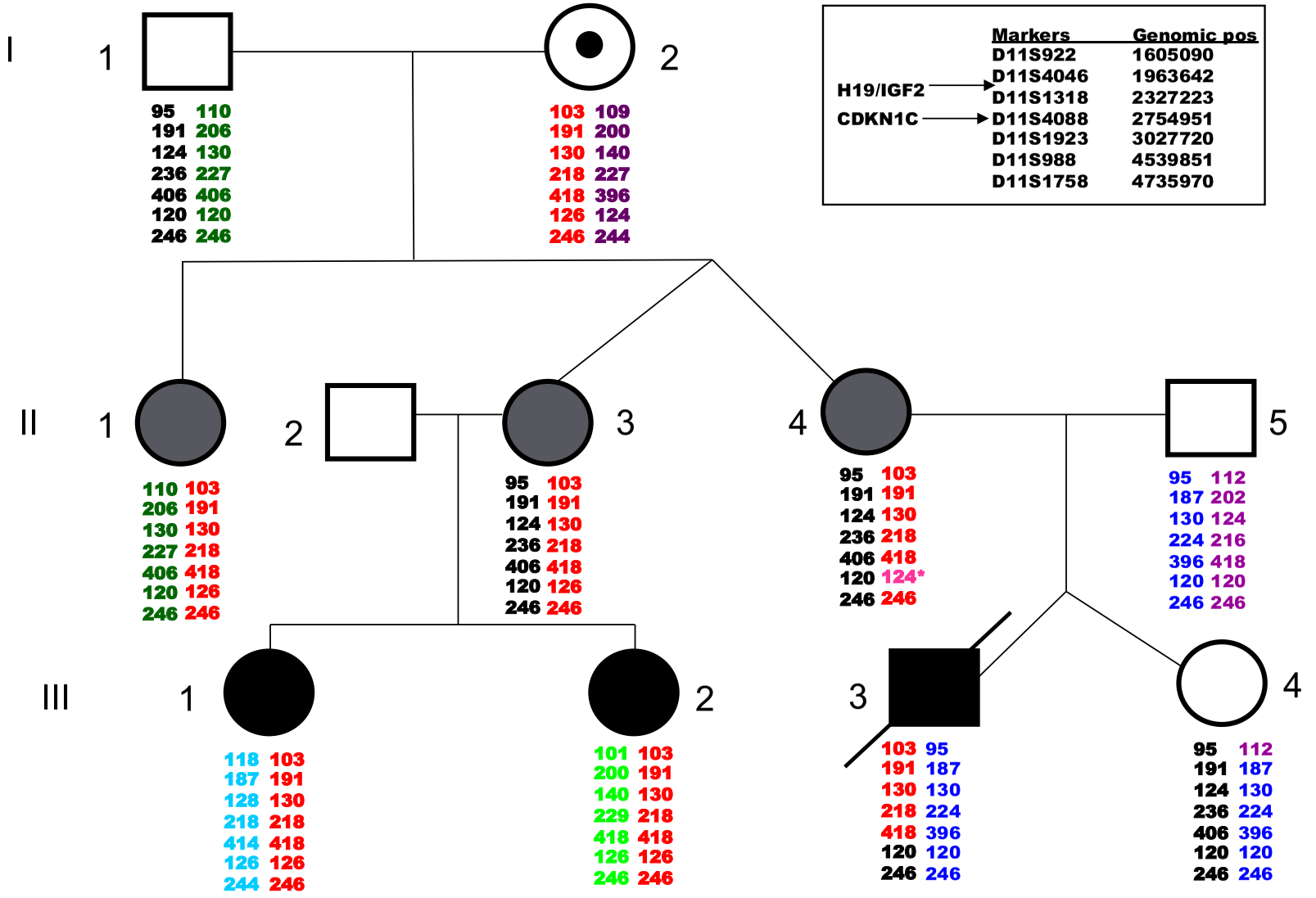
I
1
2
95 110
191 206
124 130
236 227
406 406
120 120
246 246
103 109
191 200
130 140
218 227
418 396
126 124
246 244
Markers
Genomic pos
D11S922
1605090
H19/IGF2
D11S4046
1963642
D11S1318
2327223
CDKN1C
D11S4088
2754951
D11S1923
3027720
D11S988
4539851
D11S1758
4735970
II
1
2
3
4
5
110 103
206 191
130 130
227 218
406 418
120 126
246 246
95 103
191 191
124 130
236 218
406 418
120 126
246 246
95 103
191 191
124 130
236 218
406 418
120 124*
246 246
95 112
187 202
130 124
224 216
396 418
120 120
246 246
III
1
2
3
4
118 103
187 191
128 130
218 218
414 418
126 126
244 246
101 103
200 191
140 130
229 218
418 418
126 126
246 246
103 95
191 187
130 130
218 224
418 396
120 120
246 246
95 112
191 187
124 130
236 224
406 396
120 120
246 246

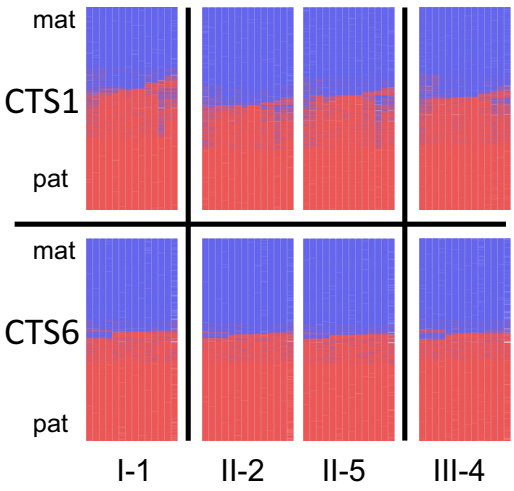
mat
CTS1
pat
mat
CTS6
pat
I-1
II-2
II-5
III-4

Supplementary Figure 1: This figure shows how the degree of methylation of an ICR1 segment (see Figure 2 for location) was measured by cloning and bisulphite sequencing, exemplified by three family members: I-2, II-4 and III-3. The segment contained 7 differentially methylated CpGs (the seven first positions) and 5 non-informative CpG positions that were excluded because of no differences between patients and controls, and stably high methylation degrees of 75-93%. The CpG positions are represented by circles, and a filled circle indicates methylation. In I-2 (grandmother), six subclones were successfully analysed, in the II-4 and III-3 eight subclones. All individual bisulphite sequencing data can be found in Figure 1 and Suppl. Table 1.

Supplementary Figure 2: Pedigree with results from the linkage analysis. The haplotypes are coloured, the red haplotype harbours the familial mutation. Upper right box shows the STR-marker names and position. The family's T>C variant is localized between the second and third marker. There are crossovers in individuals III-3 and III-4. In individual II-4, the *marks a probable polymerase slippage.

Supplementary Figure 3: DNA methylation analysis: Heat maps of the CTS1 and CTS6 methylation patterns obtained by next generation bisulphite sequencing in normal (control) individuals without the OCT4 binding site mutation. The pedigree marks below the panels are the same as in Figure 1. Lines represent sequence reads, columns CpGs. Blue – unmethylated – maternal (mat); red –methylated – paternal (pat); white - missing sequence information.

Raw data from MS-MPLA, bisulphite/subclone sequencing, and next-generation bisulphite sequencing analyses:

Methylation sensitive MLPA test using MRC-Holland kit ME030

Each data point average of 4 measurements.

DMR probe	8743-L8763	6266-L5772	11080-L11762	8744-L8764
I-1	0,55	0,44	0,44	0,50
I-2	0,47	0,48	0,52	0,47
II-1	0,82	0,67	0,71	0,74
II-3	0,67	0,58	0,62	0,61
II-4	0,72	0,66	0,85	0,75
III-1*	0,92	1,05	1,16	0,98
III-2*	0,89	0,84	0,87	0,76
III-3	0,71	0,61	0,74	0,67

Normal value ~0,5; full methylation ~1,0

*saliva-extracted DNA

Bisulphite treatment and subclone sequencing

Position	64	77	116	162	164	170	199	235	238	248	252	263
I-1	40	60	50	40	40	50	60	90	70	90	90	60
I-2	33	33	50	50	50	50	50	100	83	83	100	50
II-1	75	63	75	63	75	75	75	75	63	75	88	63
II-3	89	89	78	89	89	89	89	89	89	89	89	89
II-4	75	75	63	75	75	63	75	88	75	75	88	75
III-1*	91	100	82	91	82	91	91	100	100	100	91	82
III-2*	83	75	83	83	75	83	92	92	67	83	92	75
III-3	88	75	75	100	100	100	63	88	88	75	88	63
Ctr 1 (III-4)	73	64	64	82	100	82	80	100	91	91	100	91
Ctr 2 (II-2)	75	88	100	75	75	63	63	88	100	100	100	88
Ctr 3 (II-5)	64	73	73	55	73	64	73	82	100	91	91	73

Values show percentage of informative CpG positions that were methylated

Next-generation bisulphite sequencing

Position	CTS6	CTS1
I-1	53	58
I-2	54	55
II-1	81	95
II-3	63	93
II-4	74	94
III-1*	84	95
III-2*	73	91
III-3	85	89
Ctr 1 (III-4)	52	55
Ctr 2 (II-2)	52	50
Ctr 3 (II-5)	52	54

Values show percentage of CTS6 and CTS1 methylation
The number of reads were from 1058-4485, average 2887 reads.

OPEN ACCESS

Original research

Deep exploration of a *CDKN1C* mutation causing a mixture of Beckwith-Wiedemann and IMAGe syndromes revealed a novel transcript associated with developmental delay

Siren Berland ,[1] Bjørn Ivar Haukanes,[1] Petur Benedikt Juliusson,[2,3] Gunnar Houge[1]

► Additional material is published online only. To view, please visit the journal online (http://dx.doi.org/10.1136/jmedgenet-2020-107401).

[1]Department of Medical Genetics, Haukeland University Hospital, Bergen, Norway
[2]Department of Clinical Science, University of Bergen, Bergen, Hordaland, Norway
[3]Department of Paediatrics, Haukeland University Hospital, Bergen, Norway

Correspondence to
Dr Siren Berland, Department of Medical Genetics, Haukeland University Hospital, Bergen 5021, Norway;
siren.berland@helse-bergen.no

Received 18 August 2020
Revised 20 November 2020
Accepted 28 November 2020
Published Online First 21 December 2020

To cite: Berland S, Haukanes BI, Juliusson PB, *et al*. *J Med Genet* 2022;**59**:155–164.

ABSTRACT

Background Loss-of-function mutations in *CDKN1C* cause overgrowth, that is, Beckwith-Wiedemann syndrome (BWS), while gain-of-function variants in the gene's PCNA binding motif cause a growth-restricted condition called IMAGe syndrome. We report on a boy with a remarkable mixture of both syndromes, with developmental delay and microcephaly as additional features.

Methods Whole-exome DNA sequencing and ultra-deep RNA sequencing of leucocyte-derived and fibroblast-derived mRNA were performed in the family.

Results We found a maternally inherited variant in the IMAGe hotspot region: NM_000076.2(*CDKN1C*) c.822_826delinsGAGCTG. The asymptomatic mother had inherited this variant from her mosaic father with mild BWS features. This delins caused tissue-specific frameshifting resulting in at least three novel mRNA transcripts in the boy. First, a splice product causing CDKN1C truncation was the likely cause of BWS. Second, an alternative splice product in fibroblasts encoded IMAGe-associated amino acid substitutions. Third, we speculate that developmental delay is caused by a change in the alternative *CDKN1C-201* (ENST00000380725.1) transcript, encoding a novel isoform we call D (UniProtKB: A6NK88). Isoform D is distinguished from isoforms A and B by alternative splicing within exon 1 that changes the reading frame of the last coding exon. Remarkably, this delins changed the reading frame back to the isoform A/B type, resulting in a hybrid D–A/B isoform.

Conclusion Three different cell-type-dependent RNA products can explain the co-occurrence of both BWS and IMAGe features in the boy. Possibly, brain expression of hybrid isoform D–A/B is the cause of developmental delay and microcephaly, a phenotypic feature not previously reported in *CDKN1C* patients.

INTRODUCTION

The imprinted and predominantly maternally expressed cell cycle inhibitor *CDKN1C* located to 11p15.5 encodes a negative growth regulator also called $p57^{Kip2}$. This gene is associated with two contrasting phenotypes: the overgrowth disorder Beckwith-Wiedemann syndrome (BWS [MIM:130650]) and the growth-restricted IMAGe syndrome ([MIM:614732], an acronym for Intrauterine growth restriction, Metaphyseal dysplasia, Adrenal insufficiency and Genital abnormalities).[1] IMAGe and rare cases of Silver-Russel syndrome (SRS) are caused by gain-of-function (GoF) mutations in the PCNA-binding motif of CDKN1C, while loss-of-function (LoF) mutations are found in 8% of BWS cases.[2–4]

CDKN1C is a cyclin-dependent kinase inhibitor (CDI) belonging to the CIP/Kip family and encoded by a small gene with three to four exons of which two to three are protein coding. Other members are $p21^{Cip1}$ (CDKN1A) and $p27^{Kip1}$ (CDKN1B), which inhibit cell growth in G1 and can cause cell-cycle arrest. The ENSEMBL database (ensembl.org) contains several *CDKN1C* transcripts encoding different isoforms; *CDKN1C-202* encodes the 316aa isoform A, *CDKN1C-203* encodes an alternative isoform A with different UTRs, *CDKN1C-204* encodes the 305aa isoform B with an alternative start site and *CDKN1C-201* encodes the 131aa A6NK88 isoform that we call isoform D (see figure 1). CDKN1C has an N-terminal CDI (cyclin-dependent kinase inhibitor) domain, a central PAPA (proline-alanine) repeat and C-terminally the PCNA (proliferating cell nuclear antigen)–binding motif and an overlapping putative KRKR-containing nuclear localisation signal.

BWS is most often caused by sporadic loss-of-methylation (LoM) of imprinting centre 2 (IC2) on the maternal chromosome 11 that results in diminished *CDKN1C* expression, found in about 50%–60% of BWS, followed by paternal segmental uniparental disomy (UPD) 11p also involving the paternally methylated imprinting centre 1 (IC1) of the IGF2-H19 domain in about 20%.[5] IC1 gain-of-methylation (GoM) has been reported in 5%–10% of the patients, whereas microdeletions of IC1 and *CDKN1C* variants are important causes of familial BWS. Other chromosomal CNVs, balanced rearrangements, multilocus imprinting disturbances and mosaic genome-wide paternal UPD are rare causes of BWS. Typical features are omphalocele/umbilical hernia, macroglossia, neonatal hyperinsulinism, Wilms tumour, lateralised overgrowth, macrosomia, ear creases and pits, large internal organs, adrenal fetal cortex cytomegaly and renal abnormalities.[5 6] Genotype–phenotype correlations are reported as *CDKN1C* mutations have higher rates

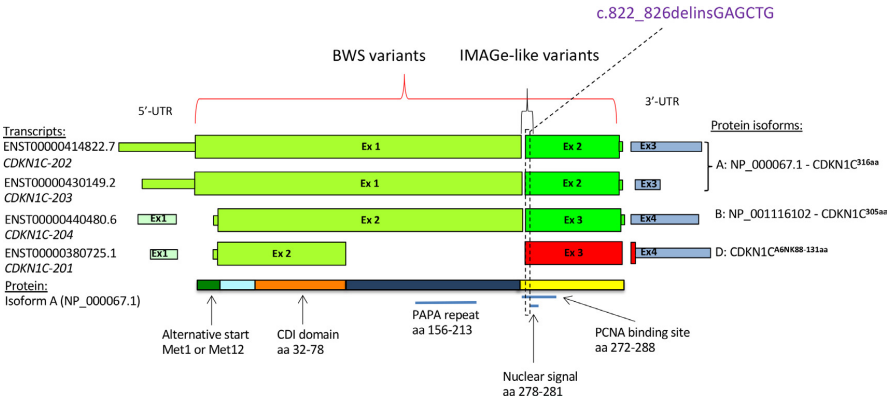

Figure 1 Overview of *CDKN1C* transcripts according to ENSEMBL GRCh38.p11, and corresponding protein isoform A. Above, the localisation of the patient's delins variant (purple and open vertical box) and reported IMAGe and Beckwith-Wiedemann syndrome (BWS) mutations. The transcripts are not drawn to scale. The narrow bars represent untranslated regions (UTRs). To the left, ENSEMBL reference transcripts, to the right protein isoforms (NCBI protein reference sequences if known). Below, isoform A (316 aa, NP_000067.1) with amino acid borders, domains, motifs, repeats and their approximate localisation. The protein isoform A of 316 aa is encoded by two different transcripts (*CDKN1C-202* and *CDKN1C-203*) with different lengths of UTRs but encoding identical amino acids. Isoform B (305 aa) uses an alternative start methionine, 11 aa downstream. A6NK88 is the UniProtKB accession code for the 131 aa protein isoform that we call isoform D. *CDKN1C-206* (encoding isoform C) is not included in this figure as this transcript was not detected in our analysis.

of preterm birth, cleft palate, abdominal wall defect, capillary malformations and ear signs, while intrauterine overgrowth and tumours are less common.[7 8] *CDKN1C*-restricted BWS features are also reported, including maternal pre-eclampsia, genital abnormalities, polydactyly, polythelia and posterior fossa abnormalities.[7 9–12]

Maternally inherited GoF variants can cause IMAGe syndrome, an SRS-like phenotype,[13] and short stature with diabetes,[14] but such variants are rare causes of growth restriction.[15–17] IMAGe was first described in 1999[18] and linked to *CDKN1C* in 2012.[4] Besides, SRS phenotype with salt-wasting due to adrenal insufficiency mimicking IMAGe was described in two patients with 11p15 maternal duplications.[19] So far, only 12 molecularly confirmed IMAGe/SRS-like families are reported, and all variants but one which we consider to be of unknown significance (VUS),[17] are located in the PCNA-binding site.[4 13 14 20–25] Most studies suggest that IMAGe/SRS variants increase protein stability,[13 20 26] although not confirmed by Kerns *et al*.[14] The mechanism is not fully elucidated but might include impaired proteasome-mediated degradation.[20] Clinical findings include short stature, neonatal adrenal hypoplasia, hypercalciuria, metaphyseal dysplasia with delayed bone age, low-set and posteriorly rotated ears, frontal bossing and relative macrocephaly, and less frequently hearing loss and craniosynostosis.[27] A *Drosophila melanogaster* IMAGe model showed impaired eye and wing growth,[4] demonstrating that cdkn1c plays a role in cell proliferation in multicellular organisms. There are no consensus criteria for IMAGe syndrome, and metaphyseal dysplasia and adrenal hypoplasia are not present in all. So far *CDKN1C* has not been associated with a neurological phenotype in humans, but developmental delay is reported in a few patients with BWS with structural brain abnormalities.[7 11 27] Furthermore, a mixture of IMAGe and BWS has not been published before.

Here, we report on a boy heterozygous for a delins variant in *CDKN1C*, replacing five nucleotides with six others in the junction between exons 1 and 2 of the main isoform. This delins caused a mixture of IMAGe and BWS-like features, and possibly also developmental delay as no alternative causes for this were found. We aimed to determine how this complex variant could have both GoF and LoF effects and to find a potential explanation for the affected brain function. Our work revealed that a novel *CDKN1C* transcript with a non-canonical C-terminal reading frame encoding isoform A6NK88 (named isoform D by us) was also affected by the delins, and as isoform D is also expressed in the brain, this could be the cause of his developmental delay.

METHODS

The boy and his family were clinically examined, given genetic counselling and consented to RNA analysis to investigate the molecular consequences of the *CDKN1C* variant.

Sanger sequencing

We used *CDKN1C* reference sequence NM_000076.2 encoding a 316 aa protein (isoform A). Sequence pilot (JSI Medical Systems, Ettenheim, Germany) software was used for interpretation. DNA was isolated from peripheral blood obtained from the boy, his parents, his mother's siblings, maternal grandparents and maternal grandfather's parents, and sequenced. To explore the mosaic pattern in the maternal grandfather, we analysed additional DNA obtained from buccal swab, urine and fibroblasts from four distinct skin biopsies.

RNA isolation, sequencing of cDNA and qPCR

Total RNA was isolated from fibroblasts from biopsies of healthy skin (two biopsies from the boy, one from his mother and four from his grandfather), one epidermal nevus in the boy and also from blood samples (from the boy, both parents and the grandfather) by using the RNeasy Mini Kit (QIAGEN, Hilden, Germany) for fibroblasts and PAXgene Blood RNA Kit (QIAGEN) for blood samples. cDNA was synthesised following the manufacturer's protocol. The variant was amplified by

quantitative qRT-PCR using different primer sets taking alternative acceptor site usage into account and also spanning the variant affecting transcript ENST00000380725.1 *CDKN1C-201* (for a full list of transcripts, see figure 1). The primer sequences are given in online supplemental file. We examined expression levels of wt (wild type) and mutant (delins) *CDKN1C*, and wt *CDKN1C-201* by qRT-PCR on RNA isolated from both blood and cultured fibroblasts from the boy (all biopsies), his mother and grandfather (where we picked the biopsy with highest mutation load), and blood from his father. Primers and probes were from Applied Biosystems, Life Technologies, and assessment of B2M (beta-2-microglobulin) RNA (Applied Biosystems) served as endogenous controls. At least two runs per experiment were performed, and two different probes for both *CDKN1C-201* and mutant *CDKN1C* were analysed.

Total RNA deep sequencing

We used blood-derived RNA from the boy, his mother and grandfather, and an unrelated healthy adult female, and fibroblast RNA from the boy's skin biopsy #2. Whole transcriptome sequencing libraries were generated using the Illumina TruSeq Stranded Total RNA kit with Ribo-Zero Gold depletion for fibroblasts and Ribo-Zero Globin depletion for blood, according to the manufacturer's protocols. Libraries were quality checked on the Agilent Bioanalyzer system and accurately quantified using the KAPA qPCR quantification kit. Libraries were paired-end sequenced on the Illumina HiSeq4000 system with a read length of 2×75 nt. Sequencing was performed ultra-deep for all libraries (~250 million reads per sample). RNA-sequencing reads were aligned to the human genome reference (GRCh38) using HISAT2 (V.2.0.5).[28 29] Reads aligned within the coding part of the genome (adequate Gencode gtf annotation file) were counted using featureCounts.[30] To resolve alternative *CDKN1C* transcripts, we created supplementary reference files in FASTA format and realigned reads. Data were visualised in IGV (Integrative Genomics Viewer V.2.3.74) (online supplemental file). We only considered splice junction tracks (SJTs) when counting reads and manually checked all reads in a region of interest. All samples were run in the same flow cell.

Whole-exome sequencing

Whole-exome sequencing (WES) was performed on genomic DNA isolated from blood from the patient and parents. DNA samples were prepared using SeqCap EZ MedExome Target Enrichment Kit (Roche NimbleGen, Madison, WI) and followed by paired-end 150 nt sequencing on an Illumina NextSeq500. The paired-end reads were aligned using the Burrows-Wheeler Alignment tool and variant calling was performed using the Genome Analysis Toolkit (GATK; Broad Institute, Cambridge, MA) according to GATK's Best Practices guidelines. Mean #reads per base pair in the exome was 83X with 97.7% of the base pairs covered at least 10 times. Data annotation and interpretation were performed using the NGS module of Cartagenia Bench Lab software (Agilent, Santa Clara, CA).

CNV and methylation analysis

The boy's DNA isolated from peripheral blood and fibroblasts (two from normal skin and one benign nevus) was analysed for 11p15 CNVs and methylation aberrations by SALSA MS-MLPA Probemix ME030-C3 BWS/RSS (MRC-Holland, Amsterdam, NL). Also, DNA from blood was tested for other imprinted diseases using the SALSA MS-MLPA Probemix ME032-A1 UPD7-UPD14, and for genomic CNVs by CytoScanHD Array (Thermo Fisher Scientific, Waltham, MA).

Table 1 Clinical findings in the patient and possible associations to *CDKN1C*-related syndromes

Clinical features	BWS (score)	IMAGe (NH-CSS)	New
Polyhydramnios	X (1)		
Pre-eclampsia in mother	X		
Omphalocele	X (2)		
Large tongue	X (2)		
Neonatal hypoglycaemia	X (1)		
Neonatal apnoea	X		
Infraorbital crease	X		
Midface retrusion	X		
Long and grooved philtrum	X		
Nevus flammeus	X (1)		
Ear creases	X (1)		
Patent ductus arteriosus	X	X	
Inguinal hernia	X	X	
Cryptorchidism, bilateral	X	X	
Small testes		X	
Small for gestational age		X (1)	
Long gracile diaphysis		X	
Broad metaphysis		X	
Delayed bone age		X	
Bifrontal bossing		X	
Low set, posteriorly rotated ears		X	
Feeding difficulties		X (1)	
Broad nasal bridge and tip		X	
Hypotonia		X	
Small kidneys		?	X
Thin upper lip			X
Strabismus	?		X
Rib synostosis			X
Developmental delay			X
Microcephaly (postnatal)			X
Relative macrocephaly at birth		X (1)	

The number in parentheses are criteria score according to Beckwith-Wiedemann syndrome (BWS) clinical consensus score and Netchine-Harbison Clinical Silver-Russel Syndrome score (NH-CSS).[6 33]

Microsatellite analysis

To determine *CDKN1C* haplotypes and allele segregation, and to explore on which parental allele the grandfather's de novo variant arose, an informative haplotype was set up by simple tandem repeat markers amplified by PCR and size determined. There were two informative markers upstream and four downstream of *CDKN1C* (online supplemental file). The haplotype analysis was performed on DNA from peripheral blood from the patient, his parents, his mother's siblings, maternal grandparents and the grandfather's parents.

RESULTS

Clinical history and findings in the boy

Clinical findings in the patient are summarised in table 1 and illustrated in figure 2. Omphalocele was discovered by routine ultrasound in week 19 of gestation, amniocentesis was performed, and the pregnancy was complicated by maternal hyperemesis, pre-eclampsia, diabetes from week 29 and later polyhydramnios. He was born after caesarean section in gestation week 34+2

Figure 2 Boy at age 3 months (A, C, D), 6 months (B) and 27 months (G, F), with clinical features of both Beckwith-Wiedemann syndrome (ie, omphalocele, midface retrusion, large cheeks, hypertelorism with down-slanted palpebral fissures, infraorbital and ear creases, a fading glabellar capillary malformation, and a long and marked philtrum with a thin upper lip, wide mouth with a high palate and macroglossia) and IMAGe (slender habitus, feeding difficulties, frontal bossing, broad nasal bridge and a wide tip, low set and posteriorly rotated ears, long and slender finger and toes). Radiographs of leg (G) showing long and slender diaphysis and broad metaphysis, with a delayed bone age of fingers (F).

with birth weight 2160 g (−1.1 SDS), birth length 42 cm (−2.5 SDS) and head circumference 32 cm (0 SDS) (all measurements adjusted for prematurity). Placental weight was on the 90th percentile. Apgar score was 3/5/7 after 1, 5 and 10 min, respectively. He had mild hypoglycaemia (1.5 mmol/L) and compromised respiration. The giant omphalocele also contained liver tissue, and he underwent several surgeries before the abdominal wall finally was closed at 3 months of age. He suffered from apnoeic spells and needed CPAP until he was discharged from the hospital 5 months of age. He was exclusively fed by nasogastric tube for the first 5 months, and the tube was removed after 12 months. At the age of 3 years, he had been through more than 20 surgeries, including for patent ductus arteriosus, inguinal hernia and cryptorchidism. He had dysmorphic features as illustrated in figure 2, small intra-abdominal testes, multiple benign epidermal nevi and mild hypotonia. At follow-up at 25 months of age, his length was 0.8 SDS, weight −2.0 SDS and he was now microcephalic (−2.7 SDS). Motor milestones were delayed; he could sit at 15 months and walk without support at 2 years and 10 months of age. At age 3 years, he could speak a few simple words, and at age 5 years he had 3–4 words sentences with articulation problems. He had a normal neurological examination, hearing, vision and social development, but marked global delayed yet without formal assessment. He received speech, education and physical therapy. Cerebral MRI was normal, repeated abdominal ultrasounds from the age of 4 months showed small kidneys bilaterally and no organomegaly. At 2.5 years, an ACTH-stimulation test did not reveal adrenal insufficiency, and skeletal X-ray showed long and slender diaphyses, broad metaphyses, a fusion of left fourth and fifth ribs, and a 1.5-year delay in bone maturation. At age 5 years, his length was −1.5 SDS, head circumference centiles unchanged, confirming a postnatal/secondary microcephaly (−2.5 SDS), and he still had a low BMI of 12.9 (−2.8 SDS). He was scheduled to cancer surveillance every sixth month until 7–8 years of age.

Family history

The boy's phenotypically normal parents are non-consanguineous, the mother was 28 and the father 42 years at his birth. Clinical examination and birth history in the mother were negative for BWS features. Head circumferences were at 99th percentile (mother) and 60th percentile (father). The maternal grandfather was >5 kg at birth, and a large tongue was commented on neonatally, suggesting macroglossia. At examination at age 58 years, he was 181 cm tall with a wide mouth, slightly short halluces, no asymmetry, a normal skeletal X-ray survey and normal cognition.

Diagnostic workup

During pregnancy, a normal male karyotype 46,XY was found in amniotic fluid cells. After birth, clinical suspicion of BWS in the boy warranted MS-MLPA of the BWS region, which was normal in DNA from blood, skin and epidermal nevus. However, sequencing of *CDKN1C* verified BWS (see next section). Due to borderline short stature, developmental delay and postnatal microcephaly, further analyses were performed with normal results: high-resolution CNV analysis, UPD screening and trio-based WES.

Interpretation of the *CDKN1C* variant

Sanger sequencing of *CDKN1C* (NM_000076.2/ENST00000414822.7) revealed a heterozygous delins variant in the sequence encoding the PCNA binding motif affecting the

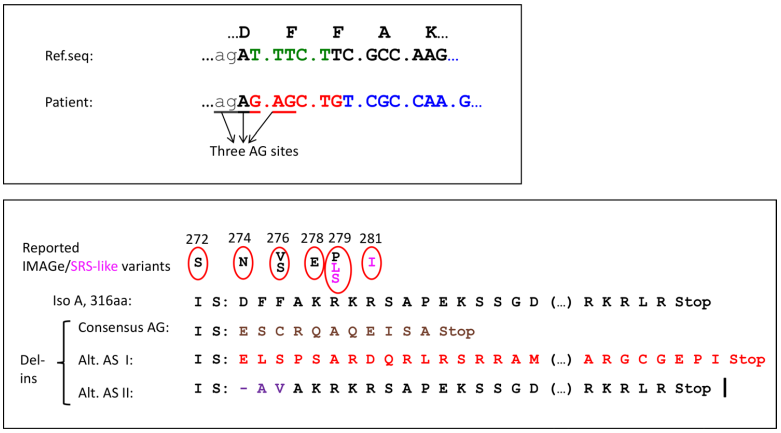

Figure 3 Predicted impact of the delins variant c.822_826delinsGAGCTG on DNA and isoform A. Upper panel shows the CDKN1C intron 2/exon 3 junction with reference amino acids on top and the reference nucleotide sequence (ENST00000414822.7, CDKN1C-202) just below. Intron sequences are written in lower case letters and exon sequences in capital letters. The five deleted nucleotides are in green. The bottom line shows the mutated sequence with the six inserted nucleotides in red, the three adjacent AGs (potential acceptor sites/AS) underlined and the out-of-frame sequence marked in blue. The lower panel shows details of the predicted amino acid sequence and changes introduced by the delins variant in amino acid numbers according to protein isoform A (316aa—NP_000067.1). On top reported IMAGe (black) and Silver-Russel syndrome (SRS)–like variants (magenta) from literature with the corresponding amino acid change, then the reference protein product, followed by the mutated products using the consensus AG (p.Asp274GlufsTer12), the protein product if alternative acceptor site I is used (p.Asp274GlufsTer47) and the protein product if alternative acceptor site II is used (p.Asp274_276delinsAlaVal). Parentheses (…) represent 21 amino acids omitted from the figure.

5′-end of exon 2: c.822_826delinsGAGCTG. The delins caused frameshifting and a premature termination codon (PTC) about 100 nucleotides upstream of the exon 2–3 junction. This change should either lead to nonsense-mediated mRNA decay (NMD) or synthesis of a truncated protein Asp274GlufsTer12, that is, an LoF change that fits with BWS phenotype. However, the delins also introduced two new putative splice junction AG acceptor sites, in addition to the consensus AG site (figure 3, upper panel). Use of alternative acceptor site I will also lead to a frameshift and a new stop codon, but in the very last protein-coding exon, that is, Asp274GlufsTer47, which should escape NMD (figure 3, lower panel). The corresponding protein product contains a modified C terminus including substitutions of four IMAGe-associated amino acids and introduce the known GoF variant Phe276Ser.[4] Use of alternative acceptor site II would be in line with the canonical reading frame of the protein's C-terminal part, but also include deletion of three and insertion of two new amino acids in the PCNA-binding motif: 274_276delinsAlaVal. This would modify one IMAGe residue (Asp274Ala), but also introduce a previously reported IMAGe-associated substitution: Phe276Val (figure 3).[4] This alternative transcript can be compared with known IMAGe-mutated transcripts, resulting in increased protein stability or affected PCNA binding.

The predicted out-of-frame C-terminal product from alternative acceptor site I, p.(Asp274GlufsTer47) (figures 3 and 4), was analysed by BLAST and found to be almost identical to *CDKN1C-201,* encoding a 131 amino acid isoform we call isoform D (UniProtKB accession A6NK88). Isoform D consists of the common CDI domain with a unique C-terminal D-tail, marked in red in figure 4, and its alternative splicing bypasses the PAPA-repeat region (figure 1). In addition to the PCNA-related amino acid substitution, the delins could also affect isoform D by introducing a frameshift that changed the reading frame back to the canonical reading frame (marked in yellow in figure 4). The predicted hybrid protein had elements from two distinct isoforms, D and A/B, where the D-type splicing causes direct connection of the CDI domain to an altered PCNA-binding motif, and where delins-induced frameshifting causes the C terminus to be of A/B type and not D type.

Diagnostic analysis of the family

The boy's asymptomatic mother was also heterozygous for the delins, compatible with a paternally imprinted allele in her, and further family studies including haplotype segregation analysis confirmed that the variant arose de novo on the grandfather's maternal allele. The mild BWS features in the grandfather indicated mosaicism, which was confirmed by DNA analyses of multiple tissues; only wt was present in fibroblasts from three out of four skin biopsies and a buccal swab, while the delins was found in blood, urine sediment and skin biopsy from the left leg. cDNA Sanger sequencing and qPCR cDNA sequencing confirmed the presence of both wt and (at a lower level) the delins allele in the boy, his mother and grandfather. Gene expression levels appeared generally low. Only in fibroblasts from the boy, the delins seemed to be more abundant than the wild-type transcript. Primers were also designed to cover the use of the two alternative splice acceptor sites illustrated in figure 3, but corresponding isoform-A/B-derived transcripts were not detected. However, sequencing demonstrated that wild-type isoform D (*CDKN1C-201*) transcript was present in blood from all family members and controls, and the delins-*CDKN1C-201* transcript was present in blood from the boy.

Semi-quantitative real time-PCR (qPCR) verified the presence of both *CDKN1C* (isoform A/B) and *CDKN1C-201* (isoform D) transcripts in blood samples from the patient, parents and grandfather. Also, isoform A/B was found in fibroblasts from all family members. Transcript levels were low compared with the B2M control and considerably lower in fibroblasts than in blood. Expression of delins-*CDKN1C* was seen in blood from

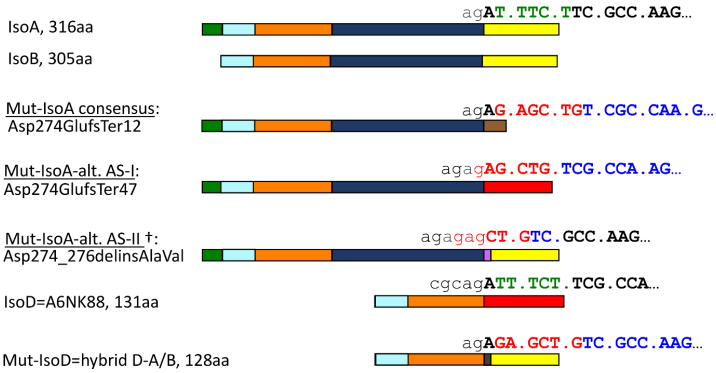

Figure 4 Overview of the predicted protein products. From top, wild-type isoform A (encoded by transcripts ENST00000414822.7=CDKN1C-202 and ENST00000430149.2=CDKN1C-203), wild-type isoform B (ENST00000440480.6=CDKN1 C-204), followed by three predicted CDKN1C protein variants of mutated isoform A depending on the splice acceptor site used; consensus acceptor site and alternative acceptor sites I or II. At the bottom, isoform D (A6NK88, encoded by ENST00000380725.1=CDKN1 C-201, with a reading frame different from isoforms A and B) and the mutated isoform D (hybrid isoform D–A/B), consensus acceptor site used. The colours correspond to regions in figures 1 and 3, where intron sequences are written in lowercase letters and exon sequence in capital letters. The five deleted nucleotides are in green. The six inserted nucleotides in the mutated (delins) sequences are shown in red, and the out-of-frame sequence marked in blue. † denotes a predicted transcript that was not found on RNA sequencing.

the boy and grandfather, but not the mother, while expression in fibroblast was very low in the boy and undetectable in others. Results from cDNA sequencing and qPCR are not shown.

NGS-based cDNA sequencing

Ultra-deep RNA-seq was done for a more quantitative non-biased analysis of all transcripts, including the delins variant. The results are illustrated in figure 5. In summary, the analysis confirmed that the level of delins was 40%–50% in the boy (higher in fibroblast than in blood), 25% in the mosaic grandfather and 6% in the mother; that activation of alternative acceptor site I occurred in the boy's fibroblasts; and that *CDKN1C-201* represented 16%–42% of the total *CDKN1C* mRNA reads but accounted for the majority of the delins reads. Neither standard nor ultra-deep RNA sequencing could verify the presence of a predicted fifth transcript *CDKN1C-206* (ENST00000647251.1) that encodes a putative 175 aa protein product labelled isoform C (CCDS86169.1).

All RNA-seq samples had in total >340 million reads after filtering, and the numbers of *CDKN1C* tracks spanning splice junctions (SJTs) were between 35 and 204 (figure 5A). Visualisation of the alignment to NCBI Build 38 is presented with the counting of SJTs (online supplemental file). No delins reads were mapped against Build 38, and we suspected mapping problems. We then created three new FASTA reference files with the delins for accurate mapping (online supplemental file), one based on the consensus splice site and two with alternative acceptor sites I and II. Alignment to one of these putative delins splice sites unmasked the delins-specific tracks, while the other two alignments did not add more data and were therefore not further analysed. Figure 5A shows the result from the mapping of transcripts *CDKN1C-202, CDKN1C-203, CDKN1C-204* (combined) and *CDKN1C-201* against the reference sequence (green columns), and the distribution was compared with the sum of other *CDKN1C* transcripts. Likewise, the pink columns show the distribution of delins-mapped reads. The total distribution of delins and *CDKN1C-201* is also presented. SJTs presented as arcs in IGV (online supplemental file) showed that the vast majority of expressed transcripts have splicing from 5′-UTRs of different lengths, including *CDKN1C-201* and *CDKN1C-204*, and both use the alternative Met11 amino acid downstream and have four exons. In contrast, *CDKN1C-202* and *CDKN1C-203* always start at Met1 and have three exons. *CDKN1C-203* uses an alternative acceptor splice site five nucleotides downstream in the last exon and can be distinguished from other transcripts. The coding part of *CDKN1C-201* continues into exon 4, while this exon is making a 3′-UTR in other transcripts.

DISCUSSION

This family, where the index case has a mixture of diametrically opposed growth-related syndromes due to the same delins variant in *CDKN1C*, illustrates that the biological complexity of this small gene goes far beyond imprinting. Due to intricate gene splicing with frameshifting, this delins has an LoF effect on some isoforms and GoF effect on another. The latter is unexpected for a five against six nucleotides exchange and is due to the creation of a new splice acceptor site two nucleotides downstream of the canonical AG. Furthermore, we demonstrate that an alternative isoform with a different C-terminal reading frame (that we call isoform D, corresponding to transcript *CDKN1C-201*) is also affected, which turns the C terminus of isoform D back to the isoform A/B reading frame. If the hybrid D–A/B isoform transcript is expressed in the brain, this could be the cause of his developmental delay.

The asymptomatic carrier mother expressed the delins at a low level, as expected for a leaky paternally imprinted allele. The maternal grandfather was mosaic for the delins on his maternal allele, in agreement with an intermediate expression level. As a cautious note, the relative levels of the transcripts are not indicative of the degree of imprinting due to variable and poor expression, also affected by presumably inconsistent and non-uniform NMD. Variation in NMD efficiency within mRNA with the same PTC and subpopulations of mRNA escaping decay are reported, and this can contribute to explaining variation between individuals and between different tissues.[31 32]

Ultra-deep RNA sequencing proved to be superior to conventional RNA analysis, particularly on fibroblast RNA. Such unbiased sequencing verified the use of alternative acceptor site I and

A

	Map: Ref seq Build 38; wt SJT ex 2-3			Map: FASTA file with delins; delins SJT ex 2-3				% delins	% Iso D	
		CDKN1C-202,203,204 Iso A+B	*CDKN1C-201* Iso D		*CDKN1C-202,203,204* Iso A+B	*CDKN1C-201* Iso D	Alt.I AC Iso A+B			Total reads passing filter
	Total Wt	% (reads)	% (reads)	Total delins	% (reads)	% (reads)	% (reads)	% (delins/total)	% (isoD/IsoABD)	
Patient –Bl	62	77.4% (48)	22.6% (14)	43	30.2% (13)	69.8% (30)	-	41.0% (43/105)	41.9% (44/105)	476,053,970
Control-Bl	45	84.4% (38)	15.6% (7)	-	-	-	-	0% (0/45)	15.6% (7/45)	371,783,318
Mother-Bl	33	60.6% (20)	39.4% (13)	2	50% (1)	50% (1)	-	5.7% (2/35)	40.0% (14/35)	379,826,523
Grandfather-Bl	58	72.4% (42)	27.6% (16)	20	20% (4)	80% (16)	-	25.6% (20/78)	41.0% (32/78)	340,350,007
Patient-Fibr	92	66.3% (61)	33.7% (31)	112	44.6% (50)	44.6% (50)	10.7% (12)	54.9% (112/204)	39.7% (81/204)	340,350,007

B

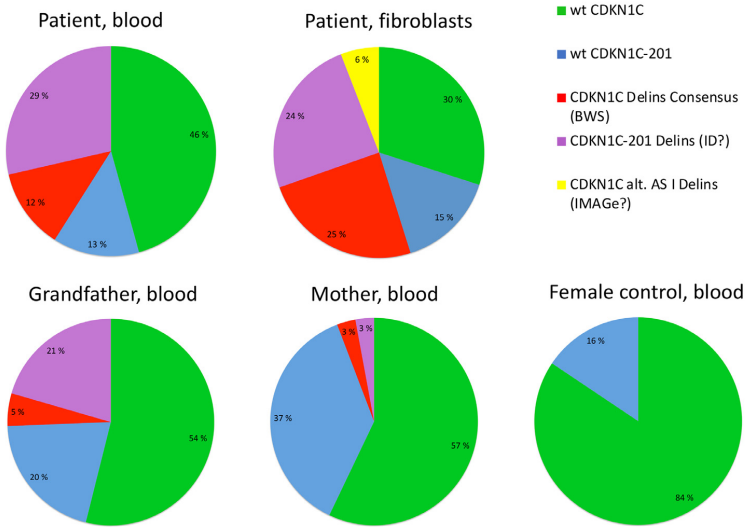

Figure 5 Result from NGS-based cDNA sequencing. (A) The number of reads spanning exon junctions (splice junction tracks, SJTs) after mapping to the reference sequence (from Genome Build 38, green background) and the delins-containing sequence (manually designed reference sequence, pink background). Reads with delins are shown in red. All reads were manually checked, and only SJTs spanning exons 2–3 are counted. Numbers are derived from figures as in the last part of the online supplemental file 1. Of note, reference sequence mapping did not detect any delins reads, probably because they were filtered out due to the complexity of the delins variant. (B) Sector diagrams illustrating the distributions of documented transcripts from RNA sequencing of RNA derived from blood samples and fibroblast. The percentages are calculated from the numbers in figure 5A. It was not possible to discriminate all *CDKN1C* transcripts by RNA sequencing, so *CDKN1C-202, CDKN1C-203* and *CDKN1C-204* are collectively referred to as *CDKN1C* in this figure, but *CDKN1C-201* transcripts (isoform D, UniProt: A6NK88) are identified. Green and blue colours represent wt reads of *CDKN1C* and *CDKN1C-201*, respectively, and red and purple colours represent delins reads using the consensus acceptor site in *CDKN1C* and *CDKN1C-201*, respectively. A fifth transcript (yellow) with delins *CDKN1C* using alternative acceptor site I, p.(Asp274GlufsTer47), was only documented in RNA from fibroblasts in the boy. The predicted or hypothetical clinical consequences of each of the four different mutated transcripts are noted in parentheses.

enabled us to quantify the expression of different transcripts, which again suggested which isoforms were most abundant. RNA sequencing as a first choice in a diagnostic pipeline would have been unsuccessful in this family as the delins could not be mapped with a single track against the reference sequence, but we solved this by mapping against dedicated reference files.

In summary, the boy fulfilled the clinical criteria of BWS—an overgrowth condition—despite being rather small and microcephalic, with a total score of 8, with two cardinal features (omphalocele and macroglossia) and four suggestive features (see table 1).[6] Macrosomia or neonatal overgrowth is common in BWS but is considered a suggestive and not a cardinal feature. There is no clinical consensus for IMAGe, but many of his non-BWS features overlap with this diagnosis. Adrenal insufficiency was never confirmed, but a mild and transient neonatal insufficiency could have been masked by continuous intravenous treatment of a leaking omphalocele. Genital abnormalities are described in both IMAGe and BWS, but small testes in IMAGe only.[22] Even though the renal size is not discussed in IMAGe (only fetal renal cortex size), his renal hypoplasia could very well be an IMAGe mirror of renal hyperplasia in BWS. Skeletal abnormalities are important findings in IMAGe, but besides asymmetry less important in SRS and are not features of BWS. Clinically, he did not pass the Netchine-Harbinson SRS score, having 3/6 criteria which is below the 4/6 limit.[33] His being small for gestational age, feeding difficulties, mild skeletal abnormalities and small testis are compatible with IMAGe, but this diagnosis is not definite as adrenal hypoplasia and metaphyseal

dysplasia were not documented. The clinical findings point to dual molecular effects with both LoF (BWS) and GoF (IMAGe) in CDKN1C. The latter can be explained by p.Asp274_276delinsAlaVal encoding transcript from alternative acceptor site II, but we could not confirm expression of this transcript in the two tissues tested. Another hypothetical GoF candidate is the p.Asp274GlufsTer47 encoding transcript from alternative acceptor site I with a verified GoF substitution Phe276Ser.[4] This transcript encodes an alternative C-terminal abolishing the PCNA-binding site, but the product might also be non-functional or degraded. Probably NMD is inefficient as a protective mechanism in *CDKN1C* as the truncated transcript from the consensus splice site, that is, encoding p.Asp274GlufsTer12 which is well within theoretical criteria for NMD, was present in both blood and fibroblasts.[34] This mutant product also substitutes IMAGe-related amino acids (figure 3) and might also have GoF effects.

A combination of opposing phenotypes due to a single mutation in the same gene is not reported earlier for *CDKN1C*, but for *GNAS*, another imprinted gene, this is not new.[35] Other genes where a variant is reported to cause both GoF and LoF effects are *RET*, *FLNA*, *GDF5* and *SMCHD1*.[36–39] In general, multinucleotide variants are potentially more damaging than single-nucleotide variants, illustrated by our family.[40]

The most intriguing finding was that the delins also affected a hitherto not confirmed transcript using a non-canonical reading frame—*CDKN1C-201*—which represented ~40% of all *CDKN1C* transcripts in the family (figure 5A). In contrast to wt *CDKN1C-201*, delins-mutated *CDKN1C-201* used the canonical reading frame, resulting in a hybrid D–A/B product that may be the cause of the unusual features in the boy. Alternative non-canonical reading frames are common in prokaryote and mitochondrial genes, but less so in eukaryotic and human genes, and another cell-cycle inhibitor gene, *CDKN2A*, is perhaps the most known example. This gene encodes at least two different proteins from different reading frames, p16(INK4) and p14(ARF). Both of these have splice variants, p16-gamma and p12, respectively, with tissue-specific expression.[41 42] Maybe this kind of regulatory complexity is a peculiarity of cyclin-dependent kinase inhibitors.

Our study identifies *CDKN1C-204* (isoform B) as the most abundant transcript, followed by *CDKN1C-201* (isoform D). The GTEx portal (gtexporal.org) suggests *CDKN1C-201* to be the most abundant isoform, particularly in the brain, followed by the isoforms encoded from *CDKN1C-204* and *CDKN1C-202,* but this could be explained by poor coverage of the PAPA-repeat region not included in the *CDKN1C-201*, that is, be artefactual. *CDKN1C-201* is only reported in humans and some higher primates.

Despite high *CDKN1C* expression in the embryonic brain, developmental delay and microcephaly are not considered features of either BWS or IMAGe, although brain abnormalities are reported in some patients.[7 11 43] However, behavioural and emotional difficulties and autistic spectrum disorders were found to be more frequent in BWS than controls, especially among patients with IC2 defects.[44] Moreover, in a cancer predisposition syndrome clinic, half of the patients with BWS or isolated hemihypertrophy needed special therapy.[45] Protein studies in embryonic brains of mice and rats suggested that Cdkn1c regulated newly formed migrating neurons,[46] and played a CDI-independent role in the maturation of midbrain dopaminergic neurons.[47] Differential spatial and temporal Cdkn1c expression in embryonic brain could be important for neurogenesis and gliogenesis, differentiation and generation of adult neural stem cells.[48–50] During cortical development, the differentiation of projection neurons was regulated via Cdkn1c.[51] According to a recent study, increased neuronal Cdkn1 expression resulted in abnormal social behaviour, implying that tightly regulated monoallelic expression is beneficial for neurological function.[52] Unexpectedly, brain-specific conditional deletion of the imprinted paternal *cdk1c* allele in mice resulted in microcephaly and thinning of the neocortex, despite low paternal expression (1%–2% of maternal levels) in control brains.[53]

The delins-mutated hybrid D–A/B transcript is our best explanation for the child's developmental delay. Brain damage due to neonatal hypoglycaemia or an untreated adrenal crisis was highly unlikely, and his brain MRI was normal, but prematurity and long hospitalisation might be contributing factors. Comparison with other IMAGe patients is difficult as many are not molecularly confirmed and could include phenocopies like MIRAGE syndrome.[54] Neither a high-resolution CNV analysis nor a trio-WES revealed alternative explanations for his developmental delay, but this cannot be excluded before further similar cases confirm a neurological association to *CDKN1C-201*. We searched the literature for other variants that may affect *CDKN1C-201* and came across a BWS family with a variant c.821–9C>A with an unknown function.[7] Unfortunately, no RNA was available to check the molecular consequence (Brioude, personal communication).

In summary, our findings demonstrate that a single delins variant can give rise to three distinct phenotypes through different molecular pathomechanisms. A hitherto not reported transcript *CDKN1C-201*, encoding an isoform D (A6NK88) with abundant brain expression, is also affected by the variant. Further functional studies or additional patients are needed to address the role of isoform D in brain development and to verify if changes to this isoform may cause a third face of the *CDKN1C* spectrum: developmental delay.

Acknowledgements We are most grateful to the family whose enthusiastic collaboration was essential to do such a complex genetic study. We also want to thank our coworkers Rita Holdhus, Hilde Rusaas, Guri Matre, Sigrid Erdal, Lene F Sandvik and Tomasz Stokowy. We also acknowledge the service from the Genomic Core Facility (GCF) at the University of Bergen, which is supported by Trond Mohn Foundation, for promoting the RNA sequencing.

Contributors SB has written and planned the article, and investigated the patients. BIH has planned and performed the molecular investigations. PBJ has contributed to the evaluation of the patient. GH has contributed to the planning and reviewing of the work.

Funding The authors have not declared a specific grant for this research from any funding agency in the public, commercial or not-for-profit sectors.

Competing interests None declared.

Patient consent for publication Parental/guardian consent obtained.

Provenance and peer review Not commissioned; externally peer reviewed.

Data availability statement All data relevant to the study are included in the article or uploaded as online supplemental information.

ORCID iD

Siren Berland http://orcid.org/0000-0002-8048-6682

REFERENCES

1 Eggermann T, Binder G, Brioude F, Maher ER, Lapunzina P, Cubellis MV, Bergadá I, Prawitt D, Begemann M. CDKN1C mutations: two sides of the same coin. *Trends Mol Med* 2014;20:614–22.
2 Hatada I, Ohashi H, Fukushima Y, Kaneko Y, Inoue M, Komoto Y, Okada A, Ohishi S, Nabetani A, Morisaki H, Nakayama M, Niikawa N, Mukai T. An imprinted gene p57KIP2 is mutated in Beckwith-Wiedemann syndrome. *Nat Genet* 1996;14:171–3.
3 Brioude F, Lacoste A, Netchine I, Vazquez M-P, Auber F, Audry G, Gauthier-Villars M, Brugieres L, Gicquel C, Le Bouc Y, Rossignol S. Beckwith-Wiedemann syndrome: growth pattern and tumor risk according to molecular mechanism, and guidelines for tumor surveillance. *Horm Res Paediatr* 2013;80:457–65.
4 Arboleda VA, Lee H, Parnaik R, Fleming A, Banerjee A, Ferraz-de-Souza B, Délot EC, Rodriguez-Fernandez IA, Braslavsky D, Bergadá I, Dell'Angelica EC, Nelson SF, Martinez-Agosto JA, Achermann JC, Vilain E. Mutations in the PCNA-binding domain of CDKN1C cause IMAGe syndrome. *Nat Genet* 2012;44:788–92.
5 Weksberg R, Shuman C, Beckwith JB. Beckwith-Wiedemann syndrome. *Eur J Hum Genet* 2010;18:8–14.
6 Brioude F, Kalish JM, Mussa A, Foster AC, Bliek J, Ferrero GB, Boonen SE, Cole T, Baker R, Bertoletti M, Cocchi G, Coze C, De Pellegrin M, Hussain K, Ibrahim A, Kilby MD, Krajewska-Walasek M, Kratz CP, Ladusans EJ, Lapunzina P, Le Bouc Y, Maas SM, Macdonald F, Õunap K, Peruzzi L, Rossignol S, Russo S, Shipster C, Skórka A, Tatton-Brown K, Tenorio J, Tortora C, Grønskov K, Netchine I, Hennekam RC, Prawitt D, Tümer Z, Eggermann T, Mackay DJG, Riccio A, Maher ER. Expert consensus document: clinical and molecular diagnosis, screening and management of Beckwith-Wiedemann syndrome: an international consensus statement. *Nat Rev Endocrinol* 2018;14:229–49.
7 Brioude F, Netchine I, Praz F, Le Jule M, Calmel C, Lacombe D, Edery P, Catala M, Odent S, Isidor B, Lyonnet S, Sigaudy S, Leheup B, Audebert-Bellanger S, Burglen L, Giuliano F, Alessandri J-L, Cormier-Daire V, Laffargue F, Blesson S, Coupier I, Lespinasse J, Blanchet P, Boute O, Baumann C, Polak M, Doray B, Verloes A, Viot G, Le Bouc Y, Rossignol S. Mutations of the imprinted CDKN1C gene as a cause of the overgrowth Beckwith-Wiedemann syndrome: clinical spectrum and functional characterization. *Hum Mutat* 2015;36:894–902.
8 Mussa A, Russo S, De Crescenzo A, Freschi A, Calzari L, Maitz S, Macchiaiolo M, Molinatto C, Baldassarre G, Mariani M, Tarani L, Bedeschi MF, Milani D, Melis D, Bartuli A, Cubellis MV, Selicorni A, Cirillo Silengo M, Larizza L, Riccio A, Ferrero GB. (Epi)genotype-phenotype correlations in Beckwith-Wiedemann syndrome. *Eur J Hum Genet* 2016;24:183–90.
9 Welsh HI, Stockley TL, Parkinson N, Ardinger HH. CDKN1C mutations and genital anomalies. *Am J Med Genet A* 2012;158A:265.
10 Romanelli V, Belinchón A, Benito-Sanz S, Martínez-Glez V, Gracia-Bouthelier R, Heath KE, Campos-Barros A, García-Miñaur S, Fernandez L, Meneses H, López-Siguero JP, Guillén-Navarro E, Gómez-Puertas P, Wesselink J-J, Mercado G, Esteban-Marfil V, Palomo R, Mena R, Sánchez A, Del Campo M, Lapunzina P. CDKN1C (p57(Kip2)) analysis in Beckwith-Wiedemann syndrome (BWS) patients: genotype–phenotype correlations, novel mutations, and polymorphisms. *Am J Med Genet A* 2010;152A:1390–7.
11 Gardiner K, Chitayat D, Choufani S, Shuman C, Blaser S, Terespolsky D, Farrell S, Reiss R, Wodak S, Pu S, Ray PN, Baskin B, Weksberg R. Brain abnormalities in patients with Beckwith-Wiedemann syndrome. *Am J Med Genet A* 2012;158A:1388–94.
12 Jurkiewicz D, Skórka A, Ciara E, Kugaudo M, Pelc M, Chrzanowska K, Krajewska-Walasek M. Rare clinical findings in three sporadic cases of Beckwith-Wiedemann syndrome due to novel mutations in the CDKN1C gene. *Clin Dysmorphol* 2020;29:28–34.
13 Brioude F, Oliver-Petit I, Blaise A, Praz F, Rossignol S, Le Jule M, Thibaud N, Faussat A-M, Tauber M, Le Bouc Y, Netchine I. CDKN1C mutation affecting the PCNA-binding domain as a cause of familial Russell Silver syndrome. *J Med Genet* 2013;50:823–30.
14 Kerns SL, Guevara-Aguirre J, Andrew S, Geng J, Guevara C, Guevara-Aguirre M, Guo M, Oddoux C, Shen Y, Zurita A, Rosenfeld RG, Ostrer H, Hwa V, Dauber A. A novel variant in CDKN1C is associated with intrauterine growth restriction, short stature, and early-adulthood-onset diabetes. *J Clin Endocrinol Metab* 2014;99:E2117–22.
15 Obermann C, Meyer E, Prager S, Tomiuk J, Wollmann HA, Eggermann T. Searching for genomic variants in IGF2 and CDKN1C in Silver-Russell syndrome patients. *Mol Genet Metab* 2004;82:246–50.
16 Suntharalingham JP, Ishida M, Buonocore F, Del Valle I, Solanky N, Demetriou C, Regan L, Moore GE, Achermann JC. Analysis of *CDKN1C* in fetal growth restriction and pregnancy loss. *F1000Res* 2019;8.
17 Inoue T, Nakamura A, Iwahashi-Odano M, Tanase-Nakao K, Matsubara K, Nishioka J, Maruo Y, Hasegawa Y, Suzumura H, Sato S, Kobayashi Y, Murakami N, Nakabayashi K, Yamazawa K, Fuke T, Narumi S, Oka A, Ogata T, Fukami M, Kagami M. Contribution of gene mutations to Silver-Russell syndrome phenotype: multigene sequencing analysis in 92 etiology-unknown patients. *Clin Epigenetics* 2020;12:86.
18 Vilain E, Le Merrer M, Lecointre C, Desangles F, Kay MA, Maroteaux P, McCabe ER. IMAGe, a new clinical association of intrauterine growth retardation, metaphyseal dysplasia, adrenal hypoplasia congenita, and genital anomalies. *J Clin Endocrinol Metab* 1999;84:4335–40.
19 Heide S, Chantot-Bastaraud S, Keren B, Harbison MD, Azzi S, Rossignol S, Michot C, Lackmy-Port Lys M, Demeer B, Heinrichs C, Newfield RS, Sarda P, Van Maldergem L, Trifard V, Giabicani E, Siffroi J-P, Le Bouc Y, Netchine I, Brioude F. Chromosomal rearrangements in the 11p15 imprinted region: 17 new 11p15.5 duplications with associated phenotypes and putative functional consequences. *J Med Genet* 2018;55:205–13.
20 Hamajima N, Johmura Y, Suzuki S, Nakanishi M, Saitoh S. Increased protein stability of CDKN1C causes a gain-of-function phenotype in patients with IMAGe syndrome. *PLoS One* 2013;8:e75137.
21 Bodian DL, Solomon BD, Khromykh A, Thach DC, Iyer RK, Link K, Baker RL, Baveja R, Vockley JG, Niederhuber JE. Diagnosis of an imprinted-gene syndrome by a novel bioinformatics analysis of whole-genome sequences from a family trio. *Mol Genet Genomic Med* 2014;2:530–8.
22 Kato F, Hamajima T, Hasegawa T, Amano N, Horikawa R, Nishimura G, Nakashima S, Fuke T, Sano S, Fukami M, Ogata T. IMAGe syndrome: clinical and genetic implications based on investigations in three Japanese patients. *Clin Endocrinol* 2014;80:706–13.
23 Homma TK, Freire BL, Honjo Kawahira RS, Dauber A, Funari MFdeA, Lerario AM, Nishi MY, Albuquerque EVde, Vasques GdeA, Collett-Solberg PF, Miura Sugayama SM, Bertola DR, Kim CA, Arnhold IJP, Malaquias AC, Jorge AAdeL. Genetic disorders in prenatal onset syndromic short stature identified by exome sequencing. *J Pediatr* 2019;215:192–8.
24 Sabir AH, Ryan G, Mohammed Z, Kirk J, Kiely N, Thyagarajan M, Cole T. Familial Russell-Silver syndrome like phenotype in the PCNA domain of the *CDKN1C* gene, a further case. *Case Rep Genet* 2019;2019:1–8.
25 Binder G, Ziegler J, Schweizer R, Habhab W, Haack TB, Heinrich T, Eggermann T. Novel mutation points to a hot spot in CDKN1C causing Silver-Russell syndrome. *Clin Epigenetics* 2020;12:152.
26 Borges KS, Arboleda VA, Vilain E. Mutations in the PCNA-binding site of CDKN1C inhibit cell proliferation by impairing the entry into S phase. *Cell Div* 2015;10:2.
27 Balasubramanian M, Sprigg A, Johnson DS. IMAGe syndrome: case report with a previously unreported feature and review of published literature. *Am J Med Genet A* 2010;152A:3138–42.
28 Kim D, Langmead B, Salzberg SL. HISAT: a fast spliced aligner with low memory requirements. *Nat Methods* 2015;12:357–60.
29 Pertea M, Kim D, Pertea GM, Leek JT, Salzberg SL. Transcript-level expression analysis of RNA-seq experiments with HISAT, StringTie and Ballgown. *Nat Protoc* 2016;11:1650–67.
30 Liao Y, Smyth GK, Shi W. featureCounts: an efficient general purpose program for assigning sequence reads to genomic features. *Bioinformatics* 2014;30:923–30.
31 Hoek TA, Khuperkar D, Lindeboom RGH, Sonneveld S, Verhagen BMP, Boersma S, Vermeulen M, Tanenbaum ME. Single-molecule imaging uncovers rules governing nonsense-mediated mRNA decay. *Mol Cell* 2019;75:e11:324–39.
32 Nguyen LS, Wilkinson MF, Gecz J. Nonsense-mediated mRNA decay: inter-individual variability and human disease. *Neurosci Biobehav Rev* 2014;46 Pt 2:175–86.
33 Wakeling EL, Brioude F, Lokulo-Sodipe O, O'Connell SM, Salem J, Bliek J, Canton APM, Chrzanowska KH, Davies JH, Dias RP, Dubern B, Elbracht M, Giabicani E, Grimberg A, Grønskov K, Hokken-Koelega ACS, Jorge AA, Kagami M, Linglart A, Maghnie M, Mohnike K, Monk D, Moore GE, Murray PG, Ogata T, Petit IO, Russo S, Said E, Toumba M, Tümer Z, Binder G, Eggermann T, Harbison MD, Temple IK, Mackay DJG, Netchine I. Diagnosis and management of Silver-Russell syndrome: first international consensus statement. *Nat Rev Endocrinol* 2017;13:105–24.
34 Fatscher T, Boehm V, Gehring NH, Mechanism GNH. Mechanism, factors, and physiological role of nonsense-mediated mRNA decay. *Cell Mol Life Sci* 2015;72:4523–44.
35 Iiri T, Herzmark P, Nakamoto JM, van Dop C, Bourne HR. Rapid GDP release from Gs alpha in patients with gain and loss of endocrine function. *Nature* 1994;371:164–8.
36 Decker RA, Peacock ML. Occurrence of MEN 2a in familial Hirschsprung's disease: a new indication for genetic testing of the RET proto-oncogene. *J Pediatr Surg* 1998;33:207–14.
37 Zenker M, Rauch A, Winterpacht A, Tagariello A, Kraus C, Rupprecht T, Sticht H, Reis A. A dual phenotype of periventricular nodular heterotopia and frontometaphyseal dysplasia in one patient caused by a single FLNA mutation leading to two functionally different aberrant transcripts. *Am J Hum Genet* 2004;74:731–7.
38 Degenkolbe E, König J, Zimmer J, Walther M, Reißner C, Nickel J, Plöger F, Raspopovic J, Sharpe J, Dathe K, Hecht JT, Mundlos S, Doelken SC, Seemann P. A GDF5 point mutation strikes twice—causing BDA1 and SYNS2. *PLoS Genet* 2013;9:e1003846.
39 Shaw ND, Brand H, Kupchinsky ZA, Bengani H, Plummer L, Jones TI, Erdin S, Williamson KA, Rainger J, Stortchevoi A, Samocha K, Currall BB, Dunican DS, Collins RL, Willer JR, Lek A, Lek M, Nassan M, Pereira S, Kammin T, Lucente D, Silva A, Seabra CM, Chiang C, An Y, Ansari M, Rainger JK, Joss S, Smith JC, Lippincott MF, Singh SS, Patel N, Jing JW, Law JR, Ferraro N, Verloes A, Rauch A, Steindl K, Zweier M, Scheer I, Sato D, Okamoto N, Jacobsen C, Tryggestad J, Chernausek S, Schimmenti LA, Brasseur B, Cesaretti C, García-Ortiz JE, Buitrago TP, Silva OP, Hoffman JD, Mühlbauer W, Ruprecht KW, Loeys BL, Shino M, Kaindl AM, Cho C-H, Morton CC, Meehan RR, van Heyningen V, Liao EC, Balasubramanian R, Hall JE, Seminara SB, Macarthur D, Moore SA, Yoshiura K-I, Gusella JF, Marsh JA, Graham JM, Lin AE, Katsanis N, Jones PL, Crowley WF, Davis EE, FitzPatrick DR, Talkowski ME. Smchd1 mutations associated

with a rare muscular dystrophy can also cause isolated arhinia and Bosma arhinia microphthalmia syndrome. *Nat Genet* 2017;49:238–48.
40 Kaplanis J, Akawi N, Gallone G, McRae JF, Prigmore E, Wright CF, Fitzpatrick DR, Firth HV, Barrett JC, Hurles ME, Deciphering Developmental Disorders study. Exome-wide assessment of the functional impact and pathogenicity of multinucleotide mutations. *Genome Res* 2019;29:1047–56.
41 Robertson KD, Jones PA. Tissue-specific alternative splicing in the human INK4a/ARF cell cycle regulatory locus. *Oncogene* 1999;18:3810–20.
42 Lin Y-C, Diccianni MB, Kim Y, Lin H-H, Lee C-H, Lin R-J, Joo SH, Li J, Chuang T-J, Yang A-S, Kuo H-H, Tsai M-D, Yu AL. Human p16gamma, a novel transcriptional variant of p16(INK4A), coexpresses with p16(INK4A) in cancer cells and inhibits cell-cycle progression. *Oncogene* 2007;26:7017–27.
43 Udayakumaran S, Onyia CU. Beckwith-Wiedemann syndrome and Chiari I malformation—a case-based review of central nervous system involvement in hemihypertrophy syndromes. *Childs Nerv Syst* 2015;31:637–41.
44 Kent L, Bowdin S, Kirby GA, Cooper WN, Maher ER. Beckwith Weidemann syndrome: a behavioral phenotype–genotype study. *Am J Med Genet B Neuropsychiatr Genet* 2008;147B:1295–7.
45 Groves AP, Gettinger K, Druley TE, Kozel BA, Shinawi M, Mohrmann C, Henry J, Jacobi C, Trinkaus K, Hayashi RJ. Special therapy and psychosocial needs identified in a multidisciplinary cancer predisposition syndrome clinic. *J Pediatr Hematol Oncol* 2019;41:133–6.
46 Itoh Y, Masuyama N, Nakayama K, Nakayama KI, Gotoh Y. The cyclin-dependent kinase inhibitors p57 and p27 regulate neuronal migration in the developing mouse neocortex. *J Biol Chem* 2007;282:390–6.
47 Joseph B, Wallén-Mackenzie A, Benoit G, Murata T, Joodmardi E, Okret S, Perlmann T. p57(Kip2) cooperates with Nurr1 in developing dopamine cells. *Proc Natl Acad Sci U S A* 2003;100:15619–24.
48 Ye W, Mairet-Coello G, Pasoreck E, Dicicco-Bloom E. Patterns of p57Kip2 expression in embryonic rat brain suggest roles in progenitor cell cycle exit and neuronal differentiation. *Dev Neurobiol* 2009;69:1–21.
49 Tury A, Mairet-Coello G, DiCicco-Bloom E. The cyclin-dependent kinase inhibitor p57Kip2 regulates cell cycle exit, differentiation, and migration of embryonic cerebral cortical precursors. *Cereb Cortex* 2011;21:1840–56.
50 Furutachi S, Miya H, Watanabe T, Kawai H, Yamasaki N, Harada Y, Imayoshi I, Nelson M, Nakayama KI, Hirabayashi Y, Gotoh Y. Slowly dividing neural progenitors are an embryonic origin of adult neural stem cells. *Nat Neurosci* 2015;18:657–65.
51 Pfurr S, Chu Y-H, Bohrer C, Greulich F, Beattie R, Mammadzada K, Hils M, Arnold SJ, Taylor V, Schachtrup K, Uhlenhaut NH, Schachtrup C. The E2A splice variant E47 regulates the differentiation of projection neurons via p57(KIP2) during cortical development. *Development* 2017;144:3917–31.
52 McNamara GI, John RM, Isles AR. Territorial behavior and social stability in the mouse require correct expression of imprinted *Cdkn1c*. *Front Behav Neurosci* 2018;12:28.
53 Imaizumi Y, Furutachi S, Watanabe T, Miya H, Kawaguchi D, Gotoh Y. Role of the imprinted allele of the CDKN1C gene in mouse neocortical development. *Sci Rep* 2020;10:1884.
54 Kim Y-M, Seo GH, Kim G-H, Ko JM, Choi J-H, Yoo H-W. A case of an infant suspected as IMAGE syndrome who were finally diagnosed with MIRAGE syndrome by targeted Mendelian exome sequencing. *BMC Med Genet* 2018;19:35.

SUPPLEMENTARY FILE

1. ***CDKN1C*** **Primer Sequences qPCR and sequencing of cDNA**
2. **RNA-Seq alignment**
3. **Haplotype analysis**
4. **RNA-seq, IGV-view**

Supplementary 1: Primers

CDKN1C Primer sequences used for RNA-sequencing (cDNA):

CDKN1C-F1	CAGGAGCCTCTCGCTGAC
CDKN1C-F2	TGTCCGGGCCTCTGATCTCCGAG
CDKN1C-F3	TGTCCGGGCCTCTGATCTCCGCTG
CDKN1C-R1	TTTGGGCTCTAAATTGGCTCAC
CDKN1C-R2	ACCGAACGCTGCTCTGCGGCA
CDKN1C-R3	AGCCGCCGC

For analysis of *CDKN1C-201* and *CDKN1C-206* (XM_005252732.4, ENS00000647521.1) that encodes a putative 175aa protein product labeled isoform C (UniProtKB A0A2R8YFP9), we also used the following primers:

CDKN1C-201/206-5UTRex1	GGACAGCCAGCACATCCACGATG
CDKN1C-201/206-5UTR	GACGCAGAAGAGTCCACCACC

RealTime-probes for RNA expression (qPCR):

Hs 00175938_m1	CDKN1C(NM_000076.2)
Hs 00908985_m1	CDKN1C-206
APZTEAZ	CDKN1C(NM_000076.2) specific mutation probe)
Hs 00187842_m1	B2M reference probe
20170628_CDKN1C.sds	Probe specific for 206-transcript: XM_005252732.4

Supplementary 2: Alignment used for generating FASTA files used as designated reference files for mapping the complex delins variant.

The two ref seq files were aligned using EMBOSS NEEDLE to illustrate where the delins is in the sequence (see line # 901 in the alignment file), deleted nucleotides are marked in green in RefSeq, and inserted nucleotides in red). Alignment parameters are included at the top of the file.

```
########################################
# Program: needle
# Rundate: Wed 22 Jan 2020 06:51:17
# Commandline: needle
#    -auto
#    -stdout
#    -asequence emboss_needle-I20200122-065114-0865-20608599-p2m.asequence
#    -bsequence emboss_needle-I20200122-065114-0865-20608599-p2m.bsequence
#    -datafile EDNAFULL
#    -gapopen 10.0
#    -gapextend 0.5
#    -endopen 10.0
#    -endextend 0.5
#    -aformat3 pair
#    -snucleotide1
#    -snucleotide2
# Align_format: pair
# Report_file: stdout
########################################

#=======================================
#
# Aligned_sequences: 2
# 1: CDKN1C_RefSeq_B38
# 2: CDKN1C_DelIns
# Matrix: EDNAFULL
# Gap_penalty: 10.0
# Extend_penalty: 0.5
#
# Length: 2802
# Identity:    2798/2802 (99.9%)
# Similarity:  2798/2802 (99.9%)
# Gaps:           1/2802 ( 0.0%)
# Score: 13968.0
#
#
#=======================================

CDKN1C_RefSeq      1 AGCACAAACAGACTGGAGTTGCAGCATTTTTCGGCCTCTTTATTTAGAAC     50
                     |||||||||||||||||||||||||||||||||||||||||||||||||||
CDKN1C_DelIns      1 AGCACAAACAGACTGGAGTTGCAGCATTTTTCGGCCTCTTTATTTAGAAC     50

CDKN1C_RefSeq     51 CCGGCGGACGAGGGGCCGGGGCAGTGGTACAGACGGCTCAGGAACCATTT    100
                     |||||||||||||||||||||||||||||||||||||||||||||||||||||
CDKN1C_DelIns     51 CCGGCGGACGAGGGGCCGGGGCAGTGGTACAGACGGCTCAGGAACCATTT    100

CDKN1C_RefSeq    101 TAACAGACTTGTCTTCAAGTTTCAGATAAACACAGTCATAATAAGAGAGA    150
                     |||||||||||||||||||||||||||||||||||||||||||||||||||||
CDKN1C_DelIns    101 TAACAGACTTGTCTTCAAGTTTCAGATAAACACAGTCATAATAAGAGAGA    150

CDKN1C_RefSeq    151 CAGCGAAAGCGCGAAGAGACTGCAAGCTAGATGGGCATGTATGGCAGCTA    200
                     |||||||||||||||||||||||||||||||||||||||||||||||||||||
CDKN1C_DelIns    151 CAGCGAAAGCGCGAAGAGACTGCAAGCTAGATGGGCATGTATGGCAGCTA    200

CDKN1C_RefSeq    201 CAGCTTGTGAGTGACCCCCTTCCCCAGAGTCCGCGATGAAAATAAAGTTA    250
                     |||||||||||||||||||||||||||||||||||||||||||||||||||||
CDKN1C_DelIns    201 CAGCTTGTGAGTGACCCCCTTCCCCAGAGTCCGCGATGAAAATAAAGTTA    250

CDKN1C_RefSeq    251 CACTTGTCAATAACCAGATGTGGGAGATGGAGAGTGCCTTTGGCATAACC    300
                     |||||||||||||||||||||||||||||||||||||||||||||||||||||
CDKN1C_DelIns    251 CACTTGTCAATAACCAGATGTGGGAGATGGAGAGTGCCTTTGGCATAACC    300

CDKN1C_RefSeq    301 AATAACCGAGCTAGTGCGTGGCAGAGCGGTCCACGCCTGGACATAAATAG    350
                     |||||||||||||||||||||||||||||||||||||||||||||||||||||
CDKN1C_DelIns    301 AATAACCGAGCTAGTGCGTGGCAGAGCGGTCCACGCCTGGACATAAATAG    350

CDKN1C_RefSeq    351 AAAATATAAGTTAGTATAACTTTAAAAACTTTTTGTACAAATATACATGG    400
                     |||||||||||||||||||||||||||||||||||||||||||||||||||||
```

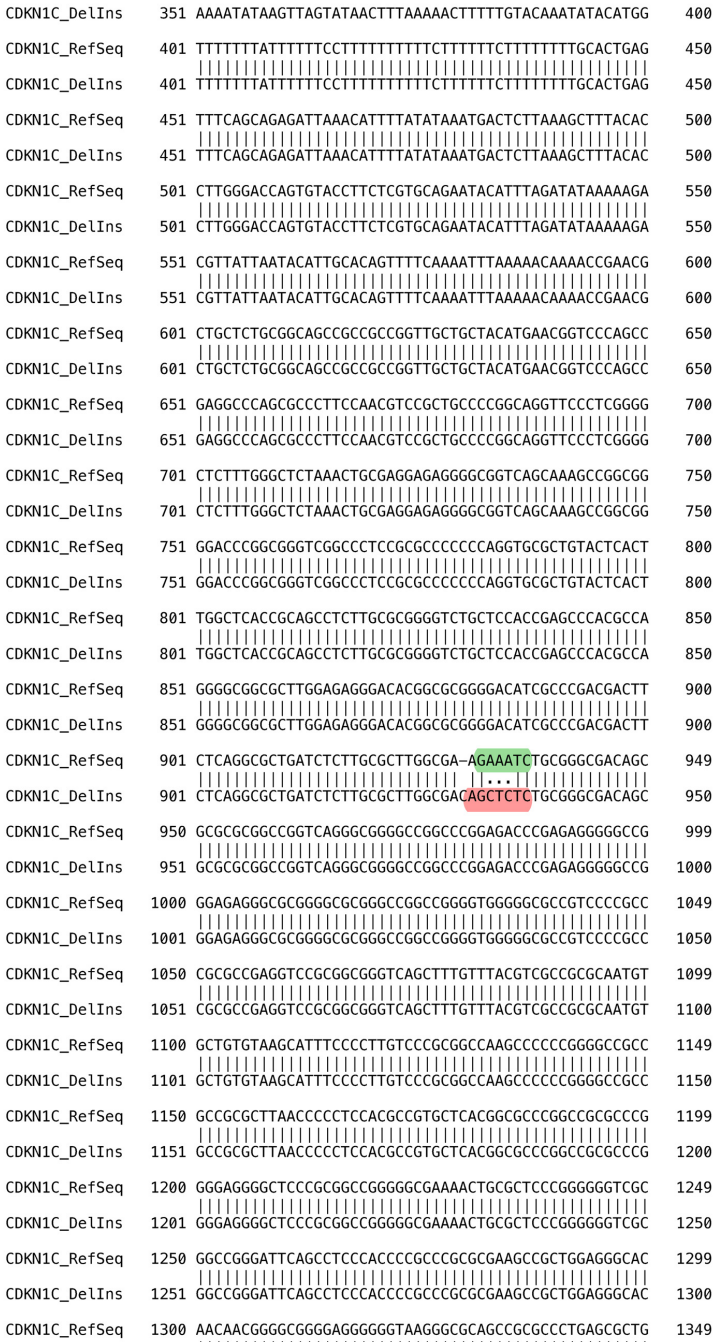
CDKN1C_DelIns 351 AAAATATAAGTTAGTATAACTTTAAAAACTTTTTGTACAAATATACATGG 400
CDKN1C_RefSeq 401 TTTTTTTATTTTTTCCTTTTTTTTTTCTTTTTTCTTTTTTTTGCACTGAG 450
CDKN1C_DelIns 401 TTTTTTTATTTTTTCCTTTTTTTTTTCTTTTTTCTTTTTTTTGCACTGAG 450
CDKN1C_RefSeq 451 TTTCAGCAGAGATTAAACATTTTATATAAATGACTCTTAAAGCTTTACAC 500
CDKN1C_DelIns 451 TTTCAGCAGAGATTAAACATTTTATATAAATGACTCTTAAAGCTTTACAC 500
CDKN1C_RefSeq 501 CTTGGGACCAGTGTACCTTCTCGTGCAGAATACATTTAGATATAAAAAGA 550
CDKN1C_DelIns 501 CTTGGGACCAGTGTACCTTCTCGTGCAGAATACATTTAGATATAAAAAGA 550
CDKN1C_RefSeq 551 CGTTATTAATACATTGCACAGTTTTCAAAATTTAAAAACAAAACCGAACG 600
CDKN1C_DelIns 551 CGTTATTAATACATTGCACAGTTTTCAAAATTTAAAAACAAAACCGAACG 600
CDKN1C_RefSeq 601 CTGCTCTGCGGCAGCCGCCGCCGGTTGCTGCTACATGAACGGTCCCAGCC 650
CDKN1C_DelIns 601 CTGCTCTGCGGCAGCCGCCGCCGGTTGCTGCTACATGAACGGTCCCAGCC 650
CDKN1C_RefSeq 651 GAGGCCCAGCGCCCTTCCAACGTCCGCTGCCCCGGCAGGTTCCCTCGGGG 700
CDKN1C_DelIns 651 GAGGCCCAGCGCCCTTCCAACGTCCGCTGCCCCGGCAGGTTCCCTCGGGG 700
CDKN1C_RefSeq 701 CTCTTTGGGCTCTAAACTGCGAGGAGAGGGGCGGTCAGCAAAGCCGGCGG 750
CDKN1C_DelIns 701 CTCTTTGGGCTCTAAACTGCGAGGAGAGGGGCGGTCAGCAAAGCCGGCGG 750
CDKN1C_RefSeq 751 GGACCCGGCGGGTCGGCCCTCCGCGCCCCCCCAGGTGCGCTGTACTCACT 800
CDKN1C_DelIns 751 GGACCCGGCGGGTCGGCCCTCCGCGCCCCCCCAGGTGCGCTGTACTCACT 800
CDKN1C_RefSeq 801 TGGCTCACCGCAGCCTCTTGCGCGGGGTCTGCTCCACCGAGCCCACGCCA 850
CDKN1C_DelIns 801 TGGCTCACCGCAGCCTCTTGCGCGGGGTCTGCTCCACCGAGCCCACGCCA 850
CDKN1C_RefSeq 851 GGGGCGGCGCTTGGAGAGGGACACGGCGCGGGGACATCGCCCGACGACTT 900
CDKN1C_DelIns 851 GGGGCGGCGCTTGGAGAGGGACACGGCGCGGGGACATCGCCCGACGACTT 900
CDKN1C_RefSeq 901 CTCAGGCGCTGATCTCTTGCGCTTGGCGA-AGAAATCTGCGGGCGACAGC 949
CDKN1C_DelIns 901 CTCAGGCGCTGATCTCTTGCGCTTGGCGACAGCTCTCTGCGGGCGACAGC 950
CDKN1C_RefSeq 950 GCGCGCGGCCGGTCAGGGCGGGGCCGGCCCGGAGACCCGAGAGGGGGCCG 999
CDKN1C_DelIns 951 GCGCGCGGCCGGTCAGGGCGGGGCCGGCCCGGAGACCCGAGAGGGGGCCG 1000
CDKN1C_RefSeq 1000 GGAGAGGGCGCGGGGCGCGGGCCGGCCGGGGTGGGGGCGCCGTCCCCGCC 1049
CDKN1C_DelIns 1001 GGAGAGGGCGCGGGGCGCGGGCCGGCCGGGGTGGGGGCGCCGTCCCCGCC 1050
CDKN1C_RefSeq 1050 CGCGCCGAGGTCCGCGGCGGGTCAGCTTTGTTTACGTCGCCGCGCAATGT 1099
CDKN1C_DelIns 1051 CGCGCCGAGGTCCGCGGCGGGTCAGCTTTGTTTACGTCGCCGCGCAATGT 1100
CDKN1C_RefSeq 1100 GCTGTGTAAGCATTTCCCCTTGTCCCGCGGCCAAGCCCCCCGGGGCCGCC 1149
CDKN1C_DelIns 1101 GCTGTGTAAGCATTTCCCCTTGTCCCGCGGCCAAGCCCCCCGGGGCCGCC 1150
CDKN1C_RefSeq 1150 GCCGCGCTTAACCCCCTCCACGCCGTGCTCACGGCGCCCGGCCGCGCCCG 1199
CDKN1C_DelIns 1151 GCCGCGCTTAACCCCCTCCACGCCGTGCTCACGGCGCCCGGCCGCGCCCG 1200
CDKN1C_RefSeq 1200 GGGAGGGGCTCCCGCGGCCGGGGGCGAAAACTGCGCTCCCGGGGGGTCGC 1249
CDKN1C_DelIns 1201 GGGAGGGGCTCCCGCGGCCGGGGGCGAAAACTGCGCTCCCGGGGGGTCGC 1250
CDKN1C_RefSeq 1250 GGCCGGGATTCAGCCTCCCACCCCGCCCGCGCGAAGCCGCTGGAGGGCAC 1299
CDKN1C_DelIns 1251 GGCCGGGATTCAGCCTCCCACCCCGCCCGCGCGAAGCCGCTGGAGGGCAC 1300
CDKN1C_RefSeq 1300 AACAACGGGGCGGGGAGGGGGGTAAGGGCGCAGCCGCGCCCTGAGCGCTG 1349

```
CDKN1C_DelIns   1301 AACAACGGGGCGGGGAGGGGGGTAAGGGCGCAGCCGCGCCCTGAGCGCTG   1350

CDKN1C_RefSeq   1350 CGGGCCCTTTAATGCCACGGGAGGAGGCGGGAACCCAGCGAGGCCCCCGA   1399
                     ||||||||||||||||||||||||||||||||||||||||||||||||||
CDKN1C_DelIns   1351 CGGGCCCTTTAATGCCACGGGAGGAGGCGGGAACCCAGCGAGGCCCCCGA   1400

CDKN1C_RefSeq   1400 GGGCTGGGGGGACCGGCCGGCCGGACAAAGCGGGGCCGGGCCGGGCCGGG   1449
                     ||||||||||||||||||||||||||||||||||||||||||||||||||
CDKN1C_DelIns   1401 GGGCTGGGGGGACCGGCCGGCCGGACAAAGCGGGGCCGGGCCGGGCCGGG   1450

CDKN1C_RefSeq   1450 GCGGGGCCGTGCGGGGCTCACCGGAGATCAGAGGCCCGGACAGCTTCTTG   1499
                     ||||||||||||||||||||||||||||||||||||||||||||||||||
CDKN1C_DelIns   1451 GCGGGGCCGTGCGGGGCTCACCGGAGATCAGAGGCCCGGACAGCTTCTTG   1500

CDKN1C_RefSeq   1500 ATCGCCGCGCCGTTGGCGCTGGCGGCCGCGGTGCCGGCCGCGGGACGTCC   1549
                     ||||||||||||||||||||||||||||||||||||||||||||||||||
CDKN1C_DelIns   1501 ATCGCCGCGCCGTTGGCGCTGGCGGCCGCGGTGCCGGCCGCGGGACGTCC   1550

CDKN1C_RefSeq   1550 CGAAATCCCCGAGTGCAGCTGGTCAGCGAGAGGCTCCTGGCCGCGCTGCC   1599
                     ||||||||||||||||||||||||||||||||||||||||||||||||||
CDKN1C_DelIns   1551 CGAAATCCCCGAGTGCAGCTGGTCAGCGAGAGGCTCCTGGCCGCGCTGCC   1600

CDKN1C_RefSeq   1600 CCTGGTTCGCGCCCTGCTCGGCGCTCTCTTGAGGCGCCGCGTCCGGGGCC   1649
                     ||||||||||||||||||||||||||||||||||||||||||||||||||
CDKN1C_DelIns   1601 CCTGGTTCGCGCCCTGCTCGGCGCTCTCTTGAGGCGCCGCGTCCGGGGCC   1650

CDKN1C_RefSeq   1650 GGGGCCGGGGCGGGGGCCGGGGCCGGGGCCGGGGCCGGGGCTGGGGCCGG   1699
                     ||||||||||||||||||||||||||||||||||||||||||||||||||
CDKN1C_DelIns   1651 GGGGCCGGGGCGGGGGCCGGGGCCGGGGCCGGGGCCGGGGCTGGGGCCGG   1700

CDKN1C_RefSeq   1700 GGCCGCGACTGGAGCCGGGGCCGGAGCCGGAGCCGGAGCCGGGGCCGGGG   1749
                     ||||||||||||||||||||||||||||||||||||||||||||||||||
CDKN1C_DelIns   1701 GGCCGCGACTGGAGCCGGGGCCGGAGCCGGAGCCGGAGCCGGGGCCGGGG   1750

CDKN1C_RefSeq   1750 CCGGGGCCAGGACCGCGACCGCGACCGGAGCCGCGACCGGAGCCGCGACC   1799
                     ||||||||||||||||||||||||||||||||||||||||||||||||||
CDKN1C_DelIns   1751 CCGGGGCCAGGACCGCGACCGCGACCGGAGCCGCGACCGGAGCCGCGACC   1800

CDKN1C_RefSeq   1800 GGAGCCGGAGCCGGGGCCGGGGCTGGAGCCAGGACCGGGACTGGGGGCGG   1849
                     ||||||||||||||||||||||||||||||||||||||||||||||||||
CDKN1C_DelIns   1801 GGAGCCGGAGCCGGGGCCGGGGCTGGAGCCAGGACCGGGACTGGGGGCGG   1850

CDKN1C_RefSeq   1850 GGTGGACGCCGGGGCCGGGACCGGGACACTAGGCAGCTGCTCCGGCGCCT   1899
                     ||||||||||||||||||||||||||||||||||||||||||||||||||
CDKN1C_DelIns   1851 GGTGGACGCCGGGGCCGGGACCGGGACACTAGGCAGCTGCTCCGGCGCCT   1900

CDKN1C_RefSeq   1900 CCTCGAGGCCGTCGAGGGACTCAGCGGCCGGCTCGAGGGGCGGGCTGACA   1949
                     ||||||||||||||||||||||||||||||||||||||||||||||||||
CDKN1C_DelIns   1901 CCTCGAGGCCGTCGAGGGACTCAGCGGCCGGCTCGAGGGGCGGGCTGACA   1950

CDKN1C_RefSeq   1950 GCCACCGCGACCGCGACGGGCCGCGGCGCCAGCAGCAGGCGGCAGCGCCC   1999
                     ||||||||||||||||||||||||||||||||||||||||||||||||||
CDKN1C_DelIns   1951 GCCACCGCGACCGCGACGGGCCGCGGCGCCAGCAGCAGGCGGCAGCGCCC   2000

CDKN1C_RefSeq   2000 CACCTGCACCGTCTCGCGGTAGAACGCGGGCACCGAGTCGCTGTCCACTT   2049
                     ||||||||||||||||||||||||||||||||||||||||||||||||||
CDKN1C_DelIns   2001 CACCTGCACCGTCTCGCGGTAGAACGCGGGCACCGAGTCGCTGTCCACTT   2050

CDKN1C_RefSeq   2050 CGGTCCACTGCAGGCGTCCAGGGCCCCGCAGCGGCATGTCCTGCTGGAAG   2099
                     ||||||||||||||||||||||||||||||||||||||||||||||||||
CDKN1C_DelIns   2051 CGGTCCACTGCAGGCGTCCAGGGCCCCGCAGCGGCATGTCCTGCTGGAAG   2100

CDKN1C_RefSeq   2100 TCGTAATCCCAGCGGTTCTGGTCCTCGGCGTTCAGCTCGGCCAGGCGGGC   2149
                     ||||||||||||||||||||||||||||||||||||||||||||||||||
CDKN1C_DelIns   2101 TCGTAATCCCAGCGGTTCTGGTCCTCGGCGTTCAGCTCGGCCAGGCGGGC   2150

CDKN1C_RefSeq   2150 CTGCAGCTCGCGGCTCAGCTCCTCGTGGTCCACCGGCCCGAAGAGGCTGC   2199
                     ||||||||||||||||||||||||||||||||||||||||||||||||||
CDKN1C_DelIns   2151 CTGCAGCTCGCGGCTCAGCTCCTCGTGGTCCACCGGCCCGAAGAGGCTGC   2200

CDKN1C_RefSeq   2200 GGCAGGCGCTGGTGCGCACTAGTACTGGGAAGGTCCCACGGGCGACAAGA   2249
                     ||||||||||||||||||||||||||||||||||||||||||||||||||
CDKN1C_DelIns   2201 GGCAGGCGCTGGTGCGCACTAGTACTGGGAAGGTCCCACGGGCGACAAGA   2250

CDKN1C_RefSeq   2250 CGCTCCATCGTGGATGTGCTGCGGAGGGACGCGTCGGACATGGCCCGGGG   2299
                     ||||||||||||||||||||||||||||||||||||||||||||||||||
```

```
CDKN1C_DelIns   2251 CGCTCCATCGTGGATGTGCTGCGGAGGGACGCGTCGGACATGGCCCGGGG   2300

CDKN1C_RefSeq   2300 CTGCGCAAACGCGGGCAGCGAGAGAGGAGAGGACAGCGAGAAGAAGGGGA   2349
                     ||||||||||||||||||||||||||||||||||||||||||||||||||
CDKN1C_DelIns   2301 CTGCGCAAACGCGGGCAGCGAGAGAGGAGAGGACAGCGAGAAGAAGGGGA   2350

CDKN1C_RefSeq   2350 AAGGAGAGGAGGAGAGGGCGGAGGCCGGGCGCAAGGGAGACCCCGCGCCG   2399
                     ||||||||||||||||||||||||||||||||||||||||||||||||||
CDKN1C_DelIns   2351 AAGGAGAGGAGGAGAGGGCGGAGGCCGGGCGCAAGGGAGACCCCGCGCCG   2400

CDKN1C_RefSeq   2400 CCCGACTCTGCGTGTGCGAGGGACGCGGCGGCTACCTGGCTGTCCGGTGG   2449
                     ||||||||||||||||||||||||||||||||||||||||||||||||||
CDKN1C_DelIns   2401 CCCGACTCTGCGTGTGCGAGGGACGCGGCGGCTACCTGGCTGTCCGGTGG   2450

CDKN1C_RefSeq   2450 TGGACTCTTCTGCGTCGGGTTCGCCTGTCTCGTCCGGACGGCAGCCGCGC   2499
                     ||||||||||||||||||||||||||||||||||||||||||||||||||
CDKN1C_DelIns   2451 TGGACTCTTCTGCGTCGGGTTCGCCTGTCTCGTCCGGACGGCAGCCGCGC   2500

CDKN1C_RefSeq   2500 CCCCTCGATGCCTGCTGGCTAGCTCGCTCGCTCAGGCCTGGCCGGCACCC   2549
                     ||||||||||||||||||||||||||||||||||||||||||||||||||
CDKN1C_DelIns   2501 CCCCTCGATGCCTGCTGGCTAGCTCGCTCGCTCAGGCCTGGCCGGCACCC   2550

CDKN1C_RefSeq   2550 CTCGAGCACAGCGCACTTGGCCTGTGGAACGCCCAGCCCGCCTGCGCCCC   2599
                     ||||||||||||||||||||||||||||||||||||||||||||||||||
CDKN1C_DelIns   2551 CTCGAGCACAGCGCACTTGGCCTGTGGAACGCCCAGCCCGCCTGCGCCCC   2600

CDKN1C_RefSeq   2600 CTTTATACGCGCGGGCCCCACCCCCGTGCGCGCGGGCCCGGCCGCGATTA   2649
                     ||||||||||||||||||||||||||||||||||||||||||||||||||
CDKN1C_DelIns   2601 CTTTATACGCGCGGGCCCCACCCCCGTGCGCGCGGGCCCGGCCGCGATTA   2650

CDKN1C_RefSeq   2650 GCATAATGTAGTATTTTCAGTTTCAACAACACCACGGCGATTGGCGGCCG   2699
                     ||||||||||||||||||||||||||||||||||||||||||||||||||
CDKN1C_DelIns   2651 GCATAATGTAGTATTTTCAGTTTCAACAACACCACGGCGATTGGCGGCCG   2700

CDKN1C_RefSeq   2700 CCCCGCTGCCCCGCCCCGCCGCGGCCCGGCCCCCGCGCACCGCCCATTGG   2749
                     ||||||||||||||||||||||||||||||||||||||||||||||||||
CDKN1C_DelIns   2701 CCCCGCTGCCCCGCCCCGCCGCGGCCCGGCCCCCGCGCACCGCCCATTGG   2750

CDKN1C_RefSeq   2750 CCGCGCGCACACCCACCGGGGGCGGGGCGGGGCGCGCGGCCGGGGCGCGC   2799
                     ||||||||||||||||||||||||||||||||||||||||||||||||||
CDKN1C_DelIns   2751 CCGCGCGCACACCCACCGGGGGCGGGGCGGGGCGCGCGGCCGGGGCGCGC   2800

CDKN1C_RefSeq   2800 GG   2801
                     ||
CDKN1C_DelIns   2801 GG   2802
```

Supplementary 3: *CDKN1C* Haplotype analysis

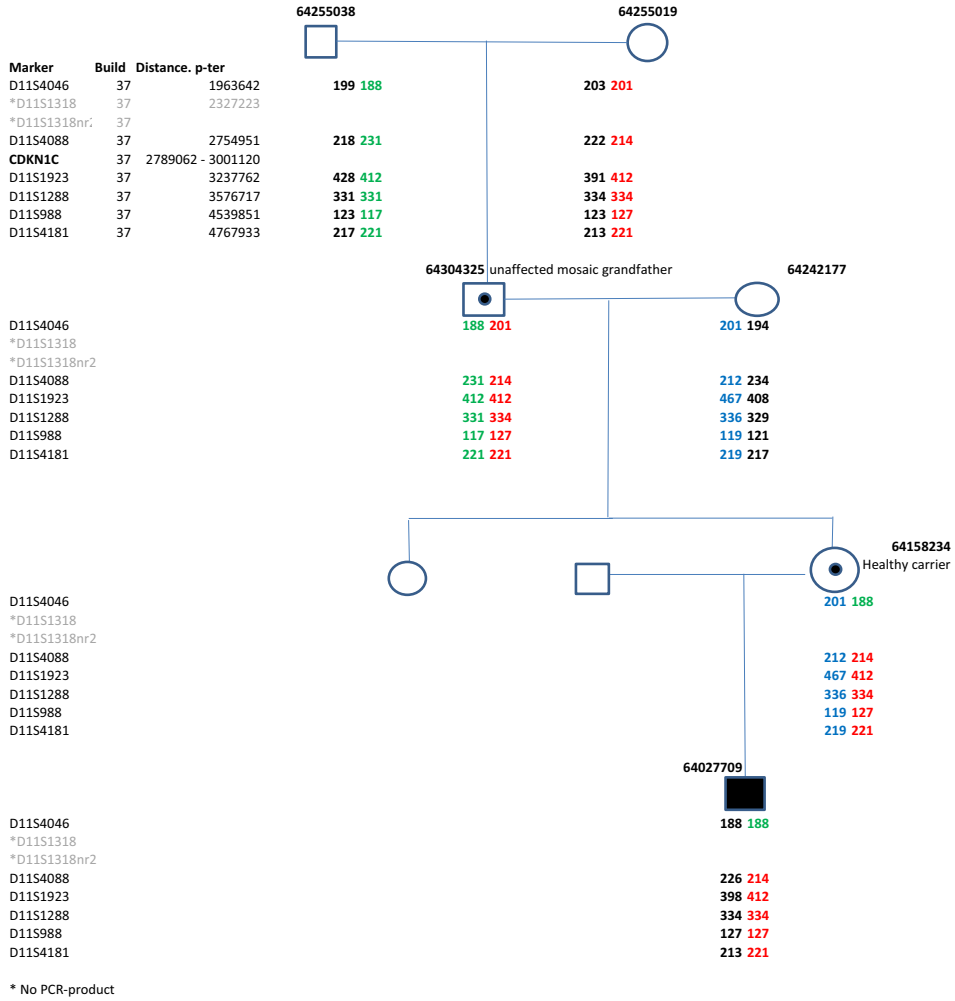

* No PCR-product

Result from haplotype analysis

Haplotype analysis in the family with informative (simple tandem repeat) markers (to the left) confirm that the *de novo CDKN1C* delins in the maternal grandfather occured on his maternal allele

Supplementary 4. Results from *CDKN1C* RNA-sequencing displaying Splice Junctions Tracks

a RefSeq; index boy and healthy control (blood)

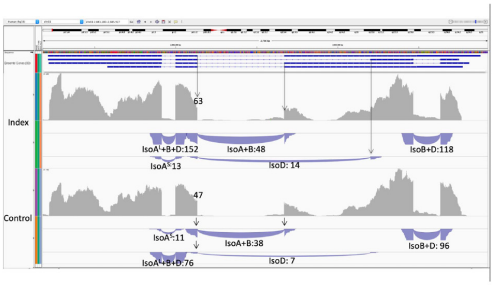

b Ref Seq; mother, maternal grandfather (blood) and index boy (fibroblasts)

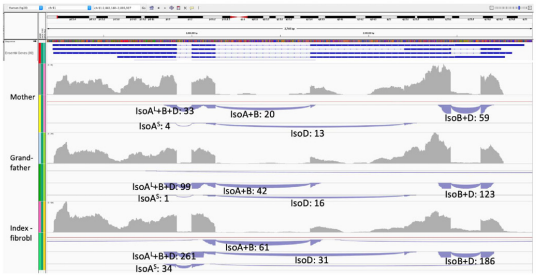

c Delins ref; index boy and control (blood)

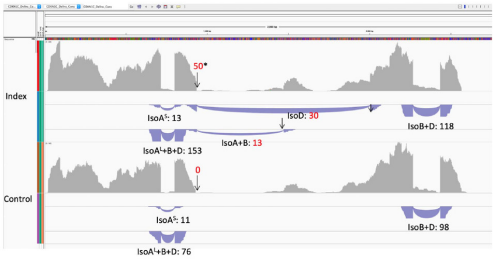

d Delins ref; mother, maternal grandfather (blood) and index boy (fibroblasts)

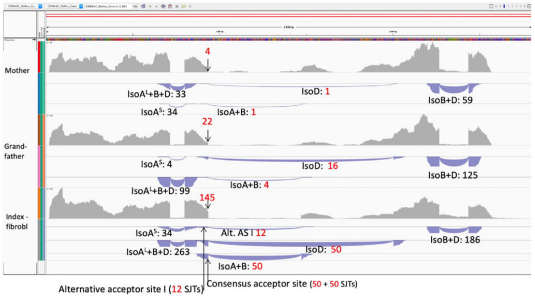

All results from RNAseq are presented in IGV (The Integrative Genomics Viewer). (a) and (b) represent mapping against reference sequence genome assembly GRCh38.p11. (c) and (d) were mapped against a FASTA file containing the delins variant, using the consensus splice site as reference.
Panel (a) and (c) show results from analysis of blood-derived RNA from index patient and a healthy control, while (b) and (d) show results from blood-derived RNA from the asymptomatic heterozygous mother, the mosaic grandfather, and at the bottom fibroblast-derived RNA from the index patient.
The four Ensembl transcripts are shown at the top; first *CDKN1C-202* (named IsoA^{L} in the figure to ease reading), then *CDKN1C-201* (IsoD), followed by *CDKN1C-204* (IsoB) and *CDKN1C-203* (IsoA^{S}). Isoform A (316aa) is encoded by two transcripts of different UTR-length, *CDKN1C-202* (L for ”long”) and *CDKN1C-203* (S for ”short”). Where the two transcript can not be distinguished, the L/S is omitted. The transcripts are read from the reverse strand (from right to left in the figures). The junctions track displays arcs connecting alignment blocks from a single read. For RNA data these connections normally arise from splice junctions, called Splice Junction Track (SJT). Below each arc, the corresponding isoform (A, B or D) and the total number of (manually checked) SJTs are reported, with delins-containing reads in red. The total number of reads at specific points are marked by arrows. SJTs on the same line do not necessarily correspond to the same transcript.

COLD SPRING HARBOR
Molecular Case Studies

RESEARCH REPORT

Double paternal uniparental isodisomy 7 and 15 presenting with Beckwith–Wiedemann spectrum features

Siren Berland,[1] Cecilie F. Rustad,[2] Mariann H. L. Bentsen,[3] Embjørg J. Wollen,[4] Gitta Turowski,[5] Stefan Johansson,[1,6] Gunnar Houge,[1] and Bjørn I. Haukanes[1]

[1]Department of Medical Genetics, Haukeland University Hospital, 5021 Bergen, Norway; [2]Department of Medical Genetics, Oslo University Hospital, 0424 Oslo, Norway; [3]Department of Pediatric and Adolescent Medicine, Haukeland University Hospital, 5021 Bergen, Norway; [4]Department of Pediatric Hepatology, Division of Pediatric and Adolescent Medicine, University of Oslo, Oslo University Hospital HF, 0424 Oslo, Norway; [5]Department of Pathology, Center for Perinatal and Pregnancy-Related Pathology, Oslo University Hospital-Ullevål, 0424 Oslo, Norway; [6]Department of Clinical Science, University of Bergen, 5007 Bergen, Norway

Abstract Here we describe for the first time double paternal uniparental isodisomy (iUPD) 7 and 15 in a baby boy with features in the Beckwith–Wiedemann syndrome spectrum (BWSp) (placentomegaly, hyperinsulinism, enlarged viscera, hemangiomas, and earlobe creases) in addition to conjugated hyperbilirubinemia. His phenotype was also reminiscent of genome-wide paternal uniparental isodisomy. We discuss the most likely origin of the UPDs: a maternal double monosomy 7 and 15 rescued by duplication of the paternal chromosomes after fertilization. So far, paternal UPD7 is not associated with an abnormal phenotype, whereas paternal UPD15 causes Angelman syndrome. Methylation analysis for other clinically relevant imprinting disorders, including BWSp, was normal. Therefore, we hypothesized that the double UPD affected other imprinted genes. To look for such effects, patient fibroblast RNA was isolated and analyzed for differential expression compared to six controls. We did not find apparent transcription differences in imprinted genes outside Chromosomes 7 and 15 in patient fibroblast. *PEG10* (7q21.3) was the only paternally imprinted gene on these chromosomes up-regulated beyond double-dose expectation (sixfold). We speculate that a high *PEG10* level could have a growth-promoting effect as his phenotype was not related to aberrations in BWS locus on 11p15.5 after DNA, RNA, and methylation testing. However, many genes in gene sets associated with growth were up-regulated. This case broadens the phenotypic spectrum of UPDs but does not show evidence of involvement of an imprinted gene network.

[Supplemental material is available for this article.]

Corresponding author:
siren.berland@helse-bergen.no

Ontology terms: conjugated hyperbilirubinemia; hyperinsulinemic hypoglycemia; large placenta; overgrowth

Published by Cold Spring Harbor Laboratory Press

doi:10.1101/mcs.a006113

INTRODUCTION

In uniparental disomy (UPD), both chromosomes in a pair are derived from the same parent (Engel 1980). The two chromosomes can be identical (isodisomy) or homologous (heterodisomy). Meiotic or mitotic recombination can result in a mixture of homozygous (identical) and heterozygous segments. Most UPDs are of maternal origin and caused by trisomy rescue after errors in the first meiotic cleavage (MI) in the oocyte (Kotzot and Utermann 2005; Nakka et al. 2019). In contrast, complete isodisomies are often of paternal origin (Scuffins et al. 2021). Gamete complementation is an anecdotal cause of UPD (Liehr 2014). Segmental UPDs due to mitotic recombination of the maternal and paternal homologs often display mosaicism.

UPDs can be phenotypically neutral but can also be associated with disease in multiple ways; imprinting disorder, low-level mosaicism of an original aneuploidy, a more complex event (supernumerary marker chromosomes, chromothripsis), or demasking of a recessive disease caused by a pathogenic variant carried by only one of the parents. Imprinted genes are tightly regulated, resulting in monoallelic expression in a parent-of-origin-specific and sometimes tissue-dependent manner. Chromosomes 6, 7, 11, 14, 15, and 20 contain imprinted genes that can result in abnormal development if the chromosome pair derives from one parent only. Remarkably, developmental disorders related to imprinting often have overlapping features. Growth disturbances are common, and paternal UPDs often lead to increased intrauterine growth (paternal UPD6/11/14/20 and mosaic genome-wide paternal UPD), whereas many maternal UPDs cause growth restrictions (maternal UPD7/11/14/15/20 and mosaic genome-wide maternal UPD). Endocrine dysregulation and neurodevelopmental delay are also frequently observed in imprinting disorders.

Complete (nonsegmental) UPDs are rare in the general population but show a higher incidence in patient populations. UPD was found in 3.73% of discarded morphologically abnormal embryos (Xu et al. 2015) and in 0.31% of about 32,000 diagnostic exome trios, of which 39% were isodisomies (Scuffins et al. 2021). No double UPD was found in this large patient study. A population screen suggested that UPD occurs in 1/2000 births (0.05%) (Nakka et al. 2019). This study also reported six double UPDs without further details, and their data suggested an incidence of double UPD of 1/50,000 births. The most frequent UPDs in this data set involved Chromosomes 1, 4, 16, 21, 22, and X. This contrasts with the UPDs found after literature search in patient populations, in which all involved imprinted chromosomes (Chromosomes 6, 7, 11, 14, and 15). The mothers of children with UPDs were significantly older than those of non-UPD children, implying a maternal age effect due to meiotic errors (Nakka et al. 2019; Scuffins et al. 2021).

Chromosome 15 is the most common chromosome involved in UPD formations in diagnostic settings, accounting for both maternal and paternal UPDs (Scuffins et al. 2021). Previous publications describing UPDs found a general overrepresentation of imprinted chromosomes like Chromosome 7 (Liehr 2014), but this probably reflects an ascertainment bias as these present with a recognizable phenotype and have readily available diagnostic tests in most developed countries (Nakka et al. 2019). UPD(15)mat (maternal UPD15) often displays heterodisomy (hUPD) or mixed hUPD and isodisomy (iUPD) and result from trisomy rescue. UPD(15)mat is found in ~25% of Prader–Willi syndrome (PWS) patients (Grugni et al. 2008), whereas UPD(15)pat (often iUPD) is a rare cause of Angelman syndrome, present in ~6% (den Besten et al. 2021). iUPD(15)pat can be caused by postzygotic monosomy 15 rescue after maternal meiotic errors, mitotic segregation errors, or rescue of an isochromosome formation. In contrast, paternal hUPD due to trisomy rescue after a paternal meiotic error is rare (Engel 2006). Angelman syndrome is caused by the lack of the maternally expressed UBE3A in the brain. The phenotype includes mild neonatal hypotonia, epilepsy, a characteristic face, microcephaly, ataxia, usually severe developmental delay without expressed language, and a normal life span, but no overgrowth (den Besten et al. 2021).

UPD(7)mat is a cause of Silver–Russell syndrome (SRS), a growth-restricted syndrome. UPD(7)pat is regarded as phenotypically neutral unless a recessive disease is demasked (Hoffmann and Heller 2011), although one report on tall stature suggested a contrasting growth effect (Nakamura et al. 2018). In total, there are seven previous clinical reports on UPD(7)pat patients, five of whom had *CFTR*-related disease (Fares et al. 2006; Feuk et al. 2006; Goh et al. 2007; Le Caignec et al. 2007), including one patient with both cystic fibrosis (CF) and *DNAH11* ciliopathy (Pan et al. 1998; Bartoloni et al. 2002). One patient had congenital chloride diarrhea (Hoglund et al. 1994). Two of seven patients had an unexplained developmental delay (Fares et al. 2006; Feuk et al. 2006). One of the patients with UPD(7)pat and CF also presented with hyperbilirubinemia and a cholestatic pattern lasting for several

months, in addition to postnatal overgrowth and delayed development (Fares et al. 2006). All but two were molecularly confirmed complete isodisomies (Feuk et al. 2006; Goh et al. 2007). In addition, a study on methylation profiling in UPD included two individuals with UPD(7)pat without phenotype information (Joshi et al. 2016), and furthermore there were three UPD(7)pat individuals found in a large population screen (Nakka et al. 2019). An overview also including nonpublished UPD(7)pat patients can be found at http://cs-tl.de/DB/CA/UPD/7-UPDp.html.

Mosaic segmental paternal UPD11p is a common cause of Beckwith–Wiedemann spectrum overgrowth disorders (BWSp). Other causes of BWSp are loss of methylation (LOM) of imprinting center 2 (*CDKNC1/KCNQ1*), gain of methylation (GOM) of imprinting center 1 (*H19/IGF2*), and mutations in the imprinting centers or the growth-inhibitor *CDKN1C*.

Complete genome-wide paternal UPD (GWpUPD), also called uniparental diploidy, is lethal and associated with a molar pregnancy, whereas mosaic GWpUPD, also called androgenetic/biparental chimerism, has been reported more than 30 times in the literature. Low-level mosaicism with tissue variations can be difficult to detect (Kalish et al. 2013; Christesen et al. 2020). Clinical features include placental mesenchymal dysplasia (PMD) and placentomegaly, BWSp, hyperinsulinism, capillary hemangiomas, elevated risk of cancer, and signs of mosaicisms like lateralized overgrowth (Kotzot 2008; Kalish et al. 2013; Postema et al. 2019; Sheppard et al. 2019). However, signs of other imprinting disorders like Angelman syndrome can sometimes be evident (Inbar-Feigenberg et al. 2013; Sheppard et al. 2019; Christesen et al. 2020). Conjugated hyperbilirubinemia is not established as a feature of imprinting disorders. However, this was documented in five girls with mosaic GWpUPD and a BWS-like phenotype with hyperinsulinism (Kalish et al. 2013; Lee et al. 2019; Christesen et al. 2020), in one case of UPD(6)pat (other methylation defects or UPDs were not ruled out in this patient) (Kenny et al. 2009), and in one case of UPD(7)pat (Fares et al. 2006).

We report on a young boy who initially presented with a phenotype overlapping BWSp and GWpUPD, but with the surprising finding of a double paternal isodisomy of the imprinted Chromosomes 7 and 15. A case of two concurrent UPDs in the same individual has not been clinically described previously. Therefore, we wanted to investigate if the double UPDs affected the transcription of other imprinted genes. We discuss the most likely mechanism of origin, suggest that paternal UPD7 might not be phenotypically neutral, and explore the gene expression pattern in patient fibroblast to find an explanation for the phenotype.

RESULTS

Clinical Presentation and Family History

The boy was born from unrelated healthy parents; the mother described the pregnancy as problematic compared to her former pregnancy, and she developed cravings for carbohydrates and felt tired constantly. Still, there were no complications and three regular ultrasound scans. Nuchal translucency was normal (1.26 mm) at gestation week 12 + 1. Spontaneous vaginal birth took place at gestation week 40 + 5, with Apgar scores 9/9/10 after 1, 5, and 10 min. He was 57 cm (2.98 SD) and weighed 4540 g (1.79 SD) at birth; head circumference was 0 SD the first week, and all growth references are according to Norwegian children growth charts (Juliusson et al. 2009). Placentomegaly with an untrimmed weight of 1.7 kg was noted, but unfortunately the placenta was not further examined. The boy was admitted to intensive care after 1.5 h as a result of hypoglycemia (lowest level 1.6 mmol/L). He developed jaundice and was diagnosed with conjugated hyperbilirubinemia, peaking at 7 wk of age with conjugated bilirubin of 109 µmol/L (<5) and elevated liver transaminases. After that, the bilirubin slowly decreased to normal levels at

4–6 mo of age, after which all medical supplements (ursodeoxycholic acid, fat-soluble vitamins) were withdrawn. Because of prolonged hypoglycemia and high insulin levels in the blood, he was diagnosed with transient hyperinsulinism that lasted 5–6 wk. He had a systolic heart murmur and clinically enlarged spleen and liver (4–5 cm below costal margin). Small palpable occipital skin tumors were present at birth, and ultrasound examination suggested hemangiomas. These disappeared within the first month of life. Regarding BWSp features, he had bilateral earlobe creases (Supplemental Fig. S1) but no asymmetry, umbilical hernia, or macroglossia. Abdominal ultrasound showed large and hyper-echogenic kidneys bilaterally, slightly enlarged normal liver, and normal pancreas and spleen, also confirmed in later scans. Echocardiography and neonatal electroencephalogram (EEG) were normal and so was an X-ray of the chest and spinal column. Explorative laparotomy and cholangiography at 5 wk of age were normal. Still, a liver biopsy revealed a possible paucity of intrahepatic bile ducts and cholestasis with minimal inflammation, no glycogenosis, and a diploid status (Haroske et al. 2001). His hyperbilirubinemia was considered secondary to hyperinsulinism. Head circumference fell from 0 SD to −1.2 SD at 10 mo of age. Height at 10 mo of age was 2.4 SD and weight 4.0 SD. He smiled at 5 wk of age and could roll over from his back at 3.5 mo. Breastfeeding was unsuccessful, but otherwise there were no feeding difficulties. At 11 mo of age, he was a happy baby with mild sleeping problems and constipation, and bilateral inguinal testes were found. There were no dysmorphic features, and he had frequent smiles, strabismus, full cheeks, no words, played with toys using both hands, could sit without support for a short period, and moved around freely by shuffling on all fours. He had moderately delayed motor milestones, but he was too young for formal assessment.

The family history was negative. Both parents were tall and slim, the father was 36 yr and 190 cm, and 54 cm and 4.25 kg at birth. The mother was 42 yr and 180 cm, and she was 3572 g at birth, 4 wk preterm. A healthy elder sister was 53 cm and 3740 g at birth, with a placenta of 520 g (trimmed weight of 394 g without fetal membranes and umbilical cord, corresponding to the 10th centile for 39 wk gestation).

The clinical scoring system of BWSp requires a minimum of four points (Brioude et al. 2018), and he scored five points—two points for hyperinsulinism lasting >1 wk, and three points from suggestive features: placentomegaly, ear creases, and nephromegaly and hepatomegaly. According to Norwegian growth charts, his birth weight of 4.45 kg is 1.79 SD, but according to World Health Organization (WHO) references, his birth weight was 2.2 SD, and this would have added another suggestive point and a total BWSp score of 6.

Diagnostic Workup

Just after birth, methylation-specific (MS) multiplex ligation-dependent probe amplification (MLPA) ME030-C1 (BWS) test, an arrayCGH test (on a 180K Agilent array), and an next-generation sequencing (NGS)-based gene panel test with genes associated with liver diseases and hyperinsulinism were performed with normal results. At admission to our hospital because of hyperinsulinism at 5 wk of age, we performed a CytoScanHD Array that revealed complete isodisomy of both Chromosomes 7 and 15, but no (likely) pathogenic copy-number variants (CNVs). As he presented with neither hypotonia (seen in PWS/UPD (15)mat) nor growth restriction (seen in Silver–Russell/UPD(7)mat), we suspected both iUPDs to be paternal or possibly representing clonal mosaicism restricted to peripheral blood. An MS-MLPA test on DNA from a separate blood sample confirmed that both UPDs were paternal, with complete LOM of *MEST/GRB10* in 7q32 and *MAGEL2/SNRP/UBE3A* in 15q11.2. Methylation patterns in differentially methylated regions (DMRs) on Chromosomes 6, 11, and 14 were normal. Trio-based whole-exome sequencing (WES) gave normal results without evidence for recessive, de novo, X-linked or imprinting

disorders and confirmed lack of biparental inheritance of single-nucleotide variants (SNVs) on Chromosomes 7 and 15. Also, *ABCC8* MLPA and *CDKN1C* Sanger sequencing were normal.

We wanted to exclude a clonal UPD event, aneuploidy-mosaicism, or GWpUPD. Chromosome analysis confirmed a normal male karyotype 46,XY in the blood (70 metaphases) and cultured skin fibroblast (39 metaphases) from a skin biopsy taken at 5 mo of age. In addition, fluorescence in situ hybridization (FISH) analysis of centromeres X and Y in 100 interphase nuclei from peripheral blood leukocytes was normal. We also repeated all three relevant MS-MLPA analyses in DNA extracted directly from the skin biopsy, with identical results to blood DNA. Parental karyotypes were both normal.

Karyotype 46,XY.arr[GRCh37] 7p22.3q36.3(44166_159119220)x2 hmz pat,
15q11.2 q26.3(22752398_102429049)x2 hmz pat

RNA Analysis

As his BWSp phenotype did not correlate with the molecular findings, RNA-seq was performed on fibroblast RNA to explore the expression of imprinted genes and other genes of interest, particularly genes involved in growth. We compared this patient to fibroblast RNA-seq results from six control samples. The results are summarized in Supplemental Table S1. Of the approximately 64,000 genes analyzed, which included alternative assemblies, 11,299 genes passed quality checks. Of these, 103 genes were up-regulated (fold change [FC] > 2), of which 99 were protein-coding genes. Similarly, 27 genes were down-regulated (FC < 0.5), of which 15 were protein-coding. There were only four imprinted differentially expressed genes (DEGs), all up-regulated. One of these (*NAP1L4)* is annotated with an unknown imprinting status, one (*PKP3*) has a predicted maternal expression, and two (*DIRAS3* and *PEG10*) had paternal expression. This analysis yielded no down-regulated imprinted gene. Gene sets that were significantly enriched (adjusted *P*-value <0.05) with DEGs fulfilling both the quality and FC criteria described above are listed in Supplemental Table

Table 1. Results from RNA expression analysis of up- or down-regulated imprinted genes on Chromosomes 7 and 15

Gene	Ensembl GeneName	Chr	FC_Index- MedianCtrls	SD	FC_{min} (>2)	FC_{max}	log_2FC	Expressed allele
PEG10	ENSG00000002746	Chr 7	6.55	2.77	4.43	12.09	2.71	Paternal
NDN	ENSG00000105825	Chr 15	2.31	1.21	*1.49*	4.61	1.21	Paternal
GLI3	ENSG00000206190	Chr 7	2.07	0.91	*0.68*	3.39	1.05	Paternal
SGCE	ENSG00000135211	Chr 7	1.59	0.36	*0.88*	1.92	0.67	Paternal
SNRPN	ENSG00000187391	Chr 15	1.54	0.47	*0.76*	1.98	0.62	Paternal
RAC1	ENSG00000158623	Chr 7	1.22	0.21	*1.06*	1.64	0.29	
UBE3A	ENSG00000106070	Chr 15	1.14	0.17	*0.85*	1.31	0.18	Maternal
CCDC71L	ENSG00000164896	Chr 7	0.87	0.18	*0.77*	1.22	–0.20	Paternal
GRB10	ENSG00000114062	Chr 7	0.81	0.17	*0.55*	0.99	–0.30	Isoform-dependent
MAGI2	ENSG00000128739	Chr 7	0.75	0.45	*0.21*	1.29	–0.42	Maternal
ATP10A	ENSG00000106571	Chr 15	0.67	0.19	*0.37*	0.86	–0.58	Maternal
TFPI2	ENSG00000182636	Chr 7	0.45	5.02	*0.16*	10.68	–1.16	Maternal
HECW1	ENSG00000242265	Chr 7	0.23	0.16	*0.17*	0.61	–2.15	Paternal

We only present genes passing the quality check with normalized RNA expression value >8 (see Supplemental Table S1). FC_Index-MedianCtrl represents the fold change between the normalized expression value of the index patient and the median normalized expression value of the six controls. FC_Min (>2) is the lowest fold change between the index and a control sample; genes not fulfilling criteria of an FC_Min >2 are marked with FC_Min in italics. FC_Max is the largest fold change between the index and a control sample.
(FC) Fold change, (Chr) corresponding chromosomal locus, (SD) standard deviation.

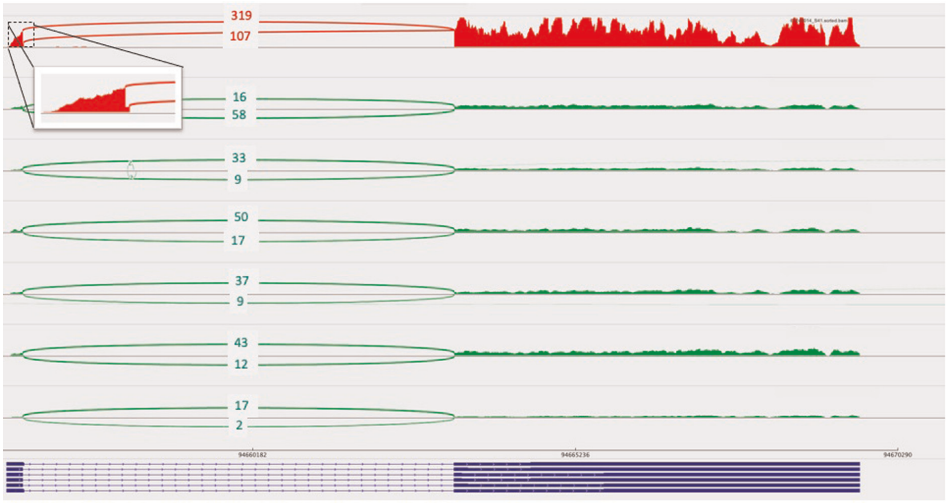

Figure 1. The Sashimi plot (IGV 2.3.74) of *PEG10* RNA-seq analysis displaying the two open reading frames (ORFs) with 11 nt difference between the two consecutive intron 1 donor sites, comparing the expression level in the index (red) to controls (green).

S1. Two relevant gene sets for growth (marked in bold) were both enriched for up-regulated genes, and according to these gene sets, 11/103 (11%) of up-regulated genes were involved in growth.

Finally, we looked at the expression status of (tentative) imprinted genes on Chromosomes 7 and 15, passing the quality check irrespectively of FC, but excluding genes with only predicted or conflicting data (Table 1). *MEST* did not pass quality criteria in five out of six controls and therefore is not included in the table. In summary, we show that the five genes with the highest FC were all paternally imprinted. No significant expression change in BWS genes like *IGF2* and *CDKN1C* was evident. *PEG10* with an FC of 6.55 and FC_min of 4.43 was the only gene also passing the FC > 2 criteria. This gene has two open reading frames (ORFs). We find ~3× higher expression for the most extended transcript in both index and controls, visualized as a Sashimi plot in Figure 1. Exon 1–intron 1 junction is shown on a large scale, confirming that in ORF1, intron 1 is 11 nt longer than in ORF2. The number of tracks spanning splice junctions is shown.

DISCUSSION

In a baby boy with a BWSp-like phenotype, we detected double paternal iUPD7 and iUPD15 (a cause of Angelman syndrome), none of which is known to affect intrauterine growth. The clinical BWSp suspicion, despite normal genetic and imprinting status for BWS locus, pointed to the existence of an "imprinted gene network" (IGN), in which imprinted genes can influence the expression of other imprinted genes even when on other chromosomes (Patten et al. 2016; Eggermann et al. 2021). Six reported patients with concurrent UPD and imprinting defects involving loci on other chromosomes provide further support to the IGN hypothesis (Arima et al. 2005; Begemann et al. 2012; Hara-Isono et al. 2020; Choufani et al. 2021).

Nevertheless, this was not confirmed by RNA-seq in our case. Therefore, we suggest that his phenotype was attributed to his double UPDs, through imprinting defects or up-regulation of nonimprinted genes involved in growth (Table 1; Supplemental Table S1). By definition, the boy has a multilocus imprinting disorder (MLID). It is possible that all MLID with paternal methylation patterns could lead to a BWSp-like phenotype, regardless of which DMRs are involved, but it is also possible that overexpression of the paternally imprinted gene *PEG10* on Chromosome 7 is growth-promoting (Fig. 1).

Overlapping phenotypic features of many imprinting disorders—in particular, SRS (LOM H19/IGF2:IG-DMR on 11p15.5), Temple syndrome (TS) (LOM DLK1/MEG3:IG-DMR on 14q32.2), and PWS (GOM SNURF:TSS-DMR on 15q11q13)—also support the IGN notion. However, genome-wide methylome analyses in these three patient groups have not revealed any apparent relationships between the methylation pattern and the shared phenotypic expression in these patients (Hara-Isono et al. 2020). In contrast, transcriptome analysis performed in patients with TS, SRS, and one mixed TS and SRS showed some overlapping features such as decreased *IGF2* expression, and TS and PWS patients showed decreased *SNURF* expression (Abi Habib et al. 2019).

Most imprinted DEGs on Chromosomes 7 and 15 in the boy showed expression changes as expected from the imprinting pattern (Table 1). *UBEA3A* shows slightly increased expression but below our fold change criteria. However, this gene is biallelically expressed in fibroblasts and only maternally expressed in the brain. The imprinting status is documented only in the placenta for the paternally expressed down-regulated genes *CCDC71L* and *HECW1* (Sanchez-Delgado et al. 2015).

In conclusion, we did not identify a single or a group of DEGs explaining the placentomegaly or overgrowth in the boy apart from high expression of *PEG10* nor a general dysregulation of known imprinted disease genes (Table 1). However, we found significant enrichment for up-regulated genes in gene sets associated with growth and, in general, about four times as many up-regulated as down-regulated DEGs.

Clinical findings were reminiscent of BWSp or mosaic GWpUPDs, which were molecularly excluded. A large placenta is a hallmark of BWS, but weight >1 kg is uncommon and a placenta of 1.9 kg has been reported in GWpUPD (Postema et al. 2019). Unfortunately, placental tissue and pathology were not available. Of note, iUPD(7)pat in postnatal overgrowth and a large and fused twin placenta of 1340 g at gestation week 34 has been reported (Nakamura et al. 2018). A partly phenotypic overlap was also found in a patient with cystic fibrosis due to iUPD(7)pat, hyperbilirubinemia with cholestatic pattern, and postnatal overgrowth (Fares et al. 2006). The imprinted genes *GRB10* on 7p12 and *MEST* (*PEG1*) on 7q32 have been suggested to be implicated in growth restriction (Carrera et al. 2016; Eggermann et al. 2019). A potential role in overgrowth in UPD(7)pat has also been discussed (Nakamura et al. 2018), and BWSp features was noted in a patient with a maternal *GRB10* deletion (Naik et al. 2011). Our study showed increased *PEG10* expression above the expected doubling from UPD, with a sixfold change (Table 1), whereas *GRB10* was not significantly down-regulated (FCmedian 0.81). Unfortunately, *MEST* did not pass quality control; thus, our study is inconclusive on the regulation on *MEST* expression. We speculate that *PEG10* (paternally expressed gene 10) on 7q21.3 might be a cause of both the fetal and placental overgrowth, being a known oncogene (Xie et al. 2018) and essential for placental development (Ono et al. 2006; Abed et al. 2019). This is in line with an SRS phenotype with normal-sized placentas in two patients with paternal isochromosomes 7p combined with maternal isochromosomes 7q (Eggerding et al. 1994; Kotzot et al. 2001). *PEG10* has two conserved ORFs (Xie et al. 2018), also confirmed by RNA-seq. *PEG10* is strongly expressed in the placenta, but also shows high expression in kidneys, lung, brain, and endocrine tissues, and it is involved in cancer proliferation, apoptosis, and metastasis.

Conjugated hyperbilirubinemia has been reported in eight patients with UPD, and 7/8 presented with hyperinsulinism. Hyperinsulinemic hypoglycemia is associated with spontaneously resolving conjugated hyperbilirubinemia in newborns (Edwards et al. 2021). A systematic review of 1692 subjects with conjugated hyperbilirubinemia in infancy does not describe any patients with UPD (Gottesman et al. 2015). Furthermore, NGS and CNV analysis did not reveal other causes of bilirubinemia in the boy. Although these methods have limitations, the clinical findings and transient and benign nature correspond well with the description of hyperbilirubinemia in UPD patients in the literature. Our report demonstrates that UPDs could very well be overlooked in patients with conjugated hyperbilirubinemia, as the UPD diagnosis in the boy was missed in the first hospital.

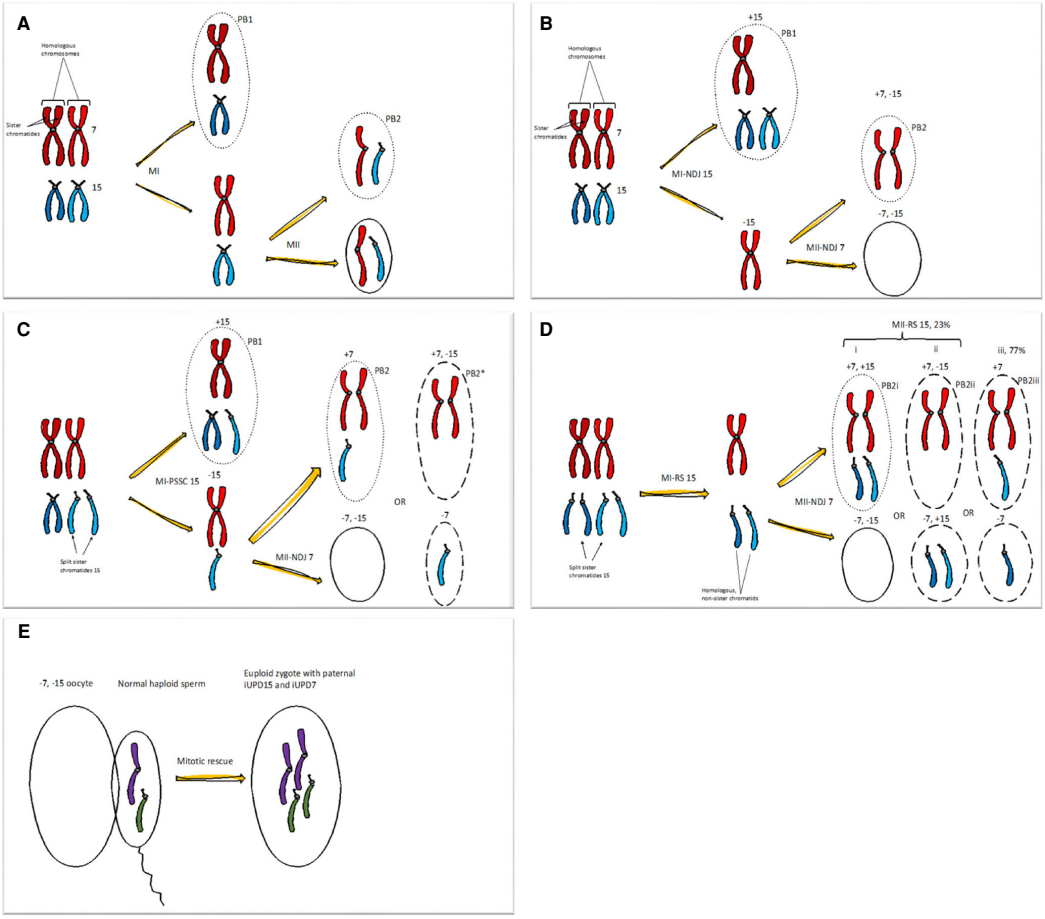

Figure 2. Abnormal female meiosis resulting in a double nullisomic oocyte, in which alternative *C* or *D* is the most likely event in our case. (*Legend continued on following page.*)

In Figure 2, we have outlined the most plausible segregation errors causing double iUPD. Because paternally derived aneuploidies are very rare, causing <1% of all meiotic errors (Tyc et al. 2020), a maternal origin of the double UPD was most likely (e.g., a correction of a double maternal monosomy). This was found in 4%–6% of the blastomeres at maternal age 40–42 yr (Tyc et al. 2020). Furthermore, an initial meiosis I (MI) error in oocytes increased the probability of a subsequent meiosis II (MII) error like nondisjunction (NDJ) by ~2.2-fold. The initial meiotic error could be of NDJ type, but premature separation (and missegregation) of sister chromatids (PSSC) (Fig. 2C) and reverse segregation are both more prevalent, particularly in advanced maternal age (Ottolini et al. 2015; Capalbo et al. 2017; Gruhn et al. 2019). Gamete complementation (a double disomic sperm meeting a double nullisomic ovum) is improbable. Complex mitotic errors are eradicated very early in embryo development. In contrast, meiotic errors are more prone to persist (McCoy et al. 2015). Thus, the most likely origin of the double paternal UPD is maternal double monosomy, causally related to increased maternal age. The meiotic errors probably involved a PSSC in MI, resulting in monosomy 15, or, alternatively, reverse segregation of Chromosome 15 in MI with missegregation in MII. The aneuploid MI oocyte was susceptible to MII-NDJ, affecting Chromosome 7. Postzygotic monosomy rescue with paternal isodisomy of both Chromosomes 15 and 7 then occurred, with a total loss of monosomic cell lines.

In conclusion, we describe for the first time a child with double paternal isodisomy UPD 7 and 15, presenting with Angelman syndrome and a Beckwith–Wiedemann spectrum phenotype. We did not find an alternative explanation for the BWSp phenotype by WES, methylation testing, and RNA-seq, but we suggest that overexpression of *PEG10* could be related

Figure 2. (*Continued.*) (*A*) Normal situation with canonical meiotic division I and II with normal segregation of Chromosomes 7 (red) and 15 (blue). The first meiotic division separates the pair of homologous chromosomes, whereas the second division separates sister chromatids. Dotted lines represent polar bodies (PB), and complete lines the oocyte. Recombinations are omitted from the figures for simplicity. (MI) Meiosis I, (MII) meiosis II. (*B*) Canonical MI and MII with nondisjunction (NDJ). At MI, homologous chromosomes should segregate to opposite spindle pools, but here the homologous Chromosome 15 missegregate. Chromosome 15 is the most frequent chromosome involved in aneuploidy and also represents the chromosomes with the strongest maternal age effect on premature separation (and missegregation) of sister chromatids (PSSC) and reverse segregation (RS) (McCoy et al. 2015; Capalbo et al. 2017; Gruhn et al. 2019). In an aneuploid oocyte, the risk of MII-NDJ increases, here depicted with NDJ of Chromosome 7, where the sister chromatids fail to separate. The double nullisomy oocyte (−7, −15) outcome is outlined. Polar body 1 (PB1) from MI-NDJ show +15 (disomy 15), and PB2 (dotted line) show +7, −15 (mixed disomy and nullisomy). The result from MII-NDJ of Chromosome 7 in an oocyte with a PB1 constitution is not drawn but would be +7,+15 (double disomy) and −7, +15 (mixed nullisomy and disomy). (*C*) Meiosis with premature (or precocious) separation of sister chromatids (PSSC), in which sister chromatids of one Chromosome 15 loose cohesins and split prematurely and separate in MI, forming a free chromatid, and segregate with (PB1, +15) or without (−15) the homologous chromosome. In addition, we include MII-NDJ of Chromosome 7. Chromatid 15 can be expelled into PB2 (+7) in MII, making a nullisomic oocyte (−7, −15). This chromatid could also stay in the oocyte during MII; see the dashed outlines of the alternative oocyte (−7) and PB2* (+7, −15). (*D*) Noncanonical meiosis with reverse segregation (RS), in which sister chromatids of Chromosome 15 segregate to different primary oocytes in MI, and homologous chromatids segregate in MII (*iii*). For simplicity, we have drawn only one of the two outcomes and also omitted PB1. RS of Chromosome 15 occurs in MI, and the three possible MII outcomes depicted all show MII-NDJ of Chromosome 7. An additional RS-MII error of the non-sister chromatids 15 occurs in the first two alternatives (*i* and *ii*), and balanced segregation of 15 in the last (*iii*). According to Ottolini et al. (2015) MI-RS error with missegregation of the non-sister chromatids into the same oocyte in MII (*i* and *ii*) will occur in 23%. We have outlined the double nullisomic oocyte; the corresponding PB2 is marked with dots (*i*), and alternative oocytes and PB2s (*ii*, *iii*) with dashes. (*E*) Fertilization with a balanced haploid sperm, followed by postzygotic double monosomy rescue via endoduplication in the zygote, producing a double paternal isodisomy of Chromosomes 7 and 15. Maternal MII completion, including extrusion of PB2, occurs after fertilization with the haploid sperm, but this is drawn separately for simplicity.

to large placental and body size. Even though clinically suspected, we could not confirm an imprinted gene network.

METHODS

DNA and RNA Isolation

DNA extracted from peripheral blood from the boy drawn at 5 wk of age was used for most analyses. DNA extracted from uncultivated fibroblasts from a skin biopsy taken at 5 mo of age was used to confirm the initial molecular analysis. RNA was extracted from cultivated fibroblasts from the same skin biopsy using the RNeasy Mini Kit (QIAGEN) and Tape station RIN value of 10. We performed chromosome analysis with conventional karyotyping and interphase FISH analysis on peripheral heparin blood and skin biopsy.

CNV, Methylation, and NGS Analysis

DNA isolated from peripheral blood and fibroblasts from the proband was analyzed for relevant CNVs and methylation aberrations by SALSA MLPA probemix ME030 BWS/RSS version C3, ME032 UPD7–UPD14 version A1, ME028 PWS/AS version C1, and P117 *ABCC8* version C2 (MRC-Holland). Also, we tested DNA from the blood for imprinted loci on Chromosomes 6 and 14 by using the ME032 kit and for genomic CNVs and long stretches of homozygosity by CytoScanHD Array (Thermo Fisher Scientific). We performed NGS analysis (trio-WES) as earlier published (Berland et al. 2020).

RNA Sequencing

We purified total RNA from cultured fibroblasts from the boy's skin biopsy. A whole transcriptome sequencing library was generated using the Illumina TruSeq Stranded Total RNA kit with Ribo-Zero Gold depletion for fibroblasts, according to the manufacturer's protocols. We quality checked the library on the Agilent Bioanalyzer system (RIN > 9) and accurately quantified it using the KAPA qPCR quantification kit. The library was paired-end sequenced on the Illumina HiSeq4000 system with a read length of 2 × 75 nt and a depth of approximately 100 million reads. RNA-seq reads were aligned to the human genome reference (assembly GRCh38.p10) using HISAT2 (v2.0.5) (Kim et al. 2015; Pertea et al. 2016). Reads aligned within the coding part of the genome (adequate GENCODE v25 gene annotation file) were counted using featureCounts (Liao et al. 2014). Read counts were further normalized and analyzed for differential expression compared to six samples from another run (three adult women and three young boys aged 5–16 yr) using DESeq2 (Love et al. 2014) with default options in the R/Bioconductor environment (Gentleman et al. 2004). We visualized data in IGV (Integrative Genomics Viewer v2.3.74). Genes were annotated by FUMA (Functional Mapping and Annotation; https://fuma.ctglab.nl/) GENE2FUNC software (Watanabe et al. 2017), and enrichment analyses were performed by GSEA software (Broad Institute; http://www.gsea-msigdb.org/gsea/index.jsp) (Subramanian et al. 2005).

RNA-seq Expression Analysis

For differential expression analysis and estimation of the fold change of RNA-seq count data, we used DESeq2, which performs an internal normalization in which we calculate a geometric mean for each gene across all samples (Love et al. 2014). The gene counts for a gene in each sample are then divided by this mean. The median of these ratios in a sample is the size factor for that sample. This procedure corrects for library size and RNA composition bias, which can arise, for example, when only a small number of genes are highly expressed in one experiment condition but not in the other. The logarithmic fold change can be viewed

as effect size and account for noisiness from genes with low expression (few counts). FC of the RNA expression level is defined as $2^{(\text{sample-controls})}$. In this case, we used the median normalized expression of all controls; FC = $2^{(\text{ExprIndex} - \text{MedExprCtrls})}$. Genes with normalized expression data values > 8 have adequate quality and were included in further analysis. We have data from six controls; none had overlapping phenotypes, UPDs, or pathogenic CNVs, and two adults are considered entirely healthy (Supplemental Table S2). For further analysis, we only included DEGs fulfilling stringent criteria; up-regulated DEGs with FC > 2 and FCmin ≥ 2, implying that all individual FC_Index-Ctrl must be ≥2, and down-regulated DEGs with FC < 0.5 but also FCmax_Index-Ctrl ≤ 0.5. We collected gene sets from http://geneontology.org/, and a list of 256 imprinted or predicted imprinted genes from https://www.geneimprint.com/site/genes-by-species in June 2021 to analyze up-regulated or down-regulated DEGs.

ADDITIONAL INFORMATION

Data Deposition and Access

Consent was not obtained to make the patient's or the control's raw DNA or RNA sequencing data publicly available.

Ethics Statement

Genetic analysis for this family was performed as clinical testing in a diagnostic setting; transcriptional analysis was performed as part of an overall assessment for interpretation of the findings. This study was undertaken as part of the clinical workup at the Department of Medical Genetics at Haukeland University Hospital, Bergen. Informed consent from the parents for publication of the family history and photographs is stored in the patient's files as a secure archive and to ensure the anonymity of the family.

Acknowledgments

We are most grateful to the family whose enthusiastic collaboration was essential to do such a complex genetic study. We also thank our coworkers Rita Holdhus, Tomasz Stokowy, Hilde Rusaas, and Sigrid Erdal, and we acknowledge the service from the Genomic Core Facility (GCF) at the University of Bergen, which is supported by Trond Mohn Foundation, for promoting the RNA sequencing.

Author Contributions

S.B., G.H., and B.I.H. designed the study. S.B., M.H.L.B., E.J.W., and C.F.R. examined, investigated, and cared for the patient and the family. G.T. examined and analyzed the liver biopsy and provided information on sibling's placenta. B.I.H. supervised the RNA-seq. S.B., S.J., G.H., and B.I.H. analyzed the data. S.J., G.H., and B.I.H. supervised the work. S.B. wrote and submitted the manuscript. All authors reviewed and provided input for the manuscript. All authors declare no conflicts of interest and have read and approved the manuscript and its submission.

Competing Interest Statement

The authors have declared no competing interest.

Received July 8, 2021; accepted in revised form August 31, 2021.

REFERENCES

Abed M, Verschueren E, Budayeva H, Liu P, Kirkpatrick DS, Reja R, Kummerfeld SK, Webster JD, Gierke S, Reichelt M, et al. 2019. The Gag protein PEG10 binds to RNA and regulates trophoblast stem cell lineage specification. *PLoS ONE* **14:** e0214110. doi:10.1371/journal.pone.0214110

Habib W A, Brioude F, Azzi S, Rossignol S, Linglart A, Sobrier ML, Giabicani E, Steunou V, Harbison MD, Le Bouc Y, et al. 2019. Transcriptional profiling at the *DLK1/MEG3* domain explains clinical overlap between imprinting disorders. *Sci Adv* **5:** eaau9425. doi:10.1126/sciadv.aau9425

Arima T, Kamikihara T, Hayashida T, Kato K, Inoue T, Shirayoshi Y, Oshimura M, Soejima H, Mukai T, Wake N. 2005. *ZAC*, *LIT1* (*KCNQ1OT1*) and $p57^{KIP2}$ *(CDKN1C)* are in an imprinted gene network that may play a role in Beckwith–Wiedemann syndrome. *Nucleic Acids Res* **33:** 2650–2660. doi:10.1093/nar/gki555

Bartoloni L, Blouin JL, Pan Y, Gehrig C, Maiti AK, Scamuffa N, Rossier C, Jorissen M, Armengot M, Meeks M, et al. 2002. Mutations in the *DNAH11* (axonemal heavy chain dynein type 11) gene cause one form of situs inversus totalis and most likely primary ciliary dyskinesia. *Proc Natl Acad Sci* **99:** 10282–10286. doi:10.1073/pnas.152337699

Begemann M, Spengler S, Kordaβ U, Schröder C, Eggermann T. 2012. Segmental maternal uniparental disomy 7q associated with *DLK1/GTL2* (14q32) hypomethylation. *Am J Med Genet A* **158A:** 423–428. doi:10.1002/ajmg.a.34412

Berland S, Haukanes BI, Juliusson PB, Houge G. 2020. Deep exploration of a *CDKN1C* mutation causing a mixture of Beckwith–Wiedemann and IMAGe syndromes revealed a novel transcript associated with developmental delay. *J Med Genet* doi:10.1136/jmedgenet-2020-107401

Brioude F, Kalish JM, Mussa A, Foster AC, Bliek J, Ferrero GB, Boonen SE, Cole T, Baker R, Bertoletti M, et al. 2018. Expert consensus document: clinical and molecular diagnosis, screening and management of Beckwith–Wiedemann syndrome: an international consensus statement. *Nat Rev Endocrinol* **14:** 229–249. doi:10.1038/nrendo.2017.166

Capalbo A, Hoffmann ER, Cimadomo D, Ubaldi FM, Rienzi L. 2017. Human female meiosis revised: new insights into the mechanisms of chromosome segregation and aneuploidies from advanced genomics and time-lapse imaging. *Hum Reprod Update* **23:** 706–722. doi:10.1093/humupd/dmx026

Carrera IA, de Zaldívar MS, Martín R, Begemann M, Soellner L, Eggermann T. 2016. Microdeletions of the 7q32.2 imprinted region are associated with Silver–Russell syndrome features. *Am J Med Genet A* **170:** 743–749. doi:10.1002/ajmg.a.37492

Choufani S, Ko JM, Lou Y, Shuman C, Fishman L, Weksberg R. 2021. Paternal uniparental disomy of the entire chromosome 20 in a child with Beckwith–Wiedemann syndrome. *Genes (Basel)* **12:** 172. doi:10.3390/genes12020172

Christesen HT, Christensen LG, Löfgren AM, Brøndum-Nielsen K, Svensson J, Brusgaard K, Samuelsson S, Elfving M, Jonson T, Gronskov K, et al. 2020. Tissue variations of mosaic genome-wide paternal uniparental disomy and phenotype of multi-syndromal congenital hyperinsulinism. *Eur J Med Genet* **63:** 103632. doi:10.1016/j.ejmg.2019.02.004

den Besten I, de Jong RF, Geerts-Haages A, Bruggenwirth HT, Koopmans M, ENCORE Expertise Center for AS 18+, Brooks A, Elgersma Y, Festen DAM, Valstar MJ. 2021. Clinical aspects of a large group of adults with Angelman syndrome. *Am J Med Genet A* **185:** 168–181. doi:10.1002/ajmg.a.61940

Edwards M, Falzone N, Harrington J. 2021. Conjugated hyperbilirubinemia among infants with hyperinsulinemic hypoglycemia. *Eur J Pediatr* **180:** 1653–1657. doi:10.1007/s00431-021-03944-0

Eggerding FA, Schonberg SA, Chehab FF, Norton ME, Cox VA, Epstein CJ. 1994. Uniparental isodisomy for paternal 7p and maternal 7q in a child with growth retardation. *Am J Hum Genet* **55:** 253–265.

Eggermann T, Begemann M, Kurth I, Elbracht M. 2019. Contribution of *GRB10* to the prenatal phenotype in Silver–Russell syndrome? Lessons from 7p12 copy number variations. *Eur J Med Genet* **62:** 103671. doi:10.1016/j.ejmg.2019.103671

Eggermann T, Davies JH, Tauber M, van den Akker E, Hokken-Koelega A, Johansson G, Netchine I. 2021. Growth restriction and genomic imprinting-overlapping phenotypes support the concept of an imprinting network. *Genes (Basel)* **12:** 585. doi:10.3390/genes12040585

Engel E. 1980. A new genetic concept: uniparental disomy and its potential effect, isodisomy. *Am J Med Genet* **6:** 137–143. doi:10.1002/ajmg.1320060207

Engel E. 2006. A fascination with chromosome rescue in uniparental disomy: Mendelian recessive outlaws and imprinting copyrights infringements. *Eur J Hum Genet* **14:** 1158–1169. doi:10.1038/sj.ejhg.5201619

Fares F, David M, Lerner A, Diukman R, Lerer I, Abeliovich D, Rivlin J. 2006. Paternal isodisomy of Chromosome 7 with cystic fibrosis and overgrowth. *Am J Med Genet A* **140:** 1785–1788. doi:10.1002/ajmg.a.31380

Feuk L, Kalervo A, Lipsanen-Nyman M, Skaug J, Nakabayashi K, Finucane B, Hartung D, Innes M, Kerem B, Nowaczyk MJ, et al. 2006. Absence of a paternally inherited *FOXP2* gene in developmental verbal dyspraxia. *Am J Hum Genet* **79:** 965–972. doi:10.1086/508902

Gentleman RC, Carey VJ, Bates DM, Bolstad B, Dettling M, Dudoit S, Ellis B, Gautier L, Ge Y, Gentry J, et al. 2004. Bioconductor: open software development for computational biology and bioinformatics. *Genome Biol* **5:** R80. doi:10.1186/gb-2004-5-10-r80

Goh DL, Zhou Y, Chong SS, Ngiam NS, Goh DY. 2007. Novel *CFTR* gene mutation in a patient with CBAVD. *J Cyst Fibros* **6:** 423–425. doi:10.1016/j.jcf.2007.02.004

Gottesman LE, Del Vecchio MT, Aronoff SC. 2015. Etiologies of conjugated hyperbilirubinemia in infancy: a systematic review of 1692 subjects. *BMC Pediatr* **15:** 192. doi:10.1186/s12887-015-0506-5

Grugni G, Crino A, Bosio L, Corrias A, Cuttini M, De Toni T, Di Battista E, Franzese A, Gargantini L, Greggio N, et al. 2008. The Italian National Survey for Prader–Willi syndrome: an epidemiologic study. *Am J Med Genet A* **146A:** 861–872. doi:10.1002/ajmg.a.32133

Gruhn JR, Zielinska AP, Shukla V, Blanshard R, Capalbo A, Cimadomo D, Nikiforov D, Chan AC, Newnham LJ, Vogel I, et al. 2019. Chromosome errors in human eggs shape natural fertility over reproductive life span. *Science* **365:** 1466–1469. doi:10.1126/science.aav7321

Hara-Isono K, Matsubara K, Fuke T, Yamazawa K, Satou K, Murakami N, Saitoh S, Nakabayashi K, Hata K, Ogata T, et al. 2020. Genome-wide methylation analysis in Silver–Russell syndrome, Temple syndrome, and Prader–Willi syndrome. *Clin Epigenetics* **12:** 159. doi:10.1186/s13148-020-00949-8

Haroske G, Baak JP, Danielsen H, Giroud F, Gschwendtner A, Oberholzer M, Reith A, Spieler P, Böcking A. 2001. Fourth updated ESACP consensus report on diagnostic DNA image cytometry. *Anal Cell Pathol* **23:** 89–95. doi:10.1155/2001/657642

Hoffmann K, Heller R. 2011. Uniparental disomies 7 and 14. *Best Pract Res Clin Endocrinol Metab* **25:** 77–100. doi:10.1016/j.beem.2010.09.004

Hoglund P, Holmberg C, de la Chapelle A, Kere J. 1994. Paternal isodisomy for Chromosome 7 is compatible with normal growth and development in a patient with congenital chloride diarrhea. *Am J Hum Genet* **55:** 747–752.

Inbar-Feigenberg M, Choufani S, Cytrynbaum C, Chen YA, Steele L, Shuman C, Ray PN, Weksberg R. 2013. Mosaicism for genome-wide paternal uniparental disomy with features of multiple imprinting disorders: diagnostic and management issues. *Am J Med Genet A* **161A:** 13–20. doi:10.1002/ajmg.a.35651

Joshi RS, Garg P, Zaitlen N, Lappalainen T, Watson CT, Azam N, Ho D, Li X, Antonarakis SE, Brunner HG, et al. 2016. DNA methylation profiling of uniparental disomy subjects provides a map of parental epigenetic bias in the human genome. *Am J Hum Genet* **99:** 555–566. doi:10.1016/j.ajhg.2016.06.032

Júlíusson PB, Roelants M, Eide GE, Moster D, Juul A, Hauspie R, Waaler PE, Bjerknes R. 2009. [Growth references for Norwegian children]. *Tidsskr Nor Laegeforen* **129:** 281–286. doi:10.4045/tidsskr.09.32473

Kalish JM, Conlin LK, Bhatti TR, Dubbs HA, Harris MC, Izumi K, Mostoufi-Moab S, Mulchandani S, Saitta S, States LJ, et al. 2013. Clinical features of three girls with mosaic genome-wide paternal uniparental isodisomy. *Am J Med Genet A* **161A:** 1929–1939. doi:10.1002/ajmg.a.36045

Kenny AP, Crimmins NA, Mackay DJ, Hopkin RJ, Bove KE, Leonis MA. 2009. Concurrent course of transient neonatal diabetes with cholestasis and paucity of interlobular bile ducts: a case report. *Pediatr Dev Pathol* **12:** 417–420. doi:10.2350/09-03-0628-CR.1

Kim D, Langmead B, Salzberg SL. 2015. HISAT: a fast spliced aligner with low memory requirements. *Nat Methods* **12:** 357–360. doi:10.1038/nmeth.3317

Kotzot D. 2008. Complex and segmental uniparental disomy updated. *J Med Genet* **45:** 545–556. doi:10.1136/jmg.2008.058016

Kotzot D, Utermann G. 2005. Uniparental disomy (UPD) other than 15: phenotypes and bibliography updated. *Am J Med Genet A* **136:** 287–305. doi:10.1002/ajmg.a.30483

Kotzot D, Holland H, Keller E, Froster UG. 2001. Maternal isochromosome 7q and paternal isochromosome 7p in a boy with growth retardation. *Am J Med Genet* **102:** 169–172. doi:10.1002/ajmg.1430

Le Caignec C, Isidor B, de Pontbriand U, David V, Audrezet MP, Ferec C, David A. 2007. Third case of paternal isodisomy for Chromosome 7 with cystic fibrosis: a new patient presenting with normal growth. *Am J Med Genet A* **143A:** 2696–2699. doi:10.1002/ajmg.a.31999

Lee CT, Tung YC, Hwu WL, Shih JC, Lin WH, Wu MZ, Kuo KT, Yang YL, Chen HL, Chen M, et al. 2019. Mosaic paternal haploidy in a patient with pancreatoblastoma and Beckwith–Wiedemann spectrum. *Am J Med Genet A* **179:** 1878–1883. doi:10.1002/ajmg.a.61276

Liao Y, Smyth GK, Shi W. 2014. featureCounts: an efficient general purpose program for assigning sequence reads to genomic features. *Bioinformatics* **30:** 923–930. doi:10.1093/bioinformatics/btt656

Liehr T. 2014. *Uniparental disomy (UPD) in clinical genetics.* Springer-Verlag, Berlin.

Love MI, Huber W, Anders S. 2014. Moderated estimation of fold change and dispersion for RNA-seq data with DESeq2. *Genome Biol* **15:** 550. doi:10.1186/s13059-014-0550-8

McCoy RC, Demko ZP, Ryan A, Banjevic M, Hill M, Sigurjonsson S, Rabinowitz M, Petrov DA. 2015. Evidence of selection against complex mitotic-origin aneuploidy during preimplantation development. *PLoS Genet* **11:** e1005601. doi:10.1371/journal.pgen.1005601

Naik S, Riordan-Eva E, Thomas NS, Poole R, Ashton M, Crolla JA, Temple IK. 2011. Large de novo deletion of 7p15.1 to 7p12.1 involving the imprinted gene GRB10 associated with a complex phenotype including

features of Beckwith–Wiedemann syndrome. *Eur J Med Genet* **54:** 89–93. doi:10.1016/j.ejmg.2010.09.006

Nakamura A, Muroya K, Ogata-Kawata H, Nakabayashi K, Matsubara K, Ogata T, Kurosawa K, Fukami M, Kagami M. 2018. A case of paternal uniparental isodisomy for Chromosome 7 associated with overgrowth. *J Med Genet* **55:** 567–570. doi:10.1136/jmedgenet-2017-104986

Nakka P, Pattillo Smith S, O'Donnell-Luria AH, McManus KF, 23andMe Research Team, Mountain JL, Ramachandran S, Sathirapongsasuti JF. 2019. Characterization of prevalence and health consequences of uniparental disomy in four million individuals from the general population. *Am J Hum Genet* **105:** 921–932. doi:10.1016/j.ajhg.2019.09.016

Ono R, Nakamura K, Inoue K, Naruse M, Usami T, Wakisaka-Saito N, Hino T, Suzuki-Migishima R, Ogonuki N, Miki H, et al. 2006. Deletion of *Peg10*, an imprinted gene acquired from a retrotransposon, causes early embryonic lethality. *Nat Genet* **38:** 101–106. doi:10.1038/ng1699

Ottolini CS, Newnham L, Capalbo A, Natesan SA, Joshi HA, Cimadomo D, Griffin DK, Sage K, Summers MC, Thornhill AR, et al. 2015. Genome-wide maps of recombination and chromosome segregation in human oocytes and embryos show selection for maternal recombination rates. *Nat Genet* **47:** 727–735. doi:10.1038/ng.3306

Pan Y, McCaskill CD, Thompson KH, Hicks J, Casey B, Shaffer LG, Craigen WJ. 1998. Paternal isodisomy of Chromosome 7 associated with complete situs inversus and immotile cilia. *Am J Hum Genet* **62:** 1551–1555. doi:10.1086/301857

Patten MM, Cowley M, Oakey RJ, Feil R. 2016. Regulatory links between imprinted genes: evolutionary predictions and consequences. *Proc Biol Sci* **283:** 20152760. doi:10.1098/rspb.2015.2760

Pertea M, Kim D, Pertea GM, Leek JT, Salzberg SL. 2016. Transcript-level expression analysis of RNA-seq experiments with HISAT, StringTie and Ballgown. *Nat Protoc* **11:** 1650–1667. doi:10.1038/nprot.2016.095

Postema FAM, Bliek J, van Noesel CJM, van Zutven L, Oosterwijk JC, Hopman SMJ, Merks JHM, Hennekam RC. 2019. Multiple tumors due to mosaic genome-wide paternal uniparental disomy. *Pediatr Blood Cancer* **66:** e27715. doi:10.1002/pbc.27715

Sanchez-Delgado M, Martin-Trujillo A, Tayama C, Vidal E, Esteller M, Iglesias-Platas I, Deo N, Barney O, Maclean K, Hata K, et al. 2015. Absence of maternal methylation in biparental hydatidiform moles from women with *NLRP7* maternal-effect mutations reveals widespread placenta-specific imprinting. *PLoS Genet* **11:** e1005644. doi:10.1371/journal.pgen.1005644

Scuffins J, Keller-Ramey J, Dyer L, Douglas G, Torene R, Gainullin V, Juusola J, Meck J, Retterer K. 2021. Uniparental disomy in a population of 32,067 clinical exome trios. *Genet Med* **23:** 1101–1107. doi:10.1038/s41436-020-01092-8

Sheppard SE, Lalonde E, Adzick NS, Beck AE, Bhatti T, De Leon DD, Duffy KA, Ganguly A, Hathaway E, Ji J, et al. 2019. Androgenetic chimerism as an etiology for Beckwith–Wiedemann syndrome: diagnosis and management. *Genet Med* **21:** 2644–2649. doi:10.1038/s41436-019-0551-9

Subramanian A, Tamayo P, Mootha VK, Mukherjee S, Ebert BL, Gillette MA, Paulovich A, Pomeroy SL, Golub TR, Lander ES, et al. 2005. Gene set enrichment analysis: a knowledge-based approach for interpreting genome-wide expression profiles. *Proc Natl Acad Sci* **102:** 15545–15550. doi:10.1073/pnas.0506580102

Tyc KM, McCoy RC, Schindler K, Xing J. 2020. Mathematical modeling of human oocyte aneuploidy. *Proc Natl Acad Sci* **117:** 10455–10464. doi:10.1073/pnas.1912853117

Watanabe K, Taskesen E, van Bochoven A, Posthuma D. 2017. Functional mapping and annotation of genetic associations with FUMA. *Nat Commun* **8:** 1826. doi:10.1038/s41467-017-01261-5

Xie T, Pan S, Zheng H, Luo Z, Tembo KM, Jamal M, Yu Z, Yu Y, Xia J, Yin Q, et al. 2018. PEG10 as an oncogene: expression regulatory mechanisms and role in tumor progression. *Cancer Cell Int* **18:** 112. doi:10.1186/s12935-018-0610-3

Xu J, Zhang M, Niu W, Yao G, Sun B, Bao X, Wang L, Du L, Sun Y. 2015. Genome-wide uniparental disomy screen in human discarded morphologically abnormal embryos. *Sci Rep* **5:** 12302. doi:10.1038/srep12302

Supplemental material

"Double paternal uniparental isodisomy 7 and 15 presenting with Beckwith-Wiedemann spectrum features"

Supplemental Figure S1: Creases of the right earlobe, clearly visible in infancy.

Legends to Supplemental Table S1: Results from RNA seq data analysis.

a) *Normalized expr. all samples*. Histogram of normalized RNA expression in all samples (RNA expression analysis using DESeq2 with default options (Love et al. 2014) in the R/Bioconductor environment (Gentleman et al. 2004). Normalized RNA expression values below 8 were considered as noise in the analysis. Only values above 8 were used in the differentially expressed gene (DEG) analysis (see Upregulated / Downregulated).

b) *Upregulated*: Results from differentially expressed genes (DEGs) analysis; upregulated genes passing quality check (normalized RNA expression values above 8). MedianExprCtrls= median of normalized expression 6 controls; ExprIndex= normalized expression index; FC_Index-MedianCtrls= fold change of expression index-medianControls (=2^(ExprIndex - MedExprCtrls)); FC_Min >2 shows lowest fold change index-single control (only FC_Min values above 2 were considered to be of interest); FC_Max shows the highest fold change between index and a single control. SD is standard deviation of the FC. Genes that either are imprinted or present in one of the two gene sets involved in growth have a notion.

c) *Downregulated*: Results from differentially expressed genes (DEGs) analysis; downregulated genes passing quality check (normalized RNA expression values above 8). FC_Max <0.5 shows the highest fold change between index and a single control (only FC_Max values below 0.5

were considered to be of interest). Among the down regulated genes, there were no imprinted gene, and no genes in one of the two enriched gene sets involved in growth.

d) GSEA (Broad Institute) (Subramanian et al. 2005) enrichment analyses of DEGs in GO Biological Processes gene sets (MsigDB c5; (Liberzon et al. 2015)). The table only display gene sets with adjusted P-value < 0.05.

Supplemental References:

Gentleman RC, Carey VJ, Bates DM, Bolstad B, Dettling M, Dudoit S, Ellis B, Gautier L, Ge Y, Gentry J et al. 2004. Bioconductor: open software development for computational biology and bioinformatics. *Genome Biol* **5**(10): R80.

Liberzon A, Birger C, Thorvaldsdottir H, Ghandi M, Mesirov JP, Tamayo P. 2015. The Molecular Signatures Database (MSigDB) hallmark gene set collection. *Cell Syst* **1**(6): 417-425.

Love MI, Huber W, Anders S. 2014. Moderated estimation of fold change and dispersion for RNA-seq data with DESeq2. *Genome Biol* **15**(12): 550.

Subramanian A, Tamayo P, Mootha VK, Mukherjee S, Ebert BL, Gillette MA, Paulovich A, Pomeroy SL, Golub TR, Lander ES et al. 2005. Gene set enrichment analysis: a knowledge-based approach for interpreting genome-wide expression profiles. *Proc Natl Acad Sci U S A* **102**(43): 15545-15550.

Graphic design: Communication Division, UiB / Print: Skipnes Kommunikasjon AS

uib.no

ISBN: 9788230866719 (print)
9788230855690 (PDF)